

**Preparation and Application of Fluoroalkyl End-Capped  
Vinyltrimethoxysilane Oligomeric Composites — Encapsulated  
a Variety of Polymetric Compounds Possessing a  
Superoleophilic/superhydrophobic Characteristic**

**Doctoral Course  
Graduate School of Science and Technology  
Hirosaki University**

**Doctoral Thesis**

**March 2019**

**Jun-ichi Suzuki**

## Contents

<b>General Introduction</b>	1
1. Fluorinated polysoap	1
2. Application to Surface Modification of Two Fluoroalkyl End-Capped Vinyltrimethoxysilane Oligomer	7
3. Application to Separation of Mixture of Oil and Water by Using Two Fluoroalkyl End-Capped Vinyltrimethoxysilane Oligomer	9
4. Thesis outline	14
<b>Chapter 1. Preparation of Fluoroalkyl End-Capped Vinyltrimethoxysilane Oligomeric Silica/ Poly(tetrafluoroethylene) Nanocomposites Possessing a Superoleophilic/ Superhydrophobic Characteristic: Application to the Separation of Oil and Water</b>	19
1.1. Introduction	20
1.2. Experimental	23
1.2.1. Measurements	23
1.2.2. Materials	23
1.2.3. Preparation of fluoroalkyl end-capped vinyltrimethoxysilane oligomeric silica/PTFE nanocomposites $[R_F-(VM-SiO_2)_n-R_F/PTFE]$	24

1.2.4.	Preparation of the modified glass treated with the $R_F-(VM-SiO_2)_n-R_F/PTFE$ nanocomposites by dipping method	25
1.3.	Results and discussion	27
1.3.1.	Preparation and thermal stability of the $R_F-(VM-SiO_2)_n-R_F/PTFE$ nanocomposites	27
1.3.2.	Surface modification of glass, PTFE sheet and filter paper by the use of the $R_F-(VM-SiO_2)_n-R_F/PTFE$ nanocomposites	31
1.3.3.	Separation of oil and water by the use of the $R_F-(VM-SiO_2)_n-R_F/PTFE$ nanocomposites	38
1.4.	Conclusion	46
<b>Chapter 2.</b>	<b>Preparation of Fluoroalkyl End-Capped Vinyltrimethoxy-silane Oligomeric Silica/Alkyl-Modified Cellulose Nanocomposites, and Use Thereof for the Modification of Glass and Filter Paper Surfaces: Creation of a Glass Thermoresponsive Switching Behavior and an Efficient Separation Paper Membrane</b>	<b>52</b>
2.1.	Introduction	53
2.2.	Experimental	56
2.2.1.	Measurements	56
2.2.2.	Materials	56
2.2.3.	Preparation of fluoroalkylated vinyltrimethoxysilane oligomeric	57

	silica/AM-Cellu nanocomposites [ $R_F$ -(VM-SiO <sub>2</sub> ) <sub>n</sub> - $R_F$ /AM-Cellu]	
2.2.4.	Surface modification of glass treated with the $R_F$ -(VM-SiO <sub>2</sub> ) <sub>n</sub> - $R_F$ /AM-Cellu nanocomposites	58
2.2.5.	Preparation of the surfactant-stabilized water in oil (1,2-dichloroethane) emulsion	59
2.3.	Results and discussion	60
2.3.1	Preparation of the $R_F$ -(VM-SiO <sub>2</sub> ) <sub>n</sub> - $R_F$ /AM-Cellu Nanocomposites	60
2.3.2	Surface Modification of Glass by Using the $R_F$ -(VM-SiO <sub>2</sub> ) <sub>n</sub> - $R_F$ /AM-Cellu Nanocomposites	61
2.3.3	Surface Modification of Filter Paper by Using the $R_F$ -(VM-SiO <sub>2</sub> ) <sub>n</sub> - $R_F$ /AM-Cellu Nanocomposites	71
2.3.4	Separation of W/O Emulsion by Using the Modified Filter Paper Treated with the $R_F$ -(VM-SiO <sub>2</sub> ) <sub>n</sub> - $R_F$ /AM-Cellu Nanocomposites as the Separation Membrane	77
2.4.	Conclusion	80
<b>Chapter 3.</b>	<b>Preparation of Fluoroalkyl End-capped Oligomer/Cyclodextrin Polymer Composites: Development of Fluorinated Composite Material Having a Higher Adsorption Ability toward Organic Molecules</b>	<b>84</b>
3.1.	Introduction	85
3.2.	Experimental	88

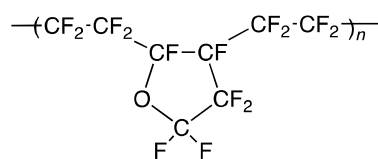
3.2.1.	Measurements	88
3.2.2.	Materials	89
3.2.3.	Preparation of fluoroalkyl end-capped vinyltrimethoxysilane oligomeric silica/ $\alpha$ -CDP composites [ $R_F-(VM-SiO_2)_n-R_F/\alpha$ -CDP]	89
3.2.4.	Surface modification of glass treated with the $R_F-(VM-SiO_2)_n-R_F/\alpha$ -CDP composites	90
3.2.5.	Preparation of the surfactant-stabilized water in oil (toluene) emulsion	91
3.2.6.	Adsorption of bisphenol A in the aqueous solution by using the $R_F-(CH_2CHSiO_2)_n-R_F/\beta$ -CDPs composites	91
3.2.7.	Adsorption of volatile organic compounds (VOCs) in the aqueous solutions by using the $R_F-(CH_2CHSiO_2)_n-R_F/CDPs$ composites	92
3.3.	Results and discussion	94
3.3.1.	Preparation of $R_F-(VM-SiO_2)_n-R_F/\alpha$ -, $\beta$ -, $\gamma$ -CDPs composites	94
3.3.2.	Surface property of $R_F-(VM-SiO_2)_n-R_F/CDPs$ composites	103
3.3.3.	Application of $R_F-(VM-SiO_2)_n-R_F/CDPs$ composites to the separation of the mixture of oil and water	107
3.3.4.	Adsorption of organic molecules by using the $R_F-(CH_2CHSiO_2)_n-R_F/CDPs$ composites	110
3.4.	Conclusion	119

<b>Conclusions</b>	126
<b>Publications</b>	130
<b>Acknowledgements</b>	132

## General Introduction

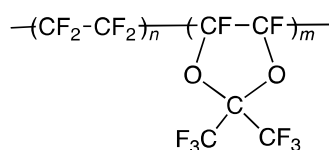
### 1. Fluorinated polysoap

It is in general well-known that perfluoropolymers such as poly(tetrafluoroethylene)  $[-(\text{CF}_2-\text{CF}_2)_n-]$  can exhibit a wide variety of unique properties such as excellent thermal stability, low surface energy, and low refractive index that set them apart from the corresponding non-fluorinated polymers.<sup>1~3)</sup> However, these fluorinated polymers give an extremely poor solubility toward organic solvents.<sup>1~3)</sup> Therefore, it is deeply desirable to develop new fluorinated polymers possessing a good solubility toward a variety of solvents. From this point of view, cyclic fluoropolymers such as CYTOP<sup>TR</sup> (see Chart 1)<sup>4)</sup> and Teflon<sup>TR</sup> AF<sup>5)</sup> (see Chart 2) have been already developed as the fluorinated polymers possessing the solubility in the selected fluorinated solvents.



CYTOP<sup>TR</sup>

Chart 1



Teflon<sup>TR</sup>AF

Chart 2

In addition, partially protonated ring-containing fluoropolymer (see Chart 3) can exhibit a higher solubility toward polar organic solvents such as acetone, acetonitrile and

*N,N*-dimethylformamide, although these fluorinated polymers have no solubility toward benzene, chloroform and methanol.<sup>6)</sup>

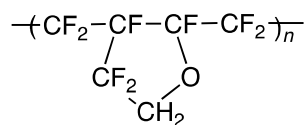


**Chart 3**

On the other hand, partially perfluoroalkylated (meth)acrylated polymers, of whose perfluoroalkyl groups are randomly introduced into polymer main chain through the ester bond, provide interesting characteristics imparted by longer perfluoroalkyl groups that set them apart from the corresponding non-fluorinated ones (see Chart 4).<sup>7)</sup> Randomly

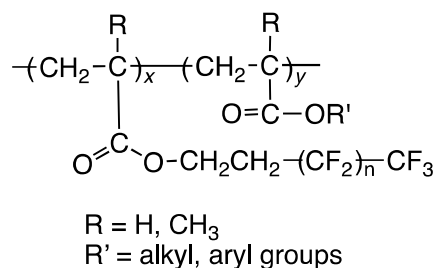


**Chart 4**

perfluoroalkylated polymers can exhibit a similar solubility to that of the partially protonated ring-containing fluoropolymer.<sup>8)</sup> However, these perfluoroalkylated polymers have a poor surface active property, compared to the usual low-molecular weight fluorinated surfactants.<sup>8)</sup> In fact, Laschewsky et al. reported on the surfactant property of the fluorinated polysoaps: that is, randomly perfluorohexylated methacrylate copolymers possessing the



hydrophilic comonomer unit such as 2-[(methacryloyloxy)ethyl]- trimethylammonium bromide, of whose perfluorohexyl units are introduced into polymeric side chain through the ester bonding (Chart 5 ).<sup>9)</sup>

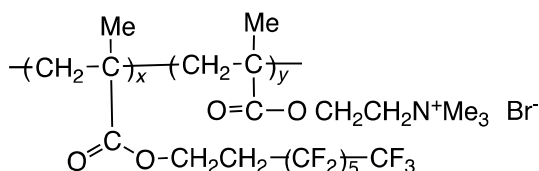


**Chart 5**

These randomly fluoroalkylated polysoaps have a poor surfactant property, compared to that of the usual low-molecular weight fluorinated surfactants, due to the entanglement of the polymer main chain in the aqueous solutions.<sup>9, 10)</sup> Therefore, it is of considerable interest to develop the partially perfluoroalkylated polymers, leading to not only the relatively good solubility toward non-polar organic solvents including water but also the surface active characteristic, similar to that of the traditional low-molecular weight fluorinated surfactants. From this point of view, a variety of block-type perfluoroalkylated copolymers (see Chart 6)

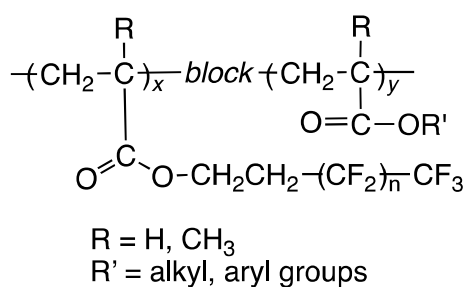
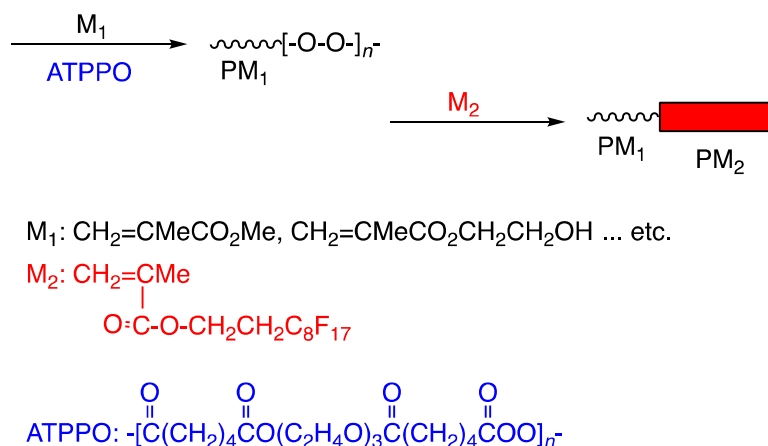


**Chart 6**

have been hitherto synthesized through RAFT (Reversible-Addition-Fragmentation-Transfer)<sup>11)</sup> and ATRP (Atom Transfer Radical Polymerization) techniques<sup>12, 13)</sup>, and the use of polymeric peroxide as a radical initiator (see Scheme 1)<sup>14)</sup>.

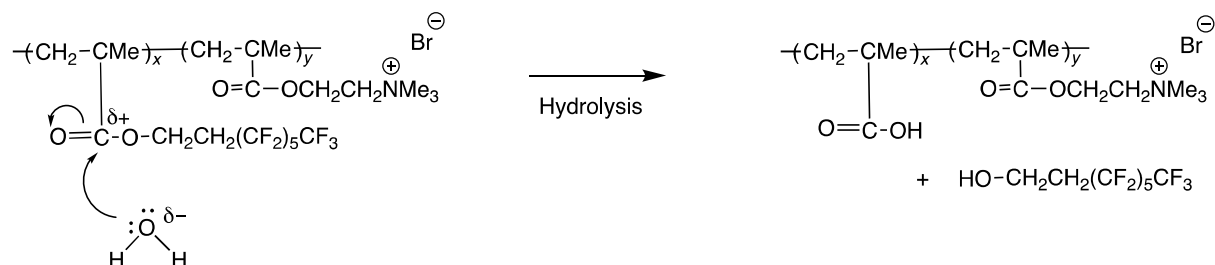


Scheme 1 Synthesis of perfluoroalkylated methacrylated block copolymer by using a polymeric peroxide (ATPPO) as a radical initiator

These block-type perfluoroalkylated copolymers (block-type fluorinated polysoaps) can exhibit relatively higher surface active characteristic and the self-assembled polymeric aggregates resembling micelle in aqueous and organic media, which cannot be achieved in the corresponding randomly fluoroalkylated polysoaps.<sup>15)</sup>

However, in these perfluoroalkylated polysoaps, perfluoroalkyl groups are in general introduced into polymeric main chain through the ester groups owing to the synthetic difficulty of the direct perfluoroalkylation with the carbon-carbon bond formation into polymeric main chain.<sup>15, 16)</sup> Such ester groups are likely to suffer the hydrolysis to produce the corresponding fluorinated alcohol as shown in Scheme 2.<sup>16)</sup> Therefore, we have some

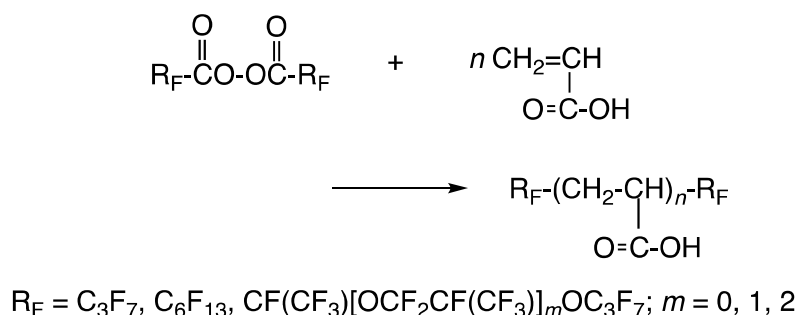
difficulty to keep the good surface active characteristic related to the perfluoroalkyl groups on their aqueous surface for a long time.



Scheme 2 Hydrolysis of randomly perfluorohexylated methacrylate copolymer

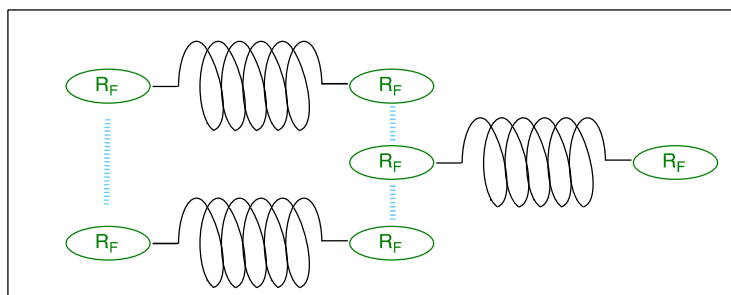
It is deeply desirable to develop new fluoroalkylated block-type polysoaps, of whose fluoroalkyl groups are directly introduced into polymeric main chain through the carbon-carbon bond formation from the developmental view point of new fluoroalkylated block-type polysoaps which can exhibit the surface active characteristic imparted by fluoroalkyl groups for a long time, quite similar to that of the low-molecular weight fluorinated surfactants. In fact, two fluoroalkyl end-capped oligomers, of whose two fluoroalkyl groups are directly introduced into both end-sites of the oligomeric main chain, have been developed by using fluoroalkanoyl peroxide  $[\text{R}_\text{F}-\text{C}(=\text{O})\text{OO}(\text{O}=\text{C})-\text{R}_\text{F}]$  as a key intermediate.<sup>17)</sup> These two fluoroalkyl end-capped oligomers  $[\text{R}_\text{F}-(\text{M})_n-\text{R}_\text{F}; \text{R}_\text{F} = \text{fluoroalkyl groups, M} = \text{radical polymerizable monomers}]$  can be synthesized by the oligomerization of radical polymerizable monomer with fluoroalkanoyl peroxide.<sup>17)</sup>

For example, acrylic acid monomer can react with fluoroalkanoyl peroxides to produce two fluoroalkyl end-capped acrylic acid oligomers as shown in Scheme 3.<sup>18, 19)</sup>



Scheme 3 Synthesis of two fluoroalkyl end-capped acrylic acid oligomers

These fluoroalkyl end-capped acrylic acid oligomers can be classified according to their structure into new ABA triblock-type fluorinated polysoap, of whose fluoroalkyl groups are directly introduced into oligomeric end-sites through the carbon-carbon bond formation.<sup>18)</sup> Especially, this fluorinated oligomer can also form the nanometer size-controlled self-assembled molecular aggregates through the aggregation of the end-capped fluoroalkyl groups in aqueous and organic media (see Scheme 4).<sup>20 ~ 24)</sup>

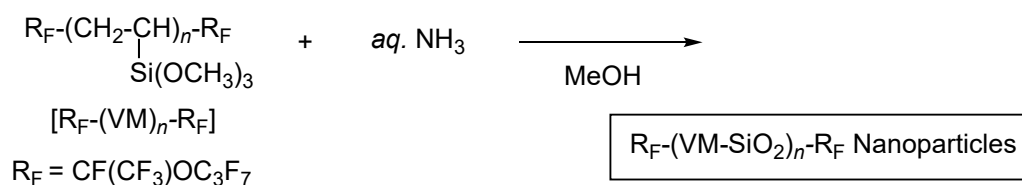


Scheme 4 Schematic illustration for the formation of self-assembled molecular aggregates with the aggregation of terminal fluoroalkyl groups in two fluoroalkyl end-capped oligomers in aqueous and organic media

## 2. Application to Surface Modification of Two Fluoroalkyl End-Capped

### Vinyltrimethoxysilane Oligomer

In a variety of two fluoroalkyl end-capped oligomers, especially, two fluoroalkyl end-capped vinyltrimethoxysilane oligomers  $[R_F-(CH_2CHSi(OMe)_3)_n-R_F; n = 2, 3; R_F = \text{fluoroalkyl groups}; R_F-(VM)_n-R_F]$  are of particular interest due to exhibiting the higher surface active characteristic and the stronger adhesion ability toward numerous substrates than those of the traditional monomeric fluoroalkyl end-capped silane coupling agents  $[R_F-CH_2CH_2-Si(OMe)_3; R_F = \text{fluoroalkyl group}]$ .<sup>25, 26)</sup> These fluoroalkyl end-capped oligomeric silane coupling agents can undergo the sol-gel reactions under alkaline conditions to produce the fluoroalkyl end-capped oligomeric silica nanoparticles  $[R_F-(VM-SiO_2)_n-R_F]$  as shown in Scheme 5.<sup>26)</sup>

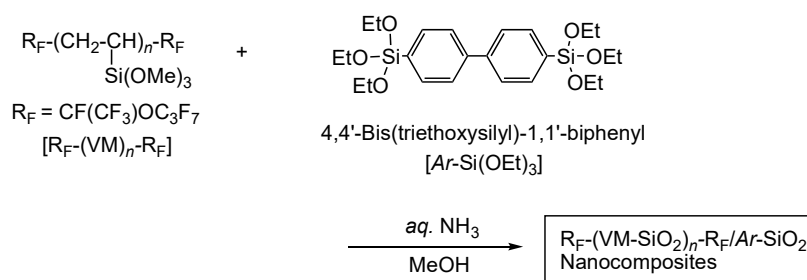


Scheme 5 Preparation of fluoroalkyl end-capped vinyltrimethoxysilane oligomeric nanoparticles

The  $R_F-(VM-SiO_2)_n-R_F$  oligomeric nanoparticles have been already applied to the surface modification of glass to supply not only a good oleophobicity but also a completely

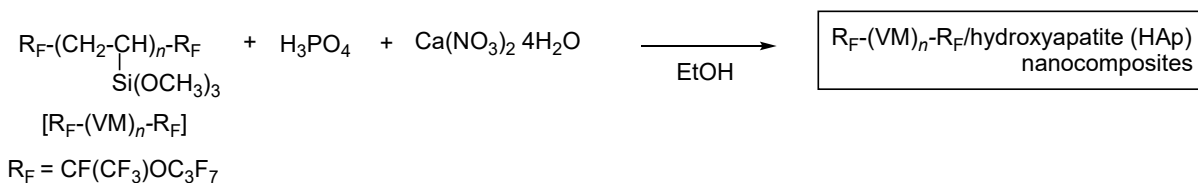
superhydrophobic characteristic (a water contact angle values; 180 degrees) with a non-wetting property against water droplets.<sup>27)</sup>

In addition, a variety of organic guest molecules such as biphenylene units can be easily encapsulated into the  $R_F-(VM-SiO_2)_n-R_F$  oligomeric nanoparticle cores to afford the corresponding fluoroalkyl end-capped oligomeric silica/biphenylene units nanocomposites, leading to the superamphiphobic characteristic on the modified glass surface (see Scheme 6).<sup>28)</sup>



Scheme 6 Preparation of fluoroalkyl end-capped vinyltrimethoxysilane oligomeric silica/biphenylene nanocomposites

Not only organic molecules but also inorganic particles such as hydroxyapatite (HAp) can be encapsulated into the  $R_F-(VM-SiO_2)_n-R_F$  oligomeric nanoparticle cores to provide the corresponding fluorinated oligomeric silica/hydroxyapatite (HAp) nanocomposites (see Scheme 7).<sup>29)</sup> These fluorinated HAp nanocomposites were applied to the surface modification of glass and poly(methyl methacrylate) to exhibit good hydro- and oleo-phobic

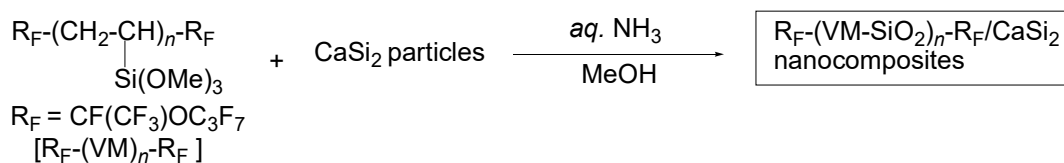


Scheme 7 Preparation of fluoroalkyl end-capped vinyltrimethoxysilane oligomeric silica/hydroxyapatite (HAp) nanocomposites

characteristics imparted by fluorine on their surface.<sup>29)</sup> Interestingly, the formation of the spherical HAp deposits was newly observed on the modified PMMA film surface treated with the  $\text{R}_\text{F}-(\text{VM}-\text{SiO}_2)_n-\text{R}_\text{F}/\text{HAp}$  nanocomposites by soaking this modified film into the simulated body fluid.<sup>29)</sup>

### 3. Application to Separation of Mixture of Oil and Water by Using Two Fluoroalkyl End-capped Vinyltrimethoxysilane Oligomer

As indicated above, a variety of inorganic particles can be effectively encapsulated into two fluoroalkyl end-capped vinyltrimethoxysilane oligomeric nanoparticle cores to provide the corresponding fluorinated oligomeric silica/inorganic particles nanocomposites. In fact, fluoroalkyl end-capped vinyltrimethoxysilane oligomeric silica/calcium silicide ( $\text{CaSi}_2$ ) nanocomposites  $[\text{R}_\text{F}-(\text{VM}-\text{SiO}_2)_n-\text{R}_\text{F}/\text{CaSi}_2]$  were prepared by the sol-gel reaction of  $\text{R}_\text{F}-(\text{CH}_2\text{CHSi}(\text{OMe})_3)_n-\text{R}_\text{F}$   $[\text{R}_\text{F}-(\text{VM})_n-\text{R}_\text{F}]$  oligomer in the presence of calcium silicide particles under alkaline conditions as shown in Scheme 8.<sup>30)</sup>  $\text{R}_\text{F}-(\text{VM}-\text{SiO}_2)_n-\text{R}_\text{F}/\text{CaSi}_2$

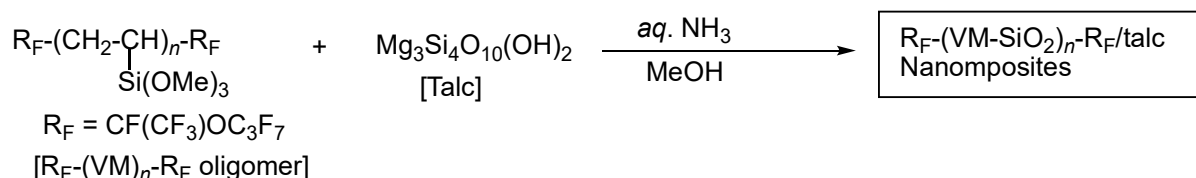


Scheme 8 Preparation of  $\text{R}_F\text{-(VM-SiO}_2)_n\text{-R}_F\text{/CaSi}_2$  nanocomposites

nanocomposites thus obtained, interestingly, can exhibit a superoleophobic/superhydrophilic characteristic on the modified glass and polyethylene terephthalate [PET] fabric surface<sup>30)</sup>, although the original  $\text{R}_F\text{-(VM-SiO}_2)_n\text{-R}_F$  oligomeric nanoparticles afford the usual oleophobic/superhydrophobic property on the modified glass surface<sup>26)</sup>. The modified PET fabric swatch treated the  $\text{R}_F\text{-(VM-SiO}_2)_n\text{-R}_F\text{/CaSi}_2$  nanocomposites possessing a superoleophobic/superhydrophilic property was applied to the separation membrane to separate the mixture of oil and water.<sup>30)</sup>

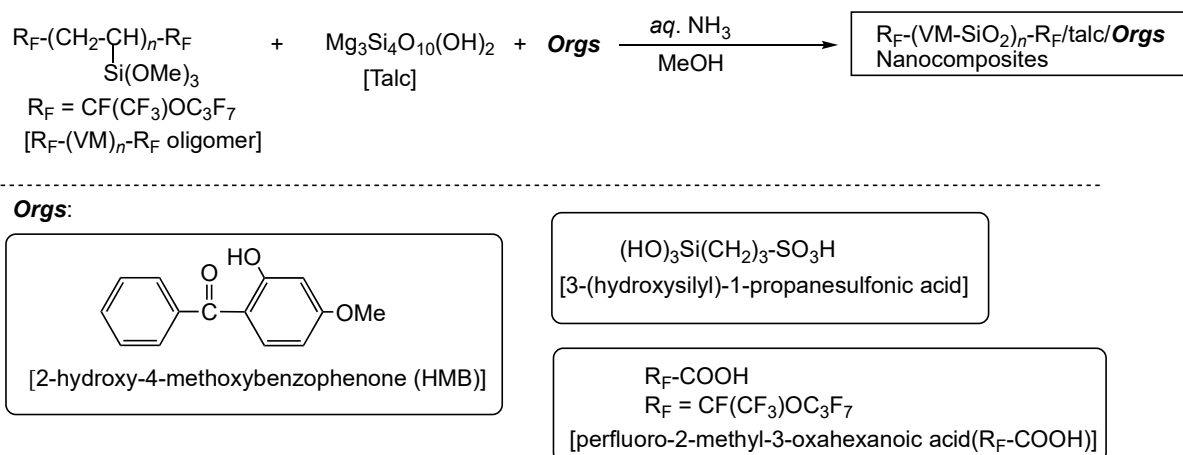
Other inorganic particles such as talc  $[\text{Mg}_3\text{Si}_4\text{O}_{10}(\text{OH})_2]$  were also applied to the encapsulation into the  $\text{R}_F\text{-(VM-SiO}_2)_n\text{-R}_F$  oligomeric nanoparticle cores, giving the corresponding fluorinated nanocomposites-encapsulated talc to exhibit a usual oleophobic/superhydrophobic characteristic (see Scheme 9),<sup>31)</sup> quite similar to that of the pristine  $\text{R}_F\text{-(VM-SiO}_2)_n\text{-R}_F$  oligomeric nanoparticles.<sup>31)</sup> However, interestingly, the encapsulation of oleophilic low-molecular weight aromatic compounds such as





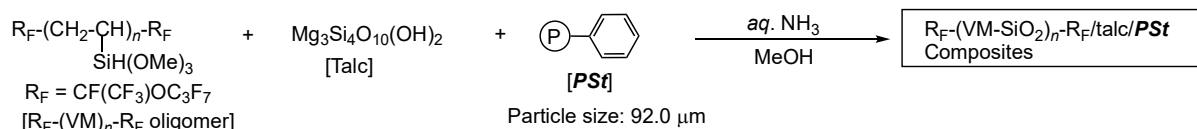
Scheme 9 Preparation of R<sub>F</sub>-(VM-SiO<sub>2</sub>)<sub>n</sub>-R<sub>F</sub>/talc nanocomposites

2-hydroxy-4-methoxybenzophenone (HMB) into the R<sub>F</sub>-(VM-SiO<sub>2</sub>)<sub>n</sub>-R<sub>F</sub> oligomeric nanoparticle cores enables the obtained nanocomposites to supply a superoleophilic/superhydrophobic characteristic on the modified surface.<sup>31)</sup> In contrast, the encapsulation of the hydrophilic low-molecular weight guest molecules such as 3-(hydroxysilyl)-1-propanesulfonic acid and perfluoro-2-methyl-3-oxahexanoic acid into the corresponding fluorinated nanocomposite cores can give not a superoleophilic/superhydrophobic but a superoleophobic/superhydrophilic property on the modified surface (see Scheme 10).<sup>31)</sup>



Scheme 10 Preparation of  $\text{R}_F\text{-(VM-SiO}_2)_n\text{-R}_F/\text{talc/Orgs}$  nanocomposites

Usually, silica gel is widely used as useful inorganic particles for the packing material for column chromatography. Thus, the fluorinated nanocomposites possessing such unique wettability are also expected to apply to the packing material for column chromatography to separate the mixture of oil and water. However, since these encapsulated low-molecular weight guest molecules in general possess extremely poor oil- and water-resistance abilities, we have some difficulties to use these composites for the packing materials for the separation of oil/water for a long time. From this point of view, cross-linked polystyrene particles (*PS**t*) possessing a good solvent resistance ability have been already applied to the guest molecule for the encapsulation into the  $\text{R}_F\text{-(VM-SiO}_2)_n\text{-R}_F/\text{talc}$  nanocomposite cores, leading to the similar superoleophilic/superhydrophobic characteristic to that of the  $\text{R}_F\text{-(VM-SiO}_2)_n\text{-R}_F/\text{talc/HMB}$  nanocomposites as shown in Scheme 10.<sup>31)</sup> In fact, the  $\text{R}_F\text{-(VM-SiO}_2)_n\text{-R}_F/\text{talc/PS}$



Scheme 11 Preparation of  $\text{R}_F\text{-(VM-SiO}_2\text{)}_n\text{-R}_F\text{/talc/PS}t$  composites

composites were applied to the separation of the fresh W/O emulsion under reduced pressure to isolate the colorless oil.<sup>31)</sup> Heretofore, fluorinated polymeric compounds possessing a good oil- and water-resistance abilities such as superhydrophobic/superoleophilic poly(vinylidene fluoride) membrane have been also applied to the separation of W/O emulsions.<sup>32)</sup>

Oil pollution caused by the petrochemical, textile, and food industries as well as the frequent oil-pollution accidents during offshore oil production or marine transportation has become one of the most urgent global environmental problems.<sup>33)</sup> Therefore, the exploration of practical methods for the collection and removal of large amounts of organic pollutants from water has become attracting global attention.<sup>34, 35)</sup> Therefore, the above-indicated fluorinated composites possessing a superoleophilic/superhydrophobic property will have high potential as a wide variety of applicable materials for oil/water separation. In the encapsulation of polymeric molecules into these fluorinated composite cores, it is of considerable importance to develop not only the cross-linked polystyrene particles but also

other polymeric compounds as the useful guest molecules toward the  $R_F-(VM-SiO_2)_n-R_F$  composite cores.

#### **4. Thesis outline**

In this thesis, preparation and applications of fluoroalkyl end-capped oligomeric silica composites - encapsulated a variety of polymeric guest molecules by using fluoroalkyl end-capped vinyltrimethoxysilane oligomer as a key intermediate will be described.

In chapter 1, poly(tetrafluoroethylene) [PTFE] fine particles are used as a polymeric guest molecule, and preparation of fluoroalkyl end-capped vinyltrimethoxysilane oligomeric silica nanocomposites - encapsulated PTFE is described. The surface modification of glass, PTFE sheet and filter paper by using these fluorinated nanocomposites is also described. Especially, application of these composite powders to the packing material for the column chromatography to separate not only the mixture of oil/water but also water-in-oil(W/O) emulsions is described in detail.

Chapter 2 focuses alkyl-modified cellulose (AM-Cellu) on a polymeric guest molecule, and preparation of fluoroalkyl end-capped vinyltrimethoxysilane oligomeric silica/AM-Cellu nanocomposites is described. The surface modification of glass and filter paper by using these fluorinated oligomeric silica/AM-Cellu nanocomposites is described.

Application of the modified filter paper to separate water-in-oil(W/O) emulsions is also described in detail.

Chapter 3 focuses  $\alpha$ -,  $\beta$ - and  $\gamma$ -cyclodextrin polymers ( $\alpha$ -,  $\beta$ - and  $\gamma$ -CDPs) on a polymeric guest molecule, and preparation of fluoroalkyl end-capped vinyltrimethoxysilane oligomeric silica/ $\alpha$ -,  $\beta$ - and  $\gamma$ -CDPs composites is described. The surface wettability of these fluorinated oligomeric silica/  $\alpha$ -,  $\beta$ -,  $\gamma$ -CDPs composites is also described. Application of these composites to the packing material for the column chromatography to separate the mixture of oil/water and water-in-oil(W/O) emulsions is also described. Application of these composites to the packing material for the solid-phase extraction cartridge is described with particular emphasis on the adsorption of the low-molecular weight compounds such as bisphenol A and bisphenol AF, and volatile organic compounds by using these composites.

## References

- 1) B. Ameduri and H. Sawada (Eds.), *Fluorinated Polymers: Volume 1, "Synthesis, Properties, Processing and Simulation"*, Cambridge, RSC (2016).
- 2) B. Ameduri and H. Sawada (Eds.), *Fluorinated Polymers: Volume 2, "Applications"*, Cambridge, RSC (2016).
- 3) D. W. Smith Jr., S. T. Iacono, and S. S. Iyer (Eds.), *Hand Book of Fluoropolymer Science and Technology*, John Wiley & Sons, Inc., Hoboken, New Jersey (2014).
- 4) G. Ogawa, N. Sugiyama, M. Kanda, and K. Okano, *Reports Res. Lab. Asahi Glass Co., Ltd.*, **55**, 47 (2005).
- 5) P. R. Resnick, and W. H. Buck, "Teflon<sup>®</sup> AF Amorphous Fluoropolymer", *Modern Fluoropolymers*, J. Scheirs (Ed.), John Wiley & Sons Ltd., Chichester, New York, 1997, pp397 ~ 419.
- 6) Z.-Y. Yang, A. E. Fering, and B. E. Smart, *J. Am. Chem. Soc.*, **116**, 4135 (1994).
- 7) B. Ameduri and B. Boutevin, *Well-Architected Fluoropolymers: Synthesis, Properties and Applications*, Elsevier, Amsterdam, 2004, pp231 ~ 348.
- 8) Y. Tanizaki, *J. Jpn. Oil Chem. Soc.*, **34**, 973 (1985).
- 9) P. Anton, O. Koberle, and A. Laschewsky, *Makromol. Chem.*, **194**, 1 (1993).
- 10) D. Cochlin, P. Hendlinger, and A. Lachewsky, *Colloid Polym. Soc.*, **273**, 1138 (1995).
- 11) D. J. Keddie, *Chem. Soc. Rev.*, **43**, 496 (2014).
- 12) K. Matyjaszewski and J. Xia, *Chem. Rev.*, **101**, 2921 (2001).
- 13) M. Kamigaito, T. Ando and M. Sawamoto, *Chem. Rev.*, **101**, 3689 (2001).
- 14) Y. Oshibe, H. Ishigaki, H. Ohmura, and T. Yamamoto, *Kobunshi Ronbunshu*, **46**, 81 (1989).
- 15) T. Imae, *Curr. Opin. Colloid Interface Sci.*, **8**, 307 (2003).
- 16) H. Sawada, *Prog. Polym. Sci.*, **32**, 509 (2007).

- 17) H. Sawada, *Chem. Rev.*, **96**, 1779 (1996).
- 18) H. Sawada, Y.-F. Gong, Y. Minoshima, T. Matsumoto, M. Nakayama, M. Kosugi, and T. Migita, *J. Chem. Soc., Chem. Commun.*, 537 (1992).
- 19) H. Sawada, Y. Minoshima, and H. Nakajima, *J. Fluorine Chem.*, **65**, 169 (1992).
- 20) H. Sawada, N. Itoh, T. Kawase, M. Mitani, H. Nakajima, M. Nishida, and Y. Moriya, *Langmuir*, **10**, 994 (1994).
- 21) H. Sawada, K. Tanba, N. Itoh, C. Hosoi, M. Oue, M. Baba, T. Kawase, M. Mitani, and H. Nakajima, *J. Fluorine Chem.*, **77**, 51 (1996).
- 22) J. Nakagawa, K. Kamogawa, H. Sakai, T. Kawase, H. Sawada, J. Manosroi, A. Manosroi, and M. Abe, *Langmuir*, **14**, 2055 (1998).
- 23) J. Nakagawa, K. Kamogawa, N. Momozawa, H. Sakai, T. Kawase, H. Sawada, Y. Sano, and M. Abe, *Langmuir*, **14**, 2061 (1998).
- 24) H. Sawada, K. Ikeno, and T. Kawase, *Macromolecules*, **35**, 4306 (2002).
- 25) H. Sawada and M. Nakayama, *J. Chem. Soc., Chem. Commun.*, 677 (1991).
- 26) H. Sawada, Y. Ikematsu, T. Kawase, and Y. Hayakawa, *Langmuir*, **12**, 3529 (1996).
- 27) H. Sawada, T. Suzuki, H. Takashima, and K. Takishita, *Colloid Polym. Sci.*, **286**, 1569 (2008).
- 28) Y. Goto, H. Takashima, K. Takishita, and H. Sawada, *J. Colloid Interface Sci.*, **362**, 375 (2011).
- 29) H. Takashima, K. Iwaki, R. Furukuwa, K. Takishita, and H. Sawada, *J. Colloid Interface Sci.*, **320**, 436 (2008).
- 30) T. Saito, Y. Tsushima, and H. Sawada, *Colloid Polym. Sci.*, **293**, 65 (2015).
- 31) Y. Oikawa, T. Saito, M. Yamada, M. Sugita, and H. Sawada, *ACS Appl. Mater. Interfaces*, **7**, 13782 (2015).
- 32) W. Zhang, Z. Shi, F. Zhang, X. Liu, J. Jin, and L. Jiang, *Adv. Mater.*, **25**, 2071 (2013).

- 33) S. E. Allan, B. W. Smith, K. A. Anderson, *Environ. Sci. Technol.*, **46**, 2033 (2012).
- 34) A. K. Kota, G. Kwon, W. Choi, J. M. Mabry, and A. Tuteja, *Nature Commun.*, **3**, 1025 (2012).
- 35) S. Parak, E. S. Lee, and W. R. W. Sulaiman, *J. Ind. Eng. Chem.* **21**, 1239 (2015).



## CHAPTER 1

# **Preparation of Fluoroalkyl End-Capped Vinyltrimethoxysilane Oligomeric Silica/Poly(tetrafluoroethylene) Nanocomposites Possessing a Superoleophilic/Superhydrophobic Characteristic: Application to the Separation of Oil and Water**

## 1.1. Introduction

Poly(tetrafluoroethylene) (PTFE), is known as Teflon<sup>TR</sup>, is a thermoplastic material with high chemical inertness, low surface energy, low friction coefficient and non-adhesive property, and is also widely used in practice as good self-lubricating material.<sup>1, 2)</sup> Such low surface energy makes PTFE an ideal candidate for the surface modification of superhydrophobic coatings, of whose coating surface has been defined as water contact angle is higher than 150°, enlarging significantly its application areas like potential self-cleaning, aerospace industry, and low-friction coatings.<sup>3 ~ 11)</sup> There have been a variety of reports for the creation of the superhydrophobic polymers by templating<sup>12 ~ 18)</sup>, etching<sup>19, 20)</sup>, spray coating<sup>21 ~ 27)</sup> and sol-gel method<sup>28, 29)</sup>, so far. Among these methods, the templating is the most convenient for the creation of the superhydrophobic PTFE surface. For example, the filter paper has been used as a template to construct a lotus-leaf structure for providing the superhydrophobic PTFE surface, after removing the template through the sintering process.<sup>30)</sup> The creation of superhydrophobic surface has hitherto been comprehensively studied by using a variety of fluoroalkyl end-capped oligomers  $[R_F-(M)_n-R_F]$ ; M = radical polymerizable monomers;  $R_F$  = fluoroalkyl groups] as key intermediates.<sup>31 ~ 34)</sup> In these fluorinated oligomers, fluoroalkyl end-capped

vinyltrimethoxysilane oligomers  $[\text{R}_\text{F}-(\text{CH}_2\text{CHSi}(\text{OMe})_3)_n-\text{R}_\text{F}]$  ( $\text{R}_\text{F}-(\text{VM})_n-\text{R}_\text{F}$ );  $\text{R}_\text{F} = \text{CF}(\text{CF}_3)\text{OC}_3\text{F}_7$ ;  $n = 2, 3$ ]<sup>35)</sup> can undergo the sol-gel reaction under alkaline conditions to provide the corresponding fluorinated oligomeric silica nanoparticles  $[\text{R}_\text{F}-(\text{VM}-\text{SiO}_2)_n-\text{R}_\text{F}]$ .<sup>36)</sup> Especially, the modified glass surface treated with these fluorinated oligomeric silica nanoparticles can exhibit the completely superhydrophobic characteristic (water contact angle value:  $180^\circ$ ) with a good oleophobicity.<sup>36)</sup>  $\text{R}_\text{F}-(\text{VM})_n-\text{R}_\text{F}$  oligomer can also undergo the similar sol-gel reactions in the presence of biphenylene unit-containing silane coupling agent  $[\text{Ar}-\text{Si}(\text{OEt})_3]$  to afford the  $\text{R}_\text{F}-(\text{VM}-\text{SiO}_2)_n-\text{R}_\text{F}/\text{Ar}-\text{SiO}_2$  nanocomposites.<sup>37)</sup> It was demonstrated that these nanocomposites provide the superamphiphobic characteristic on the modified glass surface.<sup>37)</sup> In this way,  $\text{R}_\text{F}-(\text{VM})_n-\text{R}_\text{F}$  oligomer is effective for controlling the surface morphology by the encapsulation of the guest molecule such as the specified silane coupling agent into the corresponding fluorinated oligomeric silica nanoparticle  $[\text{R}_\text{F}-(\text{VM}-\text{SiO}_2)_n-\text{R}_\text{F}]$  cores. The encapsulation of PTFE fine particles into the  $\text{R}_\text{F}-(\text{VM}-\text{SiO}_2)_n-\text{R}_\text{F}$  oligomeric nanoparticle cores is of particular interest, from the developmental viewpoints of new fluorinated oligomeric materials possessing an excellent surface active properties imparted by PTFE. This chapter shows that  $\text{R}_\text{F}-(\text{VM})_n-\text{R}_\text{F}$  oligomer can cause the sol-gel reaction in the presence of PTFE fine particles under alkaline

conditions to supply the corresponding fluorinated oligomeric silica/PTFE nanocomposites.

Interestingly, the obtained nanocomposites were found to exhibit a supeoleophilic/superhydrophobic characteristic on the modified glass, PTFE sheet and filter paper surfaces, respectively; although the oleophobic PTFE units are incorporated into the composite matrices. In contrast, the modified glass surface treated with the  $R_F-(VM-SiO_2)_n-R_F$  oligomeric nanoparticles and the original PTFE sheet surface provide the oleophobic/superhydrophobic and the usual oleophobic/hydrophobic characteristics, respectively. More interestingly, the modified filter paper treated with the  $R_F-(VM-SiO_2)_n-R_F/PTFE$  nanocomposites were applied to the oil/water separation membrane, and the fluorinated nanocomposite powders thus obtained were also applied to the packing material for column chromatography to separate not only the mixture of oil/water but also the W/O emulsions. These results will be described in this chapter.

## **1.2. Experimental**

### **1.2.1 Measurements**

Dynamic light scattering (DLS) measurements were measured by using Otsuka Electronics DLS-7000 HL (Tokyo, Japan). Thermal analyses were recorded on Bruker axs TG-DTA2000SA differential thermobalance (Kanagawa, Japan). Contact angles were measured using a Kyowa Interface Science Drop Master 300 (Saitama, Japan). Field emission scanning electron micrographs (FE-SEM) were obtained by using JEOL JSM-7000F (Tokyo, Japan). Dynamic force microscope (DFM) was recorded by using SII Nano Technology Inc. E-sweep (Chiba, Japan). Optical and fluorescence microscopies were measured by using OLYMPUS Corporation BX51 (Tokyo, Japan).

### **1.2.2. Materials**

PTFE fine particles with an average particle size of 282 nm (20 % aqueous dispersed solution: KD-500 AS<sup>TR</sup>) were obtained from Kitamura Limited (Aichi, Japan) and used as received. Span 80 (sorbitan monooleate) was purchased from Tokyo Chemical Industrial

Co., Ltd. (Tokyo, Japan). Toluene, 1, 2-dichloroethane and 25 wt % ammonia were provided by Wako Pure Chemical Industries (Osaka, Japan). Fluoroalkyl end-capped vinyltrimethoxysilane oligomer was prepared according to the previously reported method.<sup>35)</sup> Glass plate (borosilicate glass) [micro cover glass: 18 mm x 18 mm] was purchased from Matunami glass Ind. Ltd. (Osaka, Japan) and was used after washing well with 1, 2-dichloroethane. Filter paper (Advantec 131) and PTFE sheet were received from Advantec Toyo Kaisha, Ltd. (Tokyo, Japan) and AS ONE Corporation (Osaka, Japan), respectively.

### **1.2.3. Preparation of fluoroalkyl end-capped vinyltrimethoxysilane oligomeric silica/PTFE nanocomposites [R<sub>F</sub>-(VM-SiO<sub>2</sub>)<sub>n</sub>-R<sub>F</sub>/PTFE]**

A typical procedure for the preparation of nanocomposites is as follows: To methanol solution (5.0 ml) containing fluoroalkylated vinyltrimethoxysilane oligomer [300 mg; R<sub>F</sub>-(CH<sub>2</sub>CHSi(OMe)<sub>3</sub>)<sub>n</sub>-R<sub>F</sub>; R<sub>F</sub> = CF(CF<sub>3</sub>)OC<sub>3</sub>F<sub>7</sub>; Mn = 730 (R<sub>F</sub>-(VM)<sub>n</sub>-R<sub>F</sub> oligomer) and 20 wt % aqueous well-dispersed PTFE particle (25 mg) solution (125 mg) was added 25 % aqueous ammonia solution (2.0 ml). The mixture was stirred with a magnetic stirring bar at room temperature for 5 h. Methanol was added to the obtained crude products after the

solvent was evaporated off. The methanol suspension was stirred with magnetic stirring bar at room temperature for 1 day. The fluorinated oligomeric silica/PTFE nanocomposites were isolated after centrifugal separation for 30 min. The nanocomposite product was washed well with methanol several times, and then was dried under vacuum at 50 °C for 1 day to afford the expected nanocomposites as white powders (190 mg) (see Scheme 1-1).

#### **1.2.4. Preparation of the modified glass treated with the $R_F-(VM-SiO_2)_n-R_F$ /PTFE nanocomposites by dipping method**

To methanol solution (5.0 ml) containing  $R_F-(VM)_n-R_F$  oligomer (300 mg) was added 20 wt % aqueous well-dispersed PTFE particle solution (125 mg) and 25 % aqueous ammonia solution (2.0 ml). The mixture was stirred with a magnetic stirring bar at room temperature for 5 h. The glass plates (18 x 18 mm<sup>2</sup> pieces) were dipped into this methanol solution at room temperature and left for 1 min. These were lifted from the solution at constant rate and dried at room temperature for 1 day under vacuum to afford the modified glass. The modified filter papers (25 x 25 mm<sup>2</sup> pieces) and PTFE sheet (25 x 25 mm<sup>2</sup> pieces) were prepared under similar conditions. The contact angle values for dodecane and water were measured by depositing a drop of dodecane (2 μl) or water (2 μl) on the

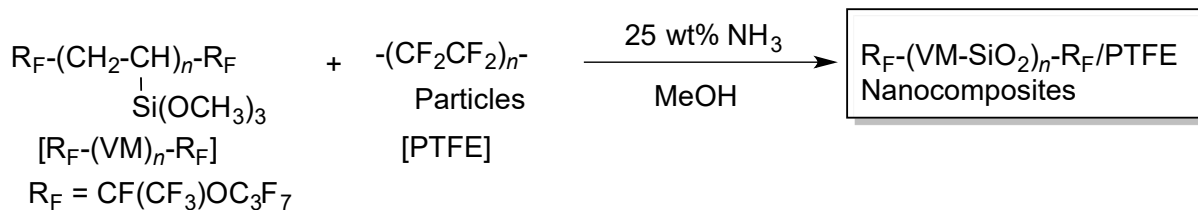
modified plate surfaces.



### 1.3. Results and discussion

#### 1.3.1. Preparation and thermal stability of the $R_F-(VM-SiO_2)_n-R_F/PTFE$ nanocomposites

Sol-gel reaction of fluoroalkyl end-capped vinyltrimethoxysilane oligomer  $[R_F-(CH_2CHSi(OMe)_3)_n-R_F]$ ;  $R_F = CF(CF_3)OC_3F_7$  ( $R_F-(VM)_n-R_F$  oligomer)] proceeded smoothly in the presence of poly(tetrafluoroethylene) (PTFE) fine particles under alkaline conditions to afford the corresponding fluorinated oligomeric silica/PTFE nanocomposites  $[R_F-(VM-SiO_2)_n-R_F/PTFE]$ . These results are shown in Scheme 1-1 and Table 1-1.



Scheme 1-1 Preparation of  $R_F-(VM-SiO_2)_n-R_F/PTFE$  nanocomposites

Table 1-1 Preparation of  $R_F-(VM-SiO_2)_n-R_F$ /PTFE Nanocomposites

Run	$R_F-(VM)_n-R_F$ (mg)	PTFE (mg)	MeOH (ml)	25 % $NH_3$ (ml)	Yield <sup>a)</sup> (%)	Size of Composites <sup>b)</sup> (nm)
1	300	25	5	2	58	$46.1 \pm 9.5$
2	300	50	5	2	59	$55.7 \pm 12.3$
3	300	100	5	2	61	$54.8 \pm 5.0$
4	300	200	5	2	58	$40.8 \pm 2.6$
5	300	300	5	2	65	$41.6 \pm 3.8$
Original PTFE						$282 \pm 29$

a) Yields were based on  $R_F-(VM)_n-R_F$  oligomer and PTFE fine particles.

b) Determined by dynamic light scattering (DLS) measurements in methanol.

As shown in Scheme 1-1 and Table 1-1, the expected composites were obtained in 58 ~ 65 % isolated yields. Fluorinated composites thus obtained were found to exhibit a good dispersibility and stability in traditional organic media such as methanol, 2-propanol, tetrahydrofuran, 1, 2-dichloroethane, *N,N*-dimethylformamide, and fluorinated aliphatic solvents [1 : 1 mixed solvents (AK-225<sup>TR</sup>) of 1, 1-dichloro-2, 2, 3, 3, 3-pentafluoropropane and 1, 3-dichloro-1, 2, 2, 3, 3-pentafluoropropane] except for water; although the parent PTFE particles have no dispersibility and stability in these solvents. Thus, the size of these fluorinated composites illustrated in Table 1-1 was measured in methanol by dynamic light-scattering (DLS) measurements at 25 °C. Each size of these fluorinated composites was found to be nanometer size-controlled fine particles: 41 ~ 56 nm (number-average diameter) as shown in Table 1-1.

FE-SEM photograph of the  $R_F-(VM-SiO_2)_n-R_F$ /PTFE nanocomposites (Run 1 in

Table 1-1) methanol solutions was recorded. The FE-SEM measurements of parent PTFE particles were also measured under similar conditions, for comparison. These results are shown in Fig. 1-1.

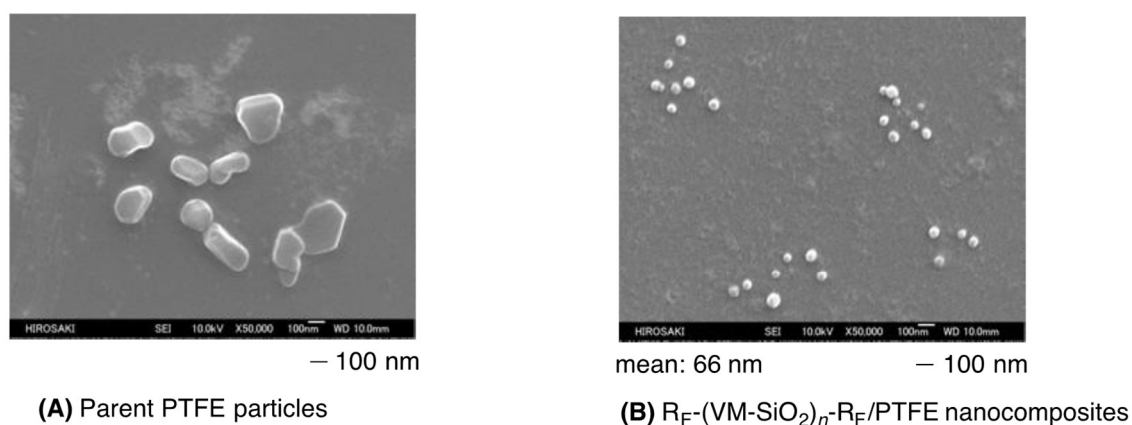


Fig. 1-1 FE-SEM (field emission scanning electron microscopy) image of the parent PTFE particles (A) and the  $R_F-(VM-SiO_2)_n-R_F/PTFE$  nanocomposites (Run 1 in Table 1-1) (B) in methanol solutions

Electron micrograph also showed the formation of fluorinated nanocomposite fine particles with a mean diameter of 66 nm, and the similar size value ( $46.1 \pm 9.5$  nm) to that of FE-SEM measurements was observed in DLS measurements (see Run 1 in Table 1-1). On the other hand, the size of the parent PTFE particles are higher than that of the  $R_F-(VM-SiO_2)_n-R_F/PTFE$  nanocomposites. This finding would be due to the coagulation or agglomeration of the original PTFE particles, and the original PTFE particles are unable to show the primary ones.

To verify the presence of the PTFE in the nanocomposites, the thermal stability of

the fluorinated nanocomposites in Table 1-1 was studied by thermogravimetric analyses, in which the weight loss of these composites was measured by raising the temperature around 800 °C (the heating rate: 10 °C min<sup>-1</sup>) in air atmosphere, and the results are shown in Fig. 1-2.

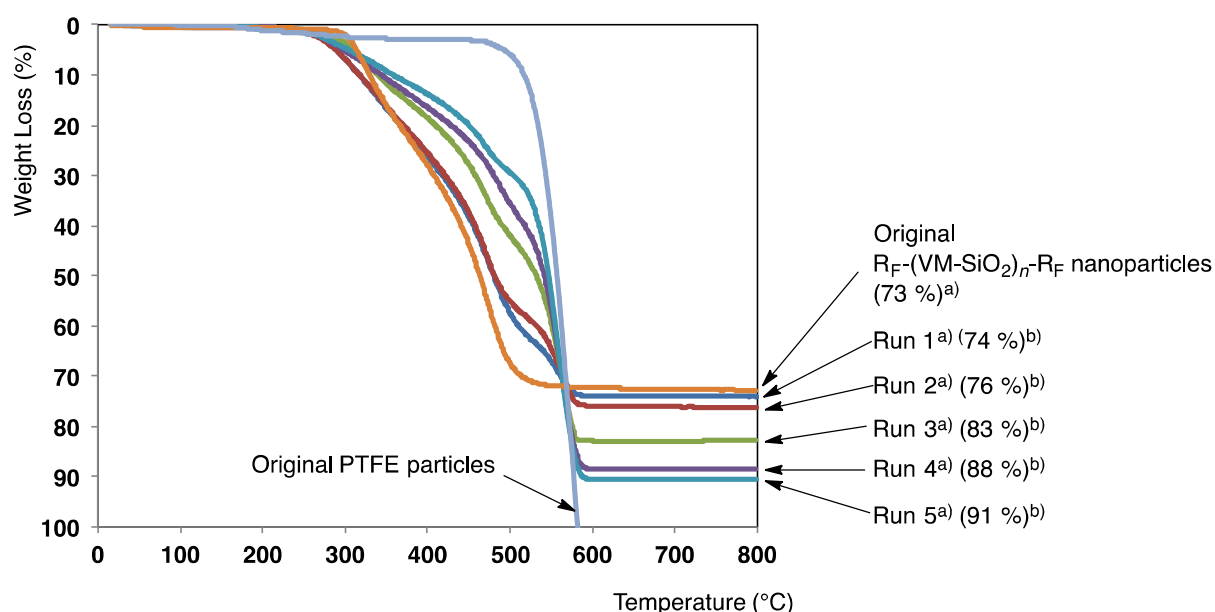


Fig. 1-2 Thermogravimetric analyses (TGA) of the  $R_F-(VM-SiO_2)_n-R_F$ /PTFE nanocomposites and the  $R_F-(VM-SiO_2)_n-R_F$  nanoparticles

- a) Each Run No. corresponds to that of Table 1-1  
b) Weight Loss at 800 °C

As shown in Fig. 1-2, the original PTFE particles give the perfect weight loss around 600 °C. The parent  $R_F-(VM-SiO_2)_n-R_F$  oligomeric nanoparticles, which were prepared by the sol-gel reaction of the  $R_F-(VM)_n-R_F$  oligomer under alkaline conditions in Scheme 1-1, afforded the 73 % weight loss around at 530 °C, owing to the partial formation

of silica gel during the calcination process. In contrast, the  $R_F-(VM-SiO_2)_n-R_F/PTFE$  nanocomposites (Runs 1 ~ 5 in Table 1-1) were found to provide the weight loss behavior in proportion to the contents of the PTFE in the nanocomposites after calcination at 800 °C, and the contents of the PTFE in the nanocomposites were estimated to be from 1 to 18 %.

### **1.3.2. Surface modification of glass, PTFE sheet and filter paper by the use of the $R_F-(VM-SiO_2)_n-R_F/PTFE$ nanocomposites**

It was previously reported that  $R_F-(VM-SiO_2)_n-R_F$  oligomeric nanoparticles are applicable to surface modification of glass to exhibit the oleophobic/superhydrophobic characteristic on the surface.<sup>36)</sup> The present  $R_F-(VM-SiO_2)_n-R_F/PTFE$  nanocomposites have been also applied to the surface modification of glass under similar conditions, and the dodecane and water contact angles on the modified glass surfaces were measured. These results are shown in Table 1-2.

Table 1-2 Contact angle values of dodecane and water on the modified glasses, PTFE sheets and filter papers treated with the  $R_F-(VM-SiO_2)_n-R_F$ /PTFE nanocomposites

Run <sup>a)</sup>	Contact Angle (degree)							
	Dodecane <sup>b)</sup>	Water <sup>c)</sup> (time)						
		0	5	10	15	20	25	30 (min)
1	0	180	-d)	-	-	-	-	-
2	0	180	-d)	-	-	-	-	-
3	0	180	-d)	-	-	-	-	-
4	0	180	-d)	-	-	-	-	-
5	0	180	-d)	-	-	-	-	-
Parent $R_F-(VM-SiO_2)_n-R_F$	48 <sup>e)</sup>	180	-d)	-	-	-	-	-
	73 <sup>f)</sup>	180	-d)	-	-	-	-	-
	21 <sup>g)</sup>	180	-d)	-	-	-	-	-
Non-treated glass	0	50						
Non-treated PTFE	33	113						

a) Each Run No. corresponds to that of Table 1-1

b) Each modified surface shows the same dodecane contact angle value.

c) Each modified surface shows the same water contact angle value.

d) The same water contact angle values to that of the initial time (0 min) was observed during 5 to 30 min.

e) Modified glass surface

f) Modified PTFE sheet surface

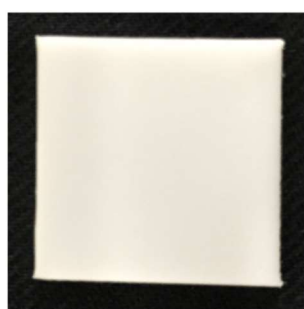
g) Modified filter paper surface

As mentioned above, dodecane and water contact angle values on the modified glass surface treated with the  $R_F-(VM-SiO_2)_n-R_F$  oligomeric nanoparticles are 48° and 180°, respectively.<sup>36)</sup> However, interestingly, the present  $R_F-(VM-SiO_2)_n-R_F$ /PTFE nanocomposites were found to provide a superoleophilic/superhydrophobic characteristic on each modified surface; because the dodecane and water contact angle values are 0° and 180° on each surface, respectively; although the oleophobic PTFE units are surely incorporated into the present nanocomposite matrices. In fact, the original PTFE sheet surface provides the usual oleophobic/hydrophobic property (water and dodecane contact

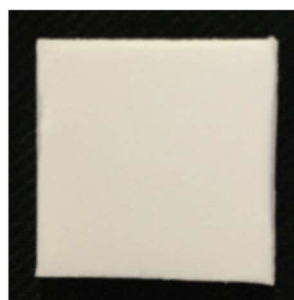
angles are 33° and 113°) (see Table 1-2).

Next, the surface modification of the PTFE sheet was tried by the use of the present  $R_F-(VM-SiO_2)_n-R_F$ /PTFE nanocomposites (Run 5 in Table 1-1).

In general, we have some difficulties to have the surface modification of the PTFE sheet due to the strong hydrophobic/oleophobic property on the surface.<sup>30)</sup> However, as shown in Fig. 1-3, the uniformly modified surface has been prepared by using the present nanocomposites.



**(A)** Parent PTFE sheet



**(B)** Modified PTFE sheet treated with the  $R_F-(VM-SiO_2)_n-R_F$ /PTFE nanocomposites

Fig. 1-3 Photograph of the parent PTFE sheet **(A)** and the modified PTFE sheet treated with the  $R_F-(VM-SiO_2)_n-R_F$ /PTFE nanocomposites (Run 5 in Table 1-1) **(B)**

This good adhesion ability toward the PTFE surface would be due to the oligomeric structures, which possess a few trimethoxysilyl  $[-Si(OMe)_3]$  units in the oligomeric main chain, quite different from the traditional monomeric fluoroalkylated silane coupling agents  $[R_F-CH_2CH_2Si(OMe)_3]$ ;  $R_F$  = longer fluoroalkyl groups]. Each modified PTFE sheet surface

treated with the nanocomposites depicted in Table 1-1 was found to supply the similar superoleophilic/superhydrophobic property (dodecane and water contact angle values are  $0^\circ$  and  $180^\circ$ , respectively) to that of the modified glass surfaces (see Table 1-2).

A similar superoleophilic/superhydrophobic characteristic behavior was observed on the modified filter papers treated with the present nanocomposites (see Table 1-2).

Superhydrophobic surface is in general realized by enhancing the surface roughness.<sup>38~41)</sup> Thus, FE-SEM measurements were used to study on the surface roughness of the modified glasses treated with the parent  $R_F-(VM-SiO_2)_n-R_F$  oligomeric nanoparticles, and with the  $R_F-(VM-SiO_2)_n-R_F/PTFE$  nanocomposites, of whose modified surfaces can exhibit an oleophobic/superhydrophobic property (dodecane and water contact angles:  $48^\circ$  and  $180^\circ$ ; see Table 1-2) and a superoleophilic/superhydrophobic characteristic (water and dodecane contact angles:  $0^\circ$  and  $180^\circ$ : Runs 1 ~ 5 in Table 1-2), respectively. These results are shown in Fig. 1-4.



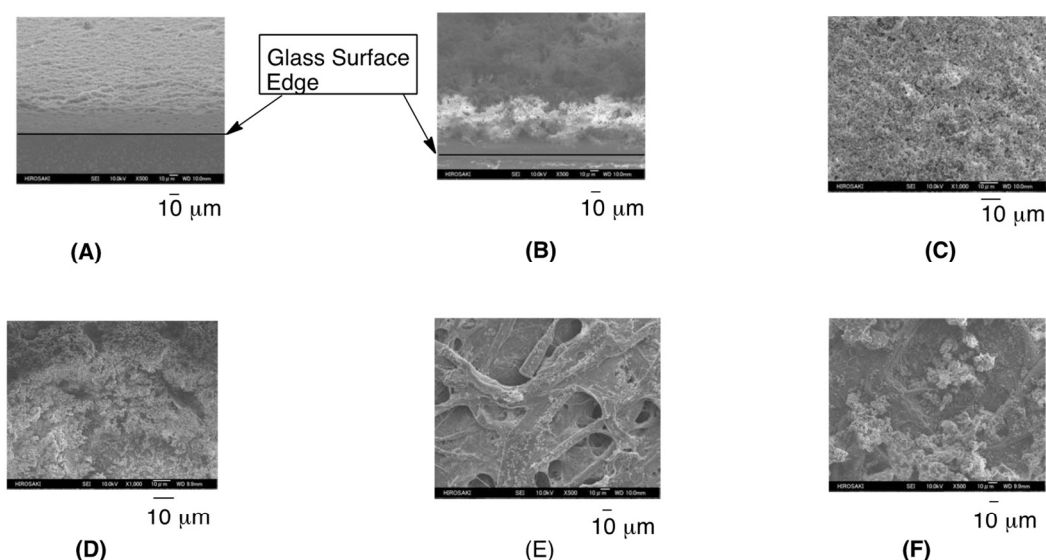


**Fig. 1-4** FE-SEM (field emission scanning electron microscopy) images of the modified glass surface treated with the  $R_F-(VM-SiO_2)_n-R_F$  nanoparticles **(A)**, the modified glass surface treated with the  $R_F-(VM-SiO_2)_n-R_F/PTFE$  nanocomposites (Run 1 in Table 1-1) **(B)**, the modified PTFE sheet surface treated with the  $R_F-(VM-SiO_2)_n-R_F$  nanoparticles **(C)**, the modified PTFE sheet surface treated with the  $R_F-(VM-SiO_2)_n-R_F/PTFE$  nanocomposites (Run 1 in Table 1-1) **(D)**, the modified filter paper surface treated with the  $R_F-(VM-SiO_2)_n-R_F$  nanoparticles **(E)**, and the modified filter paper surface treated with the  $R_F-(VM-SiO_2)_n-R_F/PTFE$  nanocomposites (Run 1 in Table 1-1) **(F)**

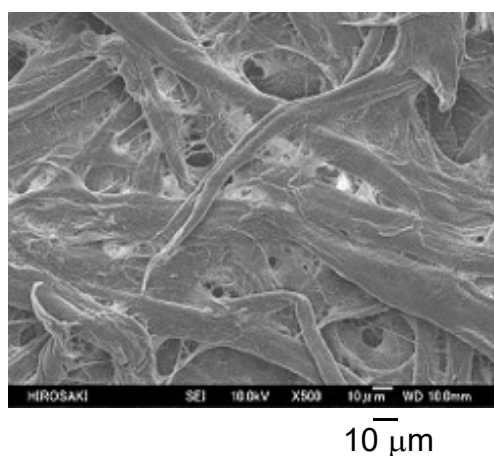


**Fig. 1-5** FE-SEM (field emission scanning electron microscopy) image of the original filter paper

As shown in Figs. 4-(B), 4-(D), and 4-(F), the architecture of the effective roughness was observed on the modified glass, PTFE sheet and filter paper surfaces treated with the  $R_F-(VM-SiO_2)_n-R_F/PTFE$  nanocomposites, compared with those (Figs. 1-4-(A),

1-4-(C), and 1-4-(E) of the parent  $R_F-(VM-SiO_2)_n-R_F$  oligomeric nanoparticles and the original filter paper (Fig. 1-5).

The DFM (dynamic force microscopy) measurements of the modified glass, PTFE sheet and the filter paper surfaces treated with the  $R_F-(VM-SiO_2)_n-R_F$ /PTFE nanocomposites have been also studied, and the results are shown in Fig. 1-6.

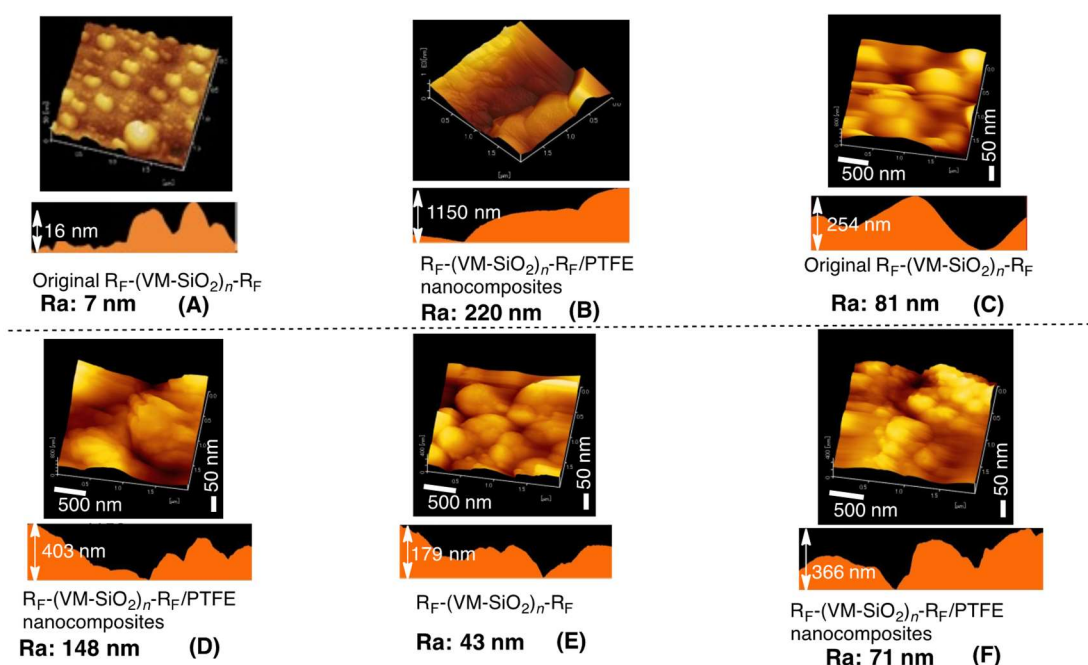


Fig. 1-6 DFM (dynamic force microscopy) topographic images of of the modified glass surface treated with the  $R_F-(VM-SiO_2)_n-R_F$  nanoparticles (A), the modified glass surface treated with the the  $R_F-(VM-SiO_2)_n-R_F$ /PTFE nanocomposites (Run 1 in Table 1-1) (B), the modified PTFE sheet surface treated with the  $R_F-(VM-SiO_2)_n-R_F$  nanoparticles (C), the modified PTFE sheet surface treated with the  $R_F-(VM-SiO_2)_n-R_F$ /PTFE nanocomposites (Run 1 in Table 1-1) (D), the modified filter paper surface treated with the  $R_F-(VM-SiO_2)_n-R_F$  nanoparticles (E), and the modified filter paper surface treated with the  $R_F-(VM-SiO_2)_n-R_F$ /PTFE nanocomposites (Run 1 in Table 1-1) (F)

Fig. 1-6-(B), 1-6-(D), and 1-6-(F) show that the topographical image of each surface can provide a roughness characteristic, and the roughness average values: Ra (220 nm, 148

nm and 71 nm) of the modified glass, PTFE sheet and filter paper surfaces possessing the superoleophilic/superhydrophobic characteristic (dodecane and water contact angles:  $0^\circ$  and  $180^\circ$ ) are extremely higher than those ( $R_a$ : 7 nm, 81 nm and 43 nm) of the modified glass surface (dodecane and water contact angle values:  $48^\circ$  and  $180^\circ$ ), the modified PTFE sheet (dodecane and water contact angle values:  $73^\circ$  and  $180^\circ$ ) and the modified filter paper (water and dodecane contact angle values:  $21^\circ$  and  $180^\circ$ ) treated with the  $R_F-(VM-SiO_2)_n-R_F$  oligomeric nanoparticles (see Figs. 1-6-(A), 1-6-(C) and 1-6-(E), and Table 1-2).

These findings suggest that the nanocomposites containing PTFE particles are essential to the architecture of rough surface. Especially, the  $R_F-(VM-SiO_2)_n-R_F$ /PTFE nanocomposite particles are effective for the fabrication of the superoleophilic and superhydrophobic fractal surface. Such higher roughness surface would be likely to interact with oils such as dodecane possessing the lower surface tension than that of water to exhibit the superoleophilic characteristic, because an oil droplet could easily penetrate the very small orifice between the composite particles. On the other hand, the fluoroalkyl groups in the  $R_F-(VM-SiO_2)_n-R_F$ /PTFE nanocomposites should be regularly arranged on the modified roughness surface to exhibit the superhydrophobic characteristic.

### **1.3.3. Separation of oil and water by the use of the $R_F-(VM-SiO_2)_n-R_F/PTFE$ nanocomposites**

The superoleophilic surface has in general a strong affinity toward oils. Thus, the surfaces possessing the superoleophilic/superhydrophobic characteristic can simultaneously repels water and strongly absorbs oils. Such behavior should be applicable to the oil/water separating materials.<sup>42 ~ 45)</sup> Thus, the separation of the mixture of the blue-colored water (water was colored with  $CuSO_4 \cdot 5H_2O$ ) and 1, 2-dichloroethane was tried by using the modified filter paper treated with the  $R_F-(VM-SiO_2)_n-R_F/PTFE$  nanocomposites (Run 1 in Table 1-1) as the liquid-liquid separation membrane. The original non-treated filter paper was also used as the liquid-liquid separation membrane under similar conditions, for comparison. These results are shown in Fig. 1-7.

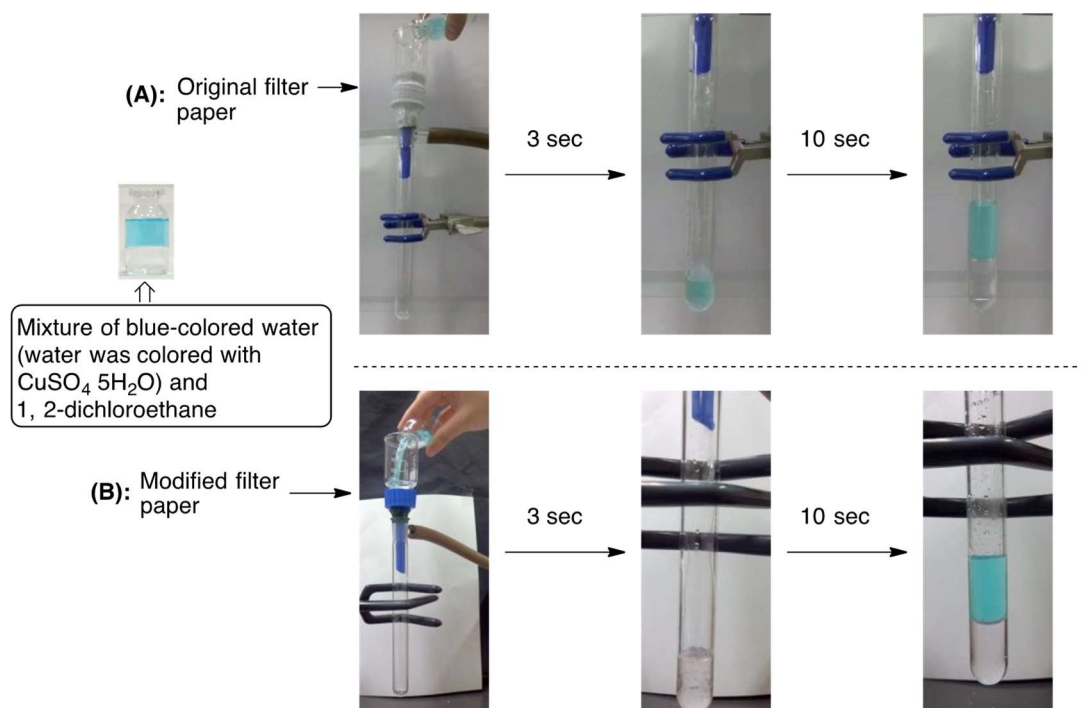


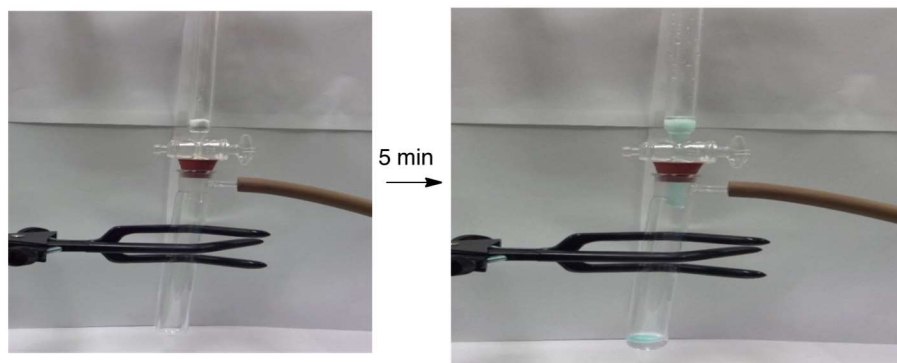
Fig. 1-7 Separation of the mixture of blue-colored water and 1, 2-dichloroethane by using the original filter paper: **(A)** and the modified filter paper treated with the  $R_F-(VM-SiO_2)_n-R_F/PTFE$  nanocomposites (Run 1 in Table 1-1): **(B)** under reduced pressure

As shown in Fig. 1-7-(A), the mixture of oil/water was unable to separate under reduced pressure conditions by the use of the original non-treated filter paper. On the other hand, the colorless oil was smoothly isolated in 3 seconds under reduced pressure due to its superoleophilic/superhydrophobic characteristic illustrated in Fig. 1-7-(B). However, the blue-colored water flowed into the isolated colorless oil after 10 seconds due to the separation process under the reduced pressure.

The present  $R_F-(VM-SiO_2)_n-R_F/PTFE$  nanocomposites depicted in Scheme 1-1 and Table 1-1 are white-colored particle powders. Especially, the modified glass surface treated with the well-dispersed  $R_F-(VM-SiO_2)_n-R_F/PTFE$  nanocomposites powders (Run 5 in Table

1-1) methanol solutions through the casting technique was found to exhibit the same superoleophilic (dodecane contact angle:  $0^\circ$ )/superhydrophobic characteristic (water contact angle:  $180^\circ$ ) to those of the Table 1-2. Thus, the present nanocomposite powders were applied to the packing materials for the column chromatography to separate not only the mixture of the blue-colored water and colorless oil illustrated in Fig. 1-7 but also the water-in-oil (W/O) emulsions. The surfactant (span 80: 30.0 mg)-stabilized water (0.05 ml)-in-oil (1, 2-dichloroethane: 5.00 ml) (W/O) emulsion and span 80 (30.0 mg)-stabilized water (0.05 ml)-in-oil (toluene: 5.00 ml) (W/O) emulsion were prepared under ultrasonic conditions for 5 min at room temperature. The  $R_F\text{-(VM-SiO}_2)_n\text{-R}_F$ /PTFE nanocomposites (Run 1 in Table 1-1) were applied to the packing material for the separation of the mixture of the blue-colored water/colorless oil and the W/O emulsions. Silica gel (Wakogel C-500HG<sup>TR</sup>) was also applied to the packing material under similar conditions, for comparison, since the silica gel is useful for the packing material for the column chromatography. These results are shown in Figs. 1-8 ~ 1-10.

**(A):** Wakogel C-500HG<sup>TR</sup>



**(B):**  $R_F-(VM-SiO_2)_n-R_F$ /PTFE nanocomposites

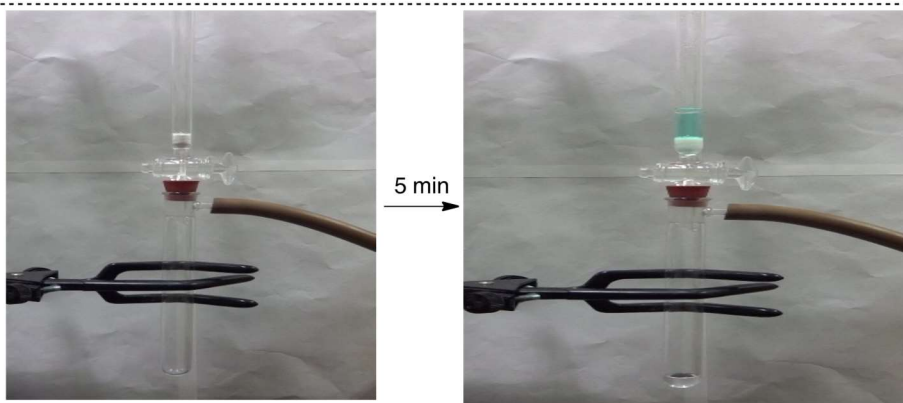


Fig. 1-8 Separation of the mixture of water and 1, 2-dichloroethane by using Wakogel C-500HG<sup>TR</sup>: **(A)** and the  $R_F-(VM-SiO_2)_n-R_F$ /PTFE nanocomposite powders (Run 1 in Table 1-1): **(B)**

As shown in Fig. 1-8-(A), the silica gel was not effective for the packing material to separate the mixture of the blue-colored water and colorless oil under reduced pressure conditions. However, interestingly, it was demonstrated that the present  $R_F-(VM-SiO_2)_n-R_F$ /PTFE nanocomposites are effective for the separation of the mixture of the blue-colored water and colorless oil, and only transparent colorless oil has been isolated under reduced pressure. The contamination of blue-colored water into the oil phase was not observed in 5 min [see Fig. 1-8-(B)].

Furthermore, the W/O emulsions were tried to separate by using the

$R_F-(VM-SiO_2)_n-R_F/PTFE$  nanocomposites. As shown in Fig. 1-9-(**B**), the nanocomposites are effective for the separation of water-in-oil (1, 2-dichloroethane) emulsion under reduced pressure to isolate the colorless oil (1, 2-dichloroethane). Similarly, water-in-oil (toluene) emulsion was smoothly separated by using the  $R_F-(VM-SiO_2)_n-R_F/PTFE$  nanocomposites as the packing material to isolate the colorless oil (toluene) [see Fig.1- 10-(**B**)].

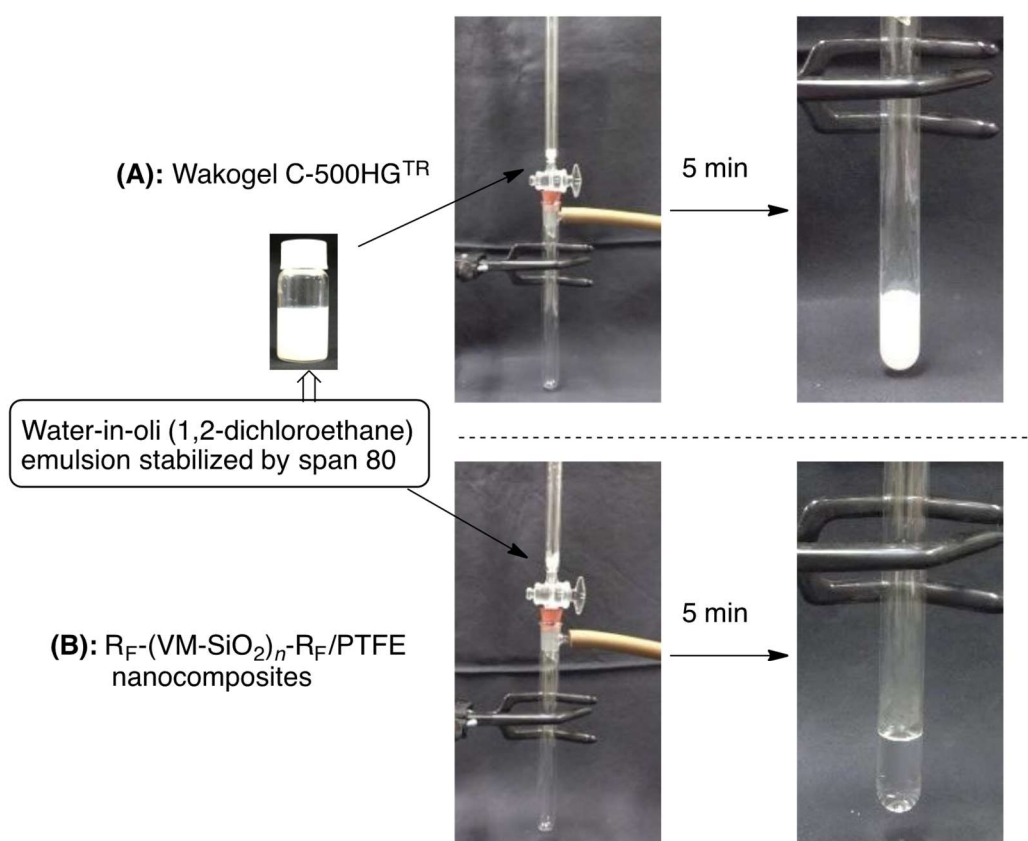


Fig. 1-9 Separation of the water-in-oil (oil: 1,2-dichloroethane) by using Wakogel C-500HG<sup>TR</sup>: (**A**) and the  $R_F-(VM-SiO_2)_n-R_F/PTFE$  nanocomposite powders (Run 1 in Table 1-1): (**B**) under reduced pressure



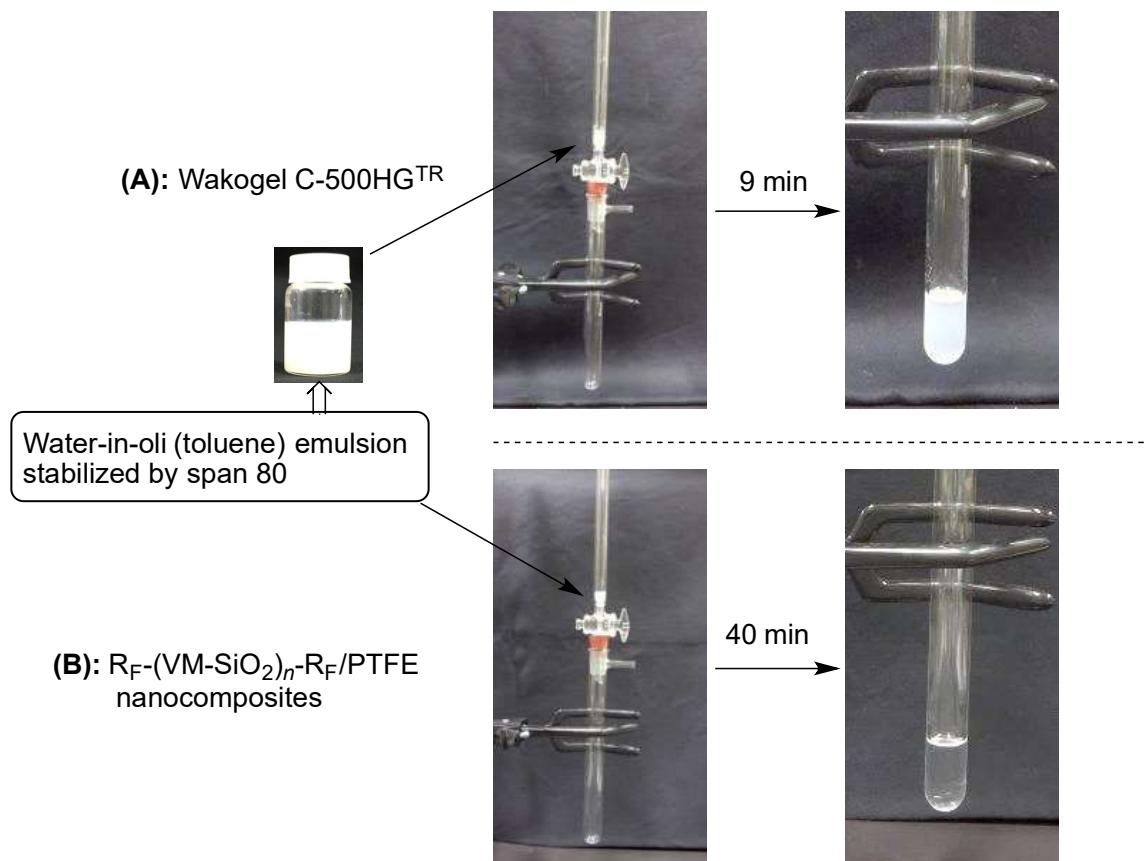


Fig.1-10 Separation of the water-in-oil (oil: toluene) by using Wakogel C-500HG<sup>TR</sup>: **(A)** and the R<sub>F</sub>-(VM-SiO<sub>2</sub>)<sub>n</sub>-R<sub>F</sub>/PTFE nanocomposite powders (Run 1 in Table 1-1): **(B)** under reduced pressure

On the other hand, the silica gel (Wakogel C-500HG<sup>TR</sup>) was unable to separate these emulsions under similar conditions in each case [see Figs. 1-9-(A) and 1-10-(A)]. As shown in Figs. 1-11 and 1-12, optical micrograph also showed that the water droplet cannot be detected at all in the isolated colorless oil in each case, although we can easily detect the water droplet in the W/O emulsions which flowed out from the column chromatography by using the silica gel (Wakogel C500-HG<sup>TR</sup>) as the packing material.

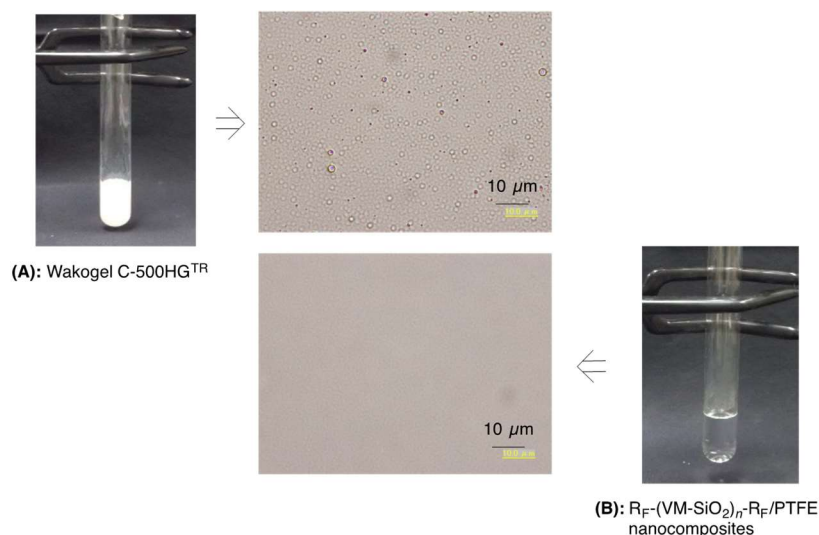


Fig. 1-11 Optical microscopy images of the eluent after the separation of the W/O (oil: 1,2-dichloroethane) emulsion by using the column chromatography with Wakogel C500-HG<sup>TR</sup> (A) and the R<sub>F</sub>-(VM-SiO<sub>2</sub>)<sub>n</sub>-R<sub>F</sub>/PTFE nanocomposites (Run 1 in Table 1-1) (B) under reduced pressure conditions

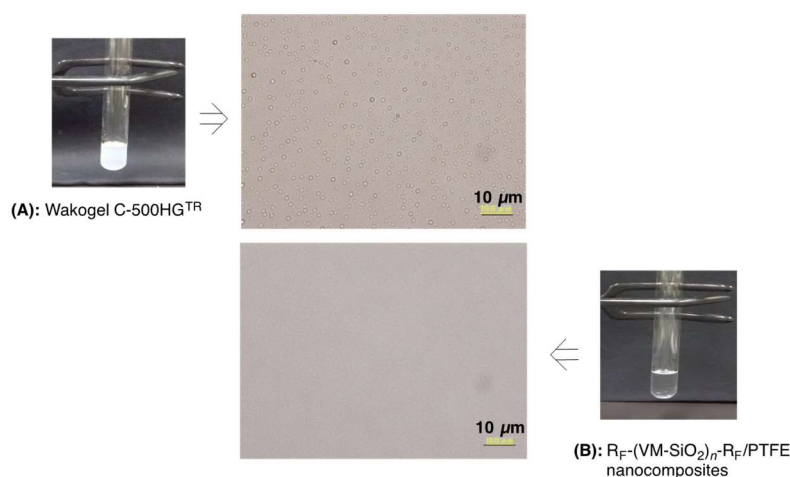


Fig. 1-12 Optical microscopy images of the eluent after the separation of the W/O (oil: toluene) emulsion by using the column chromatography with Wakogel C500-HG<sup>TR</sup> (A) and the R<sub>F</sub>-(VM-SiO<sub>2</sub>)<sub>n</sub>-R<sub>F</sub>/PTFE nanocomposites (Run 1 in Table 1-1) (B) under reduced pressure conditions

The reusability was studied for the present nanocomposite particles as not only the separation membrane for the mixture of oil/water but also the packing material for the W/O emulsions, and the results are shown in Table 1-3.

Table 1-3 Recovery rate of the separated oil from the mixture of water and 1,2-dichloroethane, the W/O (oil: 1,2-dichloroethane) emulsion, and the W/O (oil: toluene) emulsion by using the  $R_F-(VM-SiO_2)_n-R_F/PTFE$  nanocomposites (Run 1 in Table 1-1) as the packing material

Cycle	Recovery rate (%)		
	Mixture of water and 1,2-dichloroethane	W/O (oil: 1,2-dichloroethane) emulsion	W/O (oil: toluene) emulsion
1	94	80	95
2	76	83	82
3	80	76	80
4	76	80	84
5	73	80	81

Table 1-3 shows that the colorless oils were quantitatively isolated under similar conditions even after the use of the mixture of the blue-colored water and oil, and the W/O emulsions five times.

In this way, it was clarified that two kinds of W/O emulsions; one is the oil such as 1,2-dichloroethane, of whose specific gravity is higher than water and the other (toluene) is lower than water can be easily separated by using the  $R_F-(VM-SiO_2)_n-R_F/PTFE$  nanocomposites. Therefore, the present nanocomposites possessing a superoleophilic/superhydrophobic characteristic could open new developments in the separation of oil and water.

#### 1.4. Conclusion

It was demonstrated that fluoroalkyl end-capped vinyltrimethoxysilane oligomer  $[R_F-(VM)_n-R_F]$  is effective for the preparation of the corresponding fluorinated oligomeric silica/poly(tetrafluoroethylene) (PTFE) nanocomposites through the sol-gel reaction of the  $R_F-(VM)_n-R_F$  oligomer in the presence of PTFE fine particles under alkaline conditions. The  $R_F-(VM-SiO_2)_n-R_F/PTFE$  nanocomposites thus obtained were applied to the surface modification of not only glass but also PTFE sheet and filter paper to provide the superoleophilic/superhydrophobic characteristic on these modified surfaces; although the oleophobic PTFE units are certainly incorporated into the nanocomposite matrices. PTFE is well known to possess oil- and water-repellent properties.<sup>1, 2)</sup> Thus, we have some difficulties to develop the surface modification of PTFE, quite different from the traditional hydrocarbon polymers. However, it was verified that the present  $R_F-(VM-SiO_2)_n-R_F/PTFE$  nanocomposites are effective for the surface modification of the PTFE sheet through the simple sol-gel technique under room temperature. Moreover, the modified filter paper treated with the  $R_F-(VM-SiO_2)_n-R_F/PTFE$  nanocomposites possessing the superoleophilic/superhydrophobic characteristic was applicable to the separation membrane for the mixture of oil/water. Especially, the W/O emulsions can be separated by using the

$R_F-(VM-SiO_2)_n-R_F/PTFE$  nanocomposites as the packing materials for the column chromatography to isolate the transparent colorless oil from the W/O emulsions. Of particular interest, it was clarified that the present nanocomposite particle powders possess a good reusability for the packing materials even after 5 times. There has been an important worldwide problem for the oil/water separation in the area of industrial production, environmental protection and energy conservation; because, accidents of ships in the sea can often result in release of spill oil in seawater and rivers can be also contaminated by wastewater including oil generated in numerous manufacturing industries. Therefore, the present  $R_F-(VM-SiO_2)_n-R_F/PTFE$  nanocomposites may have high potential to develop into the practical oil-water separation materials in a wide variety of fields, since these nanocomposites contain the PTFE units, which have an excellent resistance to chemical reagents and high temperature stability.

## References

- 1) J. G. Drobny, “Technology of Fluoropolymers”, CRC Press (2014).
- 2) S. Ebnesajjad, “Introduction to Fluoropolymers - Materials, Technology and Applications”, Elsevier (2013).
- 3) H.Y. Erbil, A.L. Demirel, Y. Avci, and O. Mert, *Science.*, **299**, 1377 (2003) .
- 4) H. Zhang, H.Y. Hu, W.C. Ye, and F. Zhou, *J. Appl. Polym. Sci.*, **122**, 3145 (2011).
- 5) V. N. Aderikha, and V. A. Shapovalov, *Wear.*, **271**, 970 (2011).
- 6) J. R. Vail, B. A. Krick, K. R. Marchman, and W. Gregory Sawyer, *Wear.*, **270**, 737 (2011).
- 7) G. K. Kannarpady, R. Sharma, B. Liu, S. Trigwell, C. Ryerson, and A. S. Biris, *Appl. Surf. Sci.*, **256**, 1679 (2010).
- 8) S. C. Guo, F. Wu, L. Fang, C. Y. Mao, and Y. Y. Dou, *Mater. Technol.*, **30**, 43 (2015).
- 9) A. Nakajima, K. Hashimoto, and T. Watanabe, *Monatsh. Chem.*, **132**, 31 (2001).
- 10) S. A. Kulinich, and M. Farzaneh, *Appl. Surf. Sci.*, **230**, 232 (2004).
- 11) Y. Zhou, M. Li, X. Zhong, Z. Zhu, P. Deng, and H. Liu, *Ceramics Int.* , **41**, 5341 (2015).
- 12) D. Jucius, V. Grigaliunas, M. Mikolajunas, A. Guobiene, V. Kopustinskas, A.

- Gudonyte, and P. Narmontas, *Appl. Surf. Sci.*, **257**, 2353 (2011).
- 13) D. Gong, J. Long, P. Fan, D. Jiang, H. Zhang, and M. Zhong, *Appl. Surf. Sci.*, **331**, 437 (2015).
- 14) A. Bayat, M. Ebrahimi, A. Nourmohammadi, and A.Z. Moshfegh, *Appl. Surf. Sci.*, **341**, 92 (2015).
- 15) D. Iacovetta, J. Tam, and U. Erb, *Surf. Coatings Technol.*, **279**, 134 (2015).
- 16) D. Kim, W. Hwang, H. C. Park, and K. -H. Lee, *Curr. Appl. Phys.*, **8**, 770 (2008).
- 17) K. K. S. Lau, J. Bico, K. B. K. Teo, M. Chhowalla, G. A. J. Amaratunga, W. L. Milne, G. H. Mackinley, and K. K. Gleason, *Nano Lett.*, **3**, 1701 (2003).
- 18) H. Jiang, L. Chen, S. Chai, X. Yao, F. Chen, and Q. Fu, *Composites Sci. Technol.*, **103**, 28 (2014).
- 19) H. C. Barshilia, and N. Gupta, *Vacuum*, **99**, 42 (2014).
- 20) J. -M. Wang, L. -D. Wang, and L. Feng, *J. Appl. Polym. Sci.*, **120**, 524 (2011).
- 21) A. Milionis, L. Martiradonna, G. C. Anyfantis, P. D. Cozzoli, I. S. Bayer, D. Fragouli, and A. Athanassiou, *Colloid Polym. Sci.*, **291**, 401 (2013).
- 22) S. Wang, Y. Li, X. Fei, M. Sun, C. Zhang, Y. Li, Q. Yang, and X. Hong, *J. Colloid Interface Sci.*, **359**, 380 (2011).

- 23) X. Chen, Y. Gong, D. Li, H. Li, *Coll. Surf. A: Physicochem. Eng. Aspects*, **492**, 19 (2016).
- 24) X. Chen, Y. Gong, X. Suo, J. Huang, Y. Liu, and H. Li, *Appl. Surf. Sci.*, **356**, 639 (2015).
- 25) H. Wang, E. Chen, X. Jia, L. Liang, and Q. Wang, *Appl. Surf. Sci.*, **349**, 724 (2015).
- 26) H. Wang, L. Yan, D. Gao, D. Liu, C. Wang, L. Sun, and Y. Zhu, *Wear*, **319**, 62 (2014).
- 27) K. Wang, N.-X. Hu, G. Xu, and Y. Qi, *Carbon*, **49**, 1769 (2011).
- 28) D. Su, C. Y. Huang, Y. Hu, Q. Jiang, L. Zhang, and Y. Zhu, *Appl. Sur. Sci.*, **258**, 928 (2011).
- 29) S. S. Latthe, C. Terashima, K. Nakata, M. Sakai, and A. Fujishima, *J. Mater. Chem. A*, **2** 5548 (2014).
- 30) W. Hou, and Q. Wang, *J. Colloid Interface Sci.*, **333**, 400 (2009).
- 31) H. Sawada, *Chem. Rev.*, **96**, 1779 (1996).
- 32) H. Sawada, *Prog. Polym. Sci.*, **32**, 509 (2007).
- 33) H. Sawada, *Polym. Chem.*, **3**, 46 (2012).
- 34) H. Sawada, *J. Fluorine Chem.*, **121**, 111 (2003).
- 35) H. Sawada, and M. Nakayama, *J. Chem. Soc., Chem. Commun.*, 677 (1991).



- 36) H. Sawada, T. Suzuki, H. Takashima, and K. Takishita, *Colloid Polym. Sci.*, **286**, 1569 (2008).
- 37) Y. Goto, H. Takashima, K. Takishita, and H. Sawada, *J. Colloid Interface Sci.*, **362**, 375 (2011).
- 38) Y. Si, and Z. Guo, *Chem. Lett.*, **44**, 874 (2015).
- 39) K. Liu, Y. Tian, and L. Jiang, *Prog. Mater. Sci.*, **58**, 503 (2013).
- 40) T. Darmanin, and F. Guittard, *Prog. Polym. Sci.*, **39**, 656 (2014).
- 41) E. Celia, T. Darmanin, E. T. de Givenchy, S. Amigoni, and F. Guittard, *J. Colloid Interface Sci.*, **402**, 1 (2013).
- 42) J. Li, H. Wan, Y. Ye, H. Zhou, and J. Chen, *Appl. Surface Sci.*, **261**, 470 (2012).
- 43) M. Zhang, C. Wang, S. Wang, Y. Shi, and J. Li, *Appl. Surface Sci.*, **261**, 764 (2012).
- 44) M. Zhang, C. Wang, S. Wang, Y. Shi, and J. Li, *Carbohydrate Polym.*, **97**, 59 (2013).
- 45) T. Arbatan, L. Zhang, X.-Y. Fang, and W. Shen, *Chem. Eng. J.*, **210**, 74 (2012).
- 46) A. K. Kota, G. Kwon, W. Choi, J. M. Mabry, and A. Tuteja, *Nature Commun.*, **3**, 1025 (2012).
- 47) S. Parak, E. S. Lee, and W. R. W. Sulaiman, *J. Ind. Eng. Chem.*, **21**, 1239 (2015).

## CHAPTER 2

# **Preparation of Fluoroalkyl End-Capped Vinyltrimethoxysilane Oligomeric Silica/Alkyl-Modified Cellulose Nanocomposites, and Use Thereof for the Modification of Glass and Filter Paper Surfaces: Creation of a Glass Thermoresponsive Switching Behavior and an Efficient Separation Paper Membrane**

## 2.1. Introduction

Cellulose-based materials such as paper, cloth and cotton fabrics plays an important role in a variety of fields such as the textile industry, packaging, printing and coating areas.<sup>1)~3)</sup> However, cellulose is the great sensitivity to water and moisture, quite different from the traditional plastics such as polystyrene, poly(vinyl chloride), polypropylene, polyethylene, and poly(methyl methacrylate). Therefore, the transformation of such hydrophilic materials into hydrophobic, especially superhydrophobic derivatives has been hitherto strongly desirable in order to open a new route to the development of novel cellulose-based materials. In fact, there have been numerous reports on the fabrication of superhydrophobic cellulose materials by using titania/longer alkylated silane coupling agent<sup>4)</sup>, calcium carbonate/alkyl ketene dimer<sup>5)</sup>, polydiallyldimethylammonium chloride/silica particles/longer perfluoroalkylated silane coupling agent<sup>6)</sup>, longer alkylated silane coupling agent/silica nanoparticles<sup>7)</sup>, polystyrene/PTFE (polytetrafluoroethylene)<sup>8)</sup>, polymethylsiloxane<sup>9, 10)</sup>, graft-copolymerization via atom transfer radical polymerization (ATRP) technique<sup>11, 12)</sup>, and gold nanoparticle immobilization<sup>13)</sup>. In the cellulose-based materials, filter paper is widely used for adsorption of liquid, and separation of solid and liquid due to porous structure constructed by microfibrils. Therefore, the exploration of the

cellulose derivatives including filter paper possessing a superoleophilic/superhydrophobic characteristic has been of particular interest from the applicable viewpoint of oil/water separation membrane. Hitherto, there have been comprehensively studied on the development of the fabrication of superamphiphobic<sup>14, 15)</sup>, superoleophobic/superhydrophilic<sup>16, 17)</sup> and superoleophilic/superhydrophobic<sup>16, 18, 19)</sup> surfaces by using fluoroalkyl end-capped vinyltrimethoxysilane oligomeric silica composites as a key intermediate. From this point of view, it is very important to apply the corresponding fluorinated oligomeric silica composites to the development of novel cellulose-based materials possessing a unique surface characteristic. This chapter shows that fluoroalkyl end-capped vinyltrimethoxysilane oligomeric silica/alkyl-modified cellulose (**AM-Cellu**) nanocomposites can be easily prepared by the sol-gel reaction of the corresponding oligomer in the presence of **AM-Cellu**. The modified glass surface treated with these fluorinated nanocomposites was found to exhibit a highly oleophobic/superhydrophilic characteristic at 20 °C. However, interestingly, the modified surface treated with the fluorinated nanocomposites was found to provide the switching behavior from highly oleophobic/superhydrophilic to superoleophilic/superhydrophobic characteristics on the surface by increasing the temperatures from 20 to 70 °C. The nanocomposites were also applied to the surface modification of filter paper under similar

conditions to supply a superoleophilic/superhydrophobic characteristic on the modified surface. The modified filter paper thus obtained has been applied to the separation membrane for W/O emulsion to isolate the transparent colorless oil. These results will be described in this chapter.

## **2.2. Experimental**

### **2.2.1 Measurements**

Dynamic light scattering (DLS) measurements were measured by using Otsuka Electronics DLS-7000 HL (Tokyo, Japan). Contact angles were measured using a Kyowa Interface Science Drop Master 300 (Saitama, Japan). Field emission scanning electron micrographs (FE-SEM) were obtained by using JEOL JSM-7000F (Tokyo, Japan). Dynamic force microscope (DFM) was recorded by using SII Nano Technology Inc. E-sweep (Chiba, Japan). Optical and fluorescence microscopies were measured by using OLYMPUS Corporation BX51 (Tokyo, Japan).

### **2.2.2. Materials**

Alkyl-modified cellulose (Metolose-90SH-100<sup>®</sup>) was obtained from Shin-Etsu Chemical Co., Ltd. (Tokyo, Japan) and used as received. Span 80 (sorbitan monooleate) was purchased from Tokyo Chemical Industrial Co., Ltd. (Tokyo, Japan). Fluoroalkyl end-capped vinyltrimethoxysilane oligomer was prepared according to the previously

reported method.<sup>20)</sup> Glass plate (borosilicate glass) [micro cover glass: 18 mm x 18 mm] was purchased from Matunami glass Ind. Ltd. (Osaka, Japan) and was used after washing well with 1, 2-dichloroethane. Filter paper (Advantec 131) was received from Advantec Toyo Kaisha, Ltd. (Tokyo, Japan).

### **2.2.3. Preparation of fluoroalkylated vinyltrimethoxysilane oligomeric silica/AM-Cellu nanocomposites [R<sub>F</sub>-(VM-SiO<sub>2</sub>)<sub>n</sub>-R<sub>F</sub>/AM-Cellu]**

A typical procedure for the preparation of R<sub>F</sub>-(VM-SiO<sub>2</sub>)<sub>n</sub>-R<sub>F</sub>/AM-Cellu nanocomposites is as follows: To methanol solution (3.5 ml) containing fluoroalkyl end-capped vinyltrimethoxysilane oligomer [100 mg; R<sub>F</sub>-[CH<sub>2</sub>CHSi(OMe)<sub>3</sub>]<sub>n</sub>-R<sub>F</sub>; R<sub>F</sub> = CF(CF<sub>3</sub>)OC<sub>3</sub>F<sub>7</sub>; Mn = 730 (R<sub>F</sub>-(VM)<sub>n</sub>-R<sub>F</sub>)] was added aqueous AM-Cellu (10 mg) solution (1.5 ml). The mixture was stirred with a magnetic stirring bar at room temperature for 5 h. Water was added to the obtained crude products after the solvent was evaporated off. The aqueous suspension was stirred with magnetic stirring bar at room temperature for 1 day. The fluorinated oligomeric silica/AM-Cellu nanocomposites were isolated after centrifugal separation for 30 min. The nanocomposite product was washed well with water several times, and then was dried under vacuum at 50 °C for 2 days to afford the expected

composites as white powders (28 mg) (see Scheme 2-1).

#### **2.2.4. Surface modification of glass treated with the $R_F-(VM-SiO_2)_n-R_F/AM-Cellu$ nanocomposites**

The methanol solution (3.5 ml) containing  $R_F-(VM)_n-R_F$  oligomer (100 mg) and aqueous **AM-Cellu** (100 mg) solution (1.5 ml) was stirred with a magnetic stirring bar at room temperature for 5 h at room temperature. The glass plate (18 x 18 mm<sup>2</sup> pieces) was dipped into this solution at room temperature and left for 1 min. These glass plates were lifted from the solutions at a constant rate of 0.5 mm/min and were left to dry at room temperature for 1 day; finally, these were dried under vacuum for 1 day at room temperature to afford the modified glass. The modified filter papers (25 x 25 mm<sup>2</sup> pieces) were prepared under similar conditions. The contact angles of dodecane and water were measured by the deposit of each droplet (2  $\mu$ l) on these modified glasses and filter papers, which were left in the box (55 mm x 98 mm x 26 mm) and equipped with a temperature controller after the preincubation of these modified ones left in the box at each temperature (20 ~ 70 °C) for 1 hr.



#### **2.2.5. Preparation of the surfactant-stabilized water in oil (1,2-dichloroethane)**

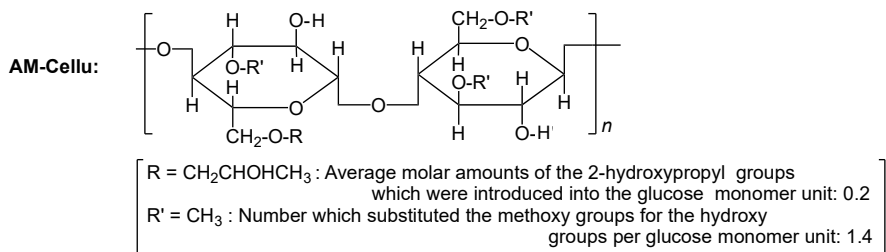
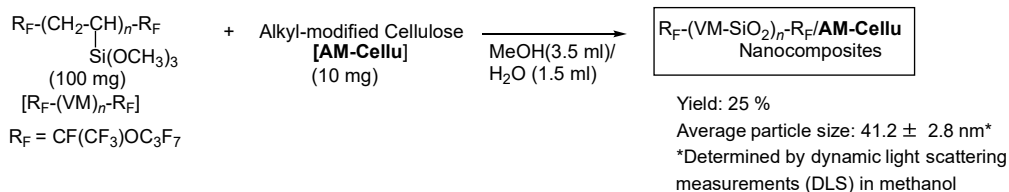
##### **emulsion**

The surfactant (span 80: 20 mg) was added into the mixture of water (0.05 ml) and 1,2-dichloroethane (5.0 ml). The expected white-colored W/O emulsion was easily prepared through the ultrasonic irradiation of the obtained mixture for 5 min at room temperature.

## 2.3. Results and discussion

### 2.3.1. Preparation of the $R_F-(VM-SiO_2)_n-R_F/AM-Cellu$ Nanocomposites

It is well-known that the original cellulose has no solubility toward not only water but also the traditional organic media. However, alkyl-modified cellulose [**AM-Cellu**] has a good solubility in water and methanol. Thus, the **AM-Cellu** was tried to use for the nanocomposite reaction with fluoroalkyl end-capped vinyltrimethoxysilane oligomer [ $R_F-(VM)_n-R_F$ ]. In fact,  $R_F-(VM)_n-R_F$  oligomer was found to undergo the sol-gel reaction in the presence of **AM-Cellu** to afford the corresponding fluorinated oligomeric silica/**AM-Cellu** composites [ $R_F-(VM-SiO_2)_n-R_F/AM-Cellu$ ] in 25 % isolated yield (see Scheme 2-1).



Scheme 2-1 Preparation of  $\text{R}_F-(\text{VM-SiO}_2)_n-\text{R}_F/\text{AM-Cellu}$  nanocomposites

The obtained composites in Scheme 2-1 were found to provide a good dispersibility and stability in methanol. Thus, the size of these fluorinated composites in methanol was measured by dynamic light-scattering (DLS) measurements at 25 °C. The size of the fluorinated composites is nanometer size-controlled fine particles: 41 nm (number-average diameter) as shown in Scheme 2-1.

### 2.3.2. Surface Modification of Glass by Using the $\text{R}_F-(\text{VM-SiO}_2)_n-\text{R}_F/\text{AM-Cellu}$ Nanocomposites

$\text{R}_F-(\text{VM-SiO}_2)_n-\text{R}_F$  oligomeric nanoparticles, which are prepared by the sol-gel reaction of the corresponding oligomer  $[\text{R}_F-(\text{VM})_n-\text{R}_F]$  under alkaline conditions, have been already applied to the surface modification of glass to exhibit an

oleophobic/superhydrophobic characteristic on the surface.<sup>21)</sup> Thus, the modified glasses have been prepared by using the  $R_F-(VM-SiO_2)_n-R_F/AM-Cellu$  nanocomposites illustrated in Scheme 2-1, and dodecane and water contact angle values on the modified glass surface were measured at 20 °C (the dodecane and water contact angle values on the original glass surface are 0° and 50°, respectively). The results are shown in Table 2-1.

Table 2-1 Temperature dependence for the contact angles of dodecane and water on the modified glass surface treated with the  $R_F-(VM-SiO_2)_n-R_F/AM-Cellu$  nanocomposites

Temperature (°C)	Contact angle (Degree)							
	Dodecane <sup>a)</sup>	Water						
		Time						
		0 m	5 m	10 m	15 m	20 m	25 m	30 m
20	69	113	95	88	63	38	0	0
30	35	124	96	86	75	51	17	0
40	23	180	┒b)	┒b)	┒b)	┒b)	┒b)	┒b)
50	17	180	┒c)	┒c)	┒c)	┒c)	┒c)	┒c)
60	18	180	┒c)	┒c)	┒c)	┒c)	┒c)	┒c)
70	0	180	┒c)	┒c)	┒c)	┒c)	┒c)	┒c)

a) A time dependence for the dodecane contact angle measurements was not observed.

b) Water contact angle was 180° in each time.

c) Water contact angle measurement was not completed due to the vaporization of water droplet.

As shown in Table 2-1, the fluorinated nanocomposites were found to afford a highly oleophobic characteristic on the modified surface; because the dodecane contact angle value is 69°, and a time dependence was not observed in the dodecane contact angle measurements.

On the other hand, the effective decrease of water contact angle values from 113° to

0° over 25 or 30 min was observed on the modified surface. The smooth flip-flop motion between hydrophobic fluoroalkyl groups and the hydrophilic **AM-Cellu** moieties in the composites would provide the superhydrophilic surface at the interface with water, and it takes 25 or 30 min to replace the fluoroalkyl groups by the **AM-Cellu** moieties, adapting itself to an environmental change from air to water on the modified surface. It was previously reported that such smooth flip-flop motion between oleophobic and hydrophilic surfaces can be observed on the modified glass surface treated with the fluoroalkyl end-capped vinyltrimethoxysilane – acryloylmorpholine cooligomer<sup>22)</sup> and fluoroalkyl end-capped vinyltrimethoxysilane oligomeric silica/calcium silicide nanocomposites<sup>17)</sup>.

It is well known that nonionic polysoaps such as poly(*N*-isopropylacrylamide) (PNIPAM) undergo a thermally induced phase separation in their aqueous solutions when heated above the lower critical solution temperature (LCST).<sup>23)</sup> In the present  $R_F-(VM-SiO_2)_n-R_F/AM-Cellu$  nanocomposites, interestingly, the **AM-Cellu** is also a temperature-sensitive polymers, and can exhibit the LCST around 70 °C in aqueous solutions as shown in Figure 2-1, indicating that it gives the transparent aqueous solution below the LCST and occurs the phase separation through the oleophilic-oleophilic interaction in the **AM-Cellu** above the LCST. From this point of view, it is expected that the oleophilic – oleophilic interaction between the oleophilic moieties in the **AM-Cellu** in

the composites and oleophilic compounds such as dodecane should accelerate the flip-flop motion between the fluoroalkyl groups and oleophilic moieties in the composites on the surface at around 70 °C (the LCST of the **AM-Cellu**) to provide the LCST-like behavior in air through the dodecane contact angle measurements. Thus, we have studied the temperature dependency for the dodecane and water contact angle measurements at 20 ~ 70 °C on the modified glass surface treated with the  $R_F-(VM-SiO_2)_n-R_F/AM-Cellu$  nanocomposites illustrated in Scheme 2-1, and the results are also shown in Table 2-1.

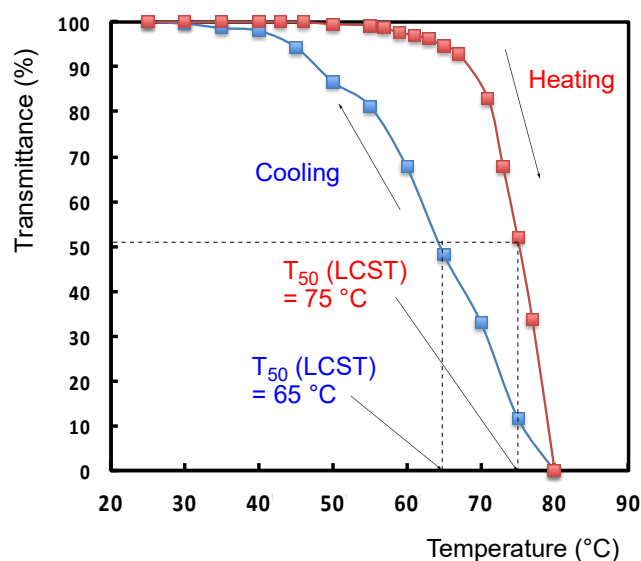


Figure 2-1 Temperature dependence of transmittance at 500 nm of aqueous solutions of the **AM-Cellu** (40 g/dm<sup>3</sup>)

As shown in Table 2-1, the dodecane contact angle values were found to decrease with the increase of the temperatures from 20 to 70 °C, providing the switching behavior

from higher oleophobic to superoleophilic characteristics on the modified surfaces. On the other hand, the wetting behavior for water on the modified surface has been changed from superhydrophilic to superhydrophobic characteristics by increasing the temperatures from 20 to over 40 °C. Because the water contact angle values increased from 0 to 180° on the surface under such conditions. In this way, it was verified that the present fluorinated nanocomposites can provide the switching behavior from highly oleophobic/superhydrophilic to superoleophilic/superhydrophobic characteristics on the modified surface by increasing the temperature on the modified surface from 20 to 70 °C. This unique temperature dependence for water and dodecane contact angle values is also illustrated in Figure 2-2.

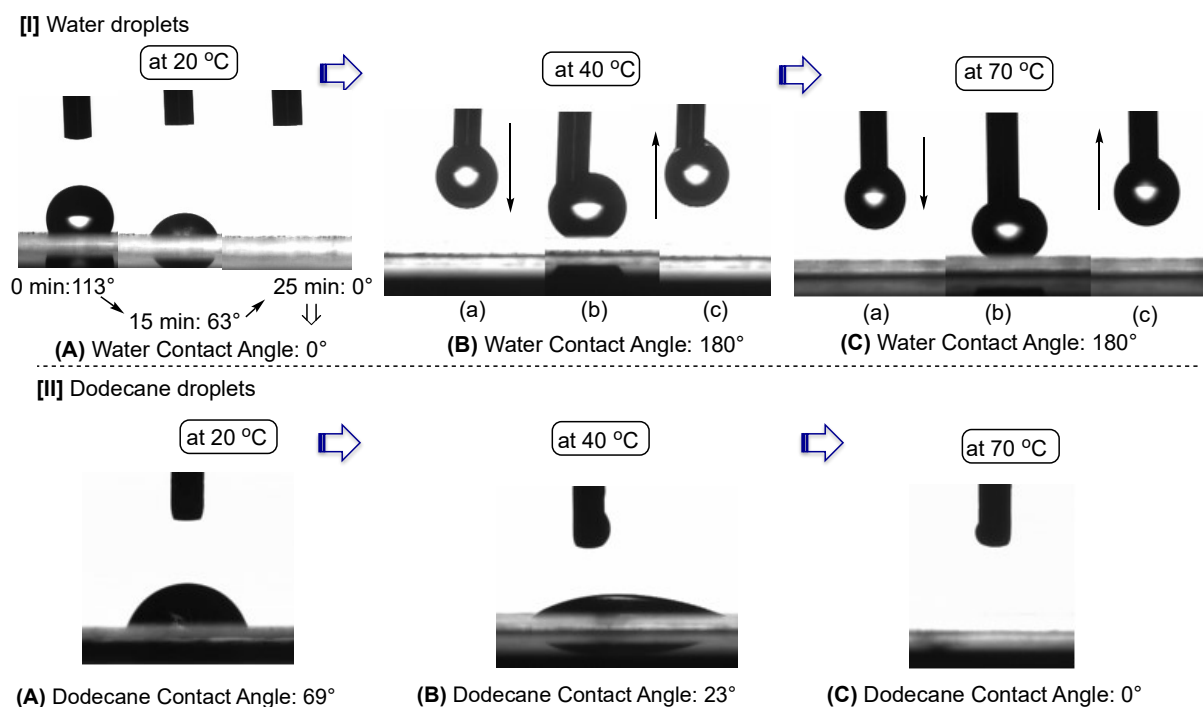


Figure 2-2 Charge coupled device camera images of the water and dodecane droplets on the modified glass surfaces treated with the  $R_F-(VM-SiO_2)_n-R_F/AM-Cellu$  nanocomposites

The time dependence for the water contact angle measurements was observed on the modified surface at 20 °C, and the effective decrease of water contact angle value from 113° to 0° over 25 min was observed to exhibit a superhydrophilic characteristic on the surface [see Figure 2-2-[I]-(A)]. On the other hand, interestingly, water contact angle value was found to increase dramatically from 0° to 180° with increasing the temperatures from 20 °C to over 40 °C [see Figure 2-2-[I]-(B) and -[I]-(C)]. Because, the water droplet that adhered to the needle tip [see Figure 2-2-[I]-(B)-(c)] even after the pull-up process of the needle from the modified surface [Figure 2-2-[I]-(B)-(b)] can be observed, indicating that the water contact angle value is 180°. A similar result was observed in the Figure



## 2-2-[I]-(C).

Figure 2-2-[II] shows the smooth decrease of dodecane contact angle value from 69° to 23°, and finally 0° with the increase of the temperatures from 20 °C to 40 °C and successively, 70 °C. Such superoleophilic characteristic on the modified surface at 70 °C would be due to the effective oleophilic - oleophilic interaction between the oleophilic moieties in the **AM-Cellu** units in the nanocomposites and dodecane; because the **AM-Cellu** can give the LCST at around 70 °C as shown in Figure 2-1.

The recyclability of the dodecane contact angle values on the modified glass surface from 20 to 70 °C was evaluated, and the results are shown in Figure 2-3.

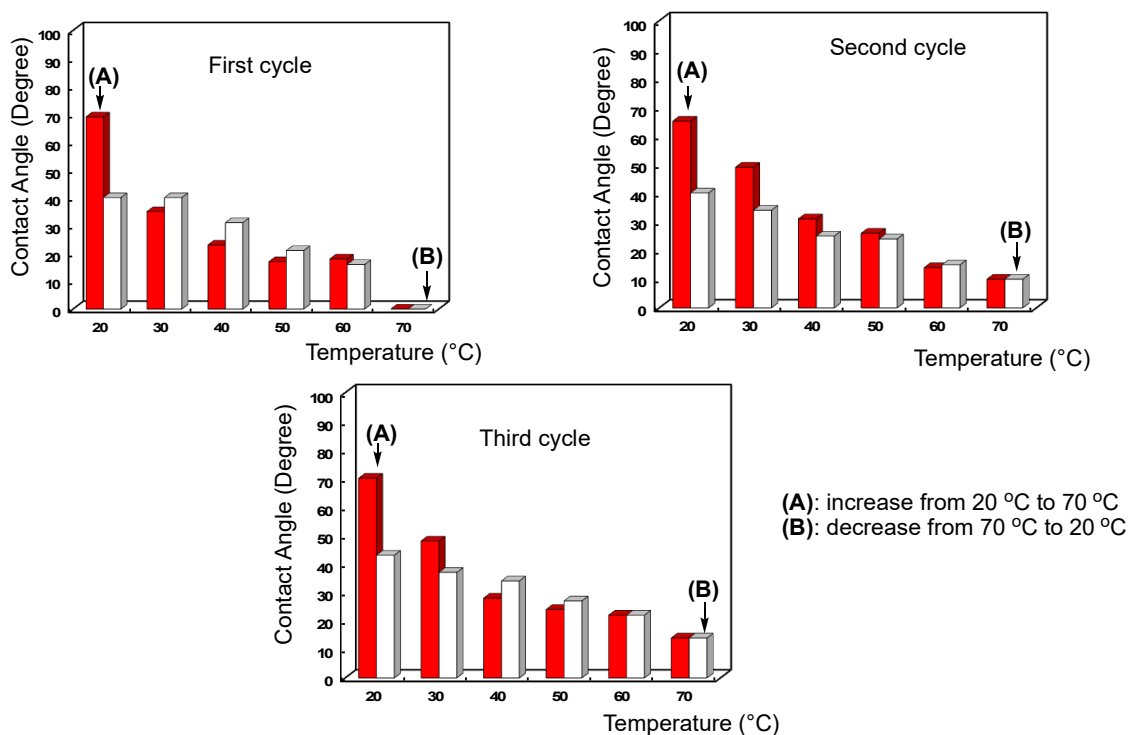


Figure 2-3 Temperature dependence of the dodecane contact angle values on the modified glass surfaces treated with the  $R_F-(VM-SiO_2)_n-R_F/AM-Cellu$  nanocomposites

As shown in first cycle in Figure 2-3-(A), dodecane contact angle values were found to decrease from 69 to 0° with increasing the temperatures from 20 to 70 °C. In contrast, interestingly, the dodecane contact angle values were found to increase from 0 to 42° with the decrease of the temperatures from 70 to 20° [see first cycle in Figure 2-3-(B)]. The process was additionally repeated two cycles, and the results are shown in second and third cycles in Figure 2-3, respectively. A similar tendency for the decrease and increase of dodecane contact angle values with the temperature changes was obtained in second and third cycles. However, the similar dodecane contact angle values during 20 ~ 70 °C were not observed in each cycle, suggesting that these modified films consist of the cross-linked silica composite networks.

Similarly, the recyclability of the water contact angle values on the modified glass surface was evaluated, and the results are shown in Figure 2-4.

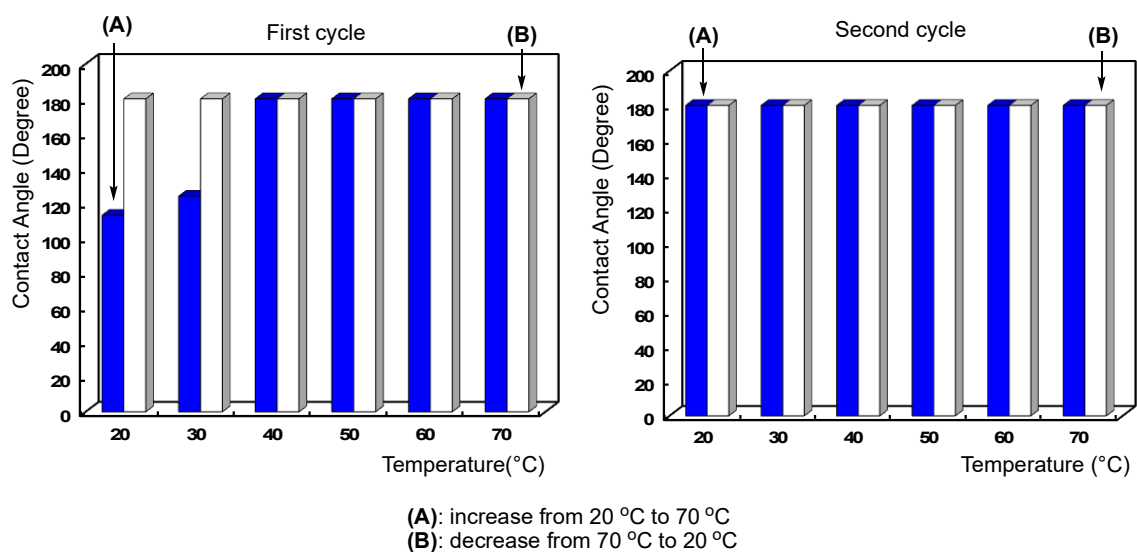


Figure 2-4 Temperature dependence of the water contact angle values on the modified glass surfaces treated with the  $R_F-(VM-SiO_2)_n-R_F/AM-Cellu$  nanocomposites

Water contact angle values were found to increase from 113° to 180° with increasing the temperatures from 20 to over 40 °C [see first cycle in Figure 2-4-(A)]. In fact, as shown in Figure 2-5, the higher roughness architecture was observed on the modified glass surface after heating at 70 °C, compared with that before heating. In addition, Figure 2-6 shows that the topographical image of the modified glass surface after heating at 70 °C can provide a higher roughness property (the roughness average:  $R_a = 159$  nm) than that ( $R_a = 23$  nm) before heating. These findings also suggest that such higher  $R_a$  value would be derived into the superhydrophobic surface toward the modified glass surface after heating.

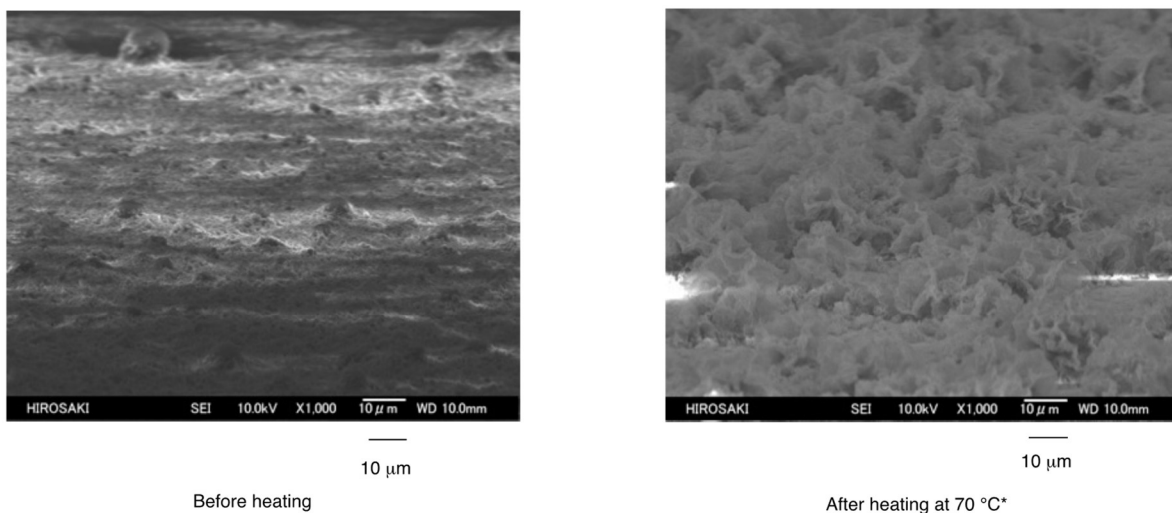


Figure 2-5 FE-SEM images of the modified glass surface treated with the  $R_F-(VM-SiO_2)_n-R_F/AM-Cellu$  nanocomposites at 20 °C (before heating) and after heating at 70 °C\*  
 \*The modified glass was used for the measurements after the decrease of the temperature from 70 to 20 °C

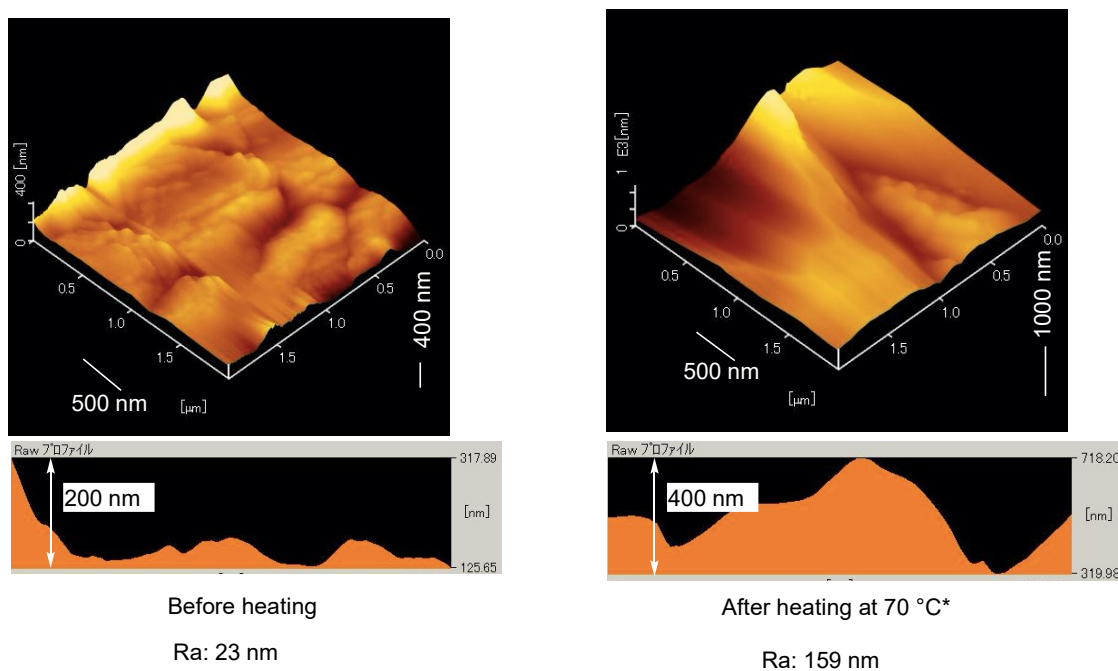


Figure 2-6 DFM (Dynamic Force Microscopy) topographic images of the modified glass surface treated with the  $R_F-(VM-SiO_2)_n-R_F/AM-Cellu$  nanocomposites at 20 °C (before heating) and after heating at 70 °C\*  
 \*The modified glass was used for the measurements after the decrease of the temperature from 70 to 20 °C

The decrease of the water contact angle values was not observed at all with the decrease of the temperatures from 70 to 20 °C as shown in first cycle in Figure 2-4-(B). The

temperature dependency of the water contact angle values was not observed at all in second cycle (or third cycle: data not shown) under similar conditions, keeping the constant value: 180° for the increase or the decrease process of the temperatures [see second cycles in Figure 2-4-(A) and (B)]. This finding would be due to the fluorinated oligomeric silica network structures on the modified surfaces.

### 2.3.3. Surface Modification of Filter Paper by Using the $R_F-(VM-SiO_2)_n-R_F/AM-Cellu$ Nanocomposites

Next, the surface modification of filter paper was tried by using the  $R_F-(VM-SiO_2)_n-R_F/AM-Cellu$  nanocomposites illustrated in Scheme 2-1. As shown in Figure 2-7, the uniformly modified filter paper has been prepared by the use of  $R_F-(VM-SiO_2)_n-R_F/AM-Cellu$  nanocomposites, quite similar to that of the original filter paper. Moreover, it was clarified that the adhesion ability of the modified filter paper surface is strong enough, and the appearance of the modified surface can not change at all even after rubbing the modified surface with the finger, due to the presence of the **AM-Cellu** units in the nanocomposites. In contrast, the adhesion ability of the modified filter paper treated with the original  $R_F-(VM-SiO_2)_n-R_F$  oligomeric nanoparticles is poor,

and the corresponding particles were easily released from the modified filter paper after rubbing the surface with the finger.

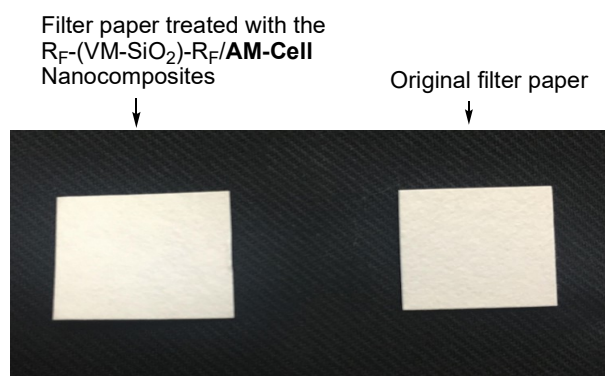


Figure 2-7 Photograph of the modified filter paper treated with the  $R_F-(VM-SiO_2)-R_F/AM-Cell$  nanocomposites and the original filter paper

The modified filter paper treated with the  $R_F-(VM-SiO_2)_n-R_F/AM-Cellu$  nanocomposites was found to exhibit a superoleophilic/superhydrophobic characteristic on the modified filter paper surface, because the dodecane and water contact angle values at 25 or 70 °C are 0 and 180°, respectively, as following; although both of the dodecane and water contact angle values on the original filter paper are 0° under similar conditions.

	25 °C	70 °C
Dodecane contact angle:	0°	0°
Water contact angle:	180°	180°

Unexpectedly, the temperature dependency for these contact angles was not observed at all with the increase or decrease of the temperatures during 20 to 70 °C, and the same contact angle values were observed in each case.

Creation of superhydrophobic surface is in general realized by enhancing the surface roughness.<sup>24 ~ 26)</sup> Thus, the surface roughness of the modified filter papers treated with the  $R_F-(VM-SiO_2)_n-R_F/AM-Cellu$  nanocomposites illustrated in Scheme 2-1 has been studied by using FE-SEM measurements. The original filter paper was also studied under similar conditions, for comparison. These results are shown in Figures 2-8 and 2-9.

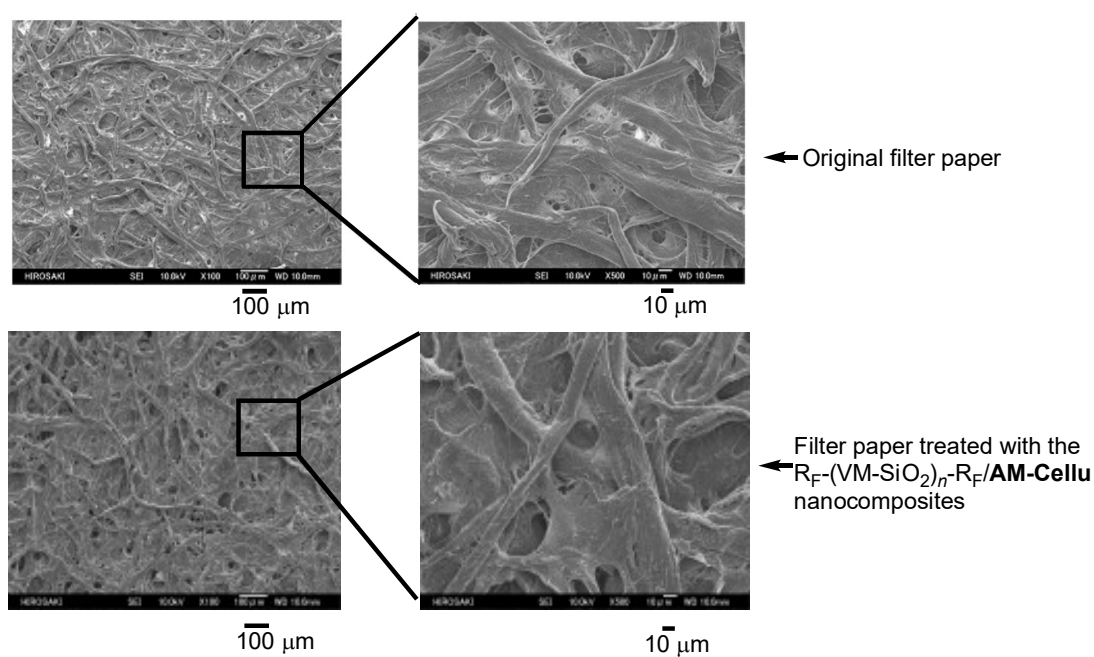


Figure 2-8 FE-SEM images of the modified filter paper surface treated with the  $R_F-(VM-SiO_2)_n-R_F/AM-Cellu$  nanocomposites

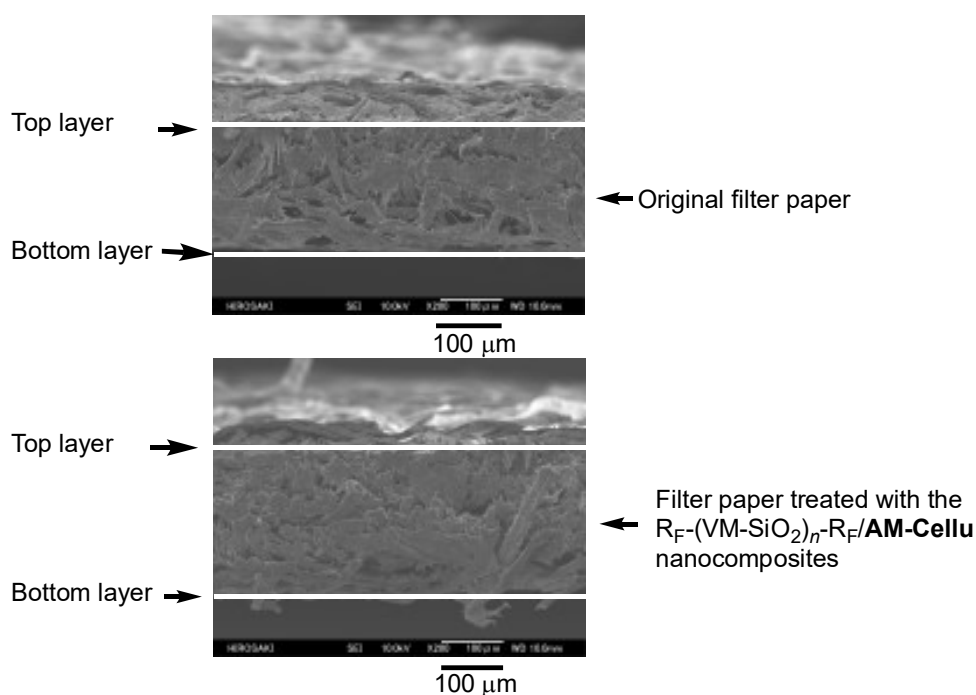


Figure 2-9 FE-SEM images of the cross section of the modified filter paper surface treated with the  $R_F-(VM-SiO_2)_n-R_F/AM-Cellu$  nanocomposites

As shown in Figure 2-8, the similar roughness on the modified filter paper surface to



that of the original filter paper was observed, and the surface appearance is quite similar to that of the original one. In addition, the similar FEM-SEM image of the cross section of the modified filter paper to that of the original one was observed as shown in Figure 2-9.

The DFM (dynamic force microscopy) measurements of the modified filter paper including the original filter paper have been also studied, and the results are shown in Figure 2-10.

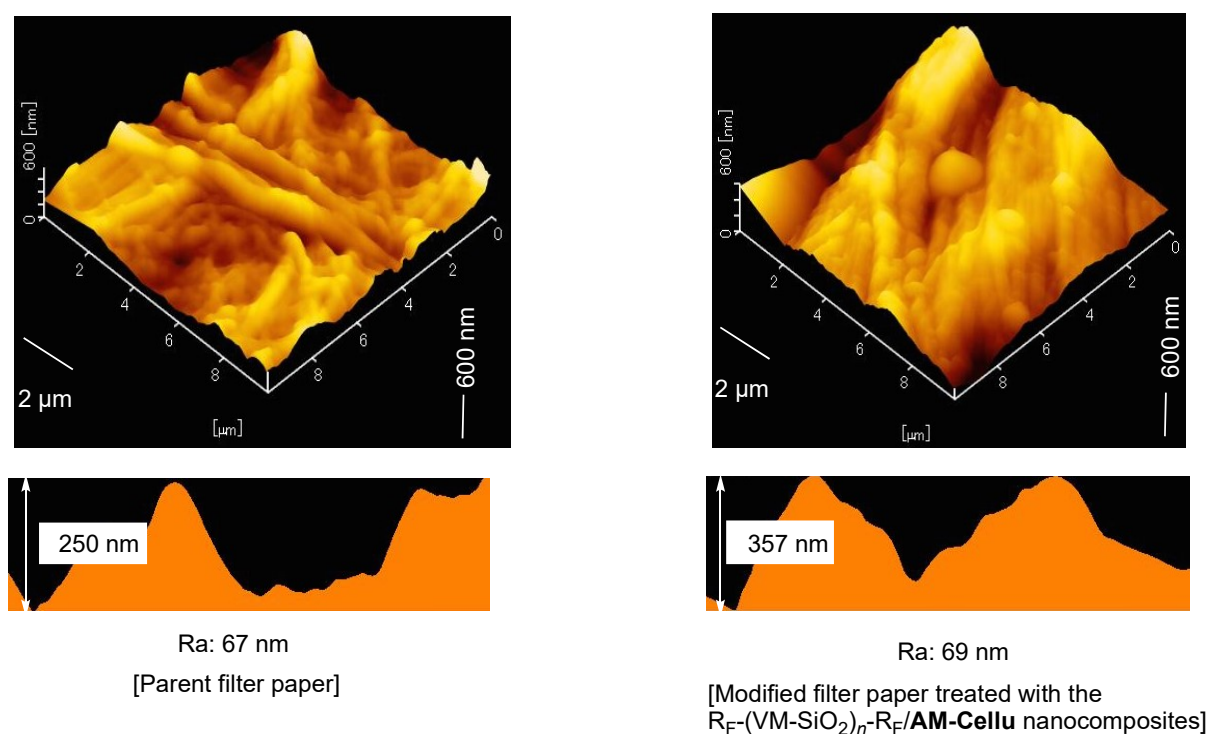


Figure 2-10 DFM topographic images of the parent filter paper surface and the modified filter paper surface treated with the  $R_F-(VM-SiO_2)_n-R_F/AM-Cellu$  nanocomposites

As shown in Figure 2-10, unexpectedly, the modified filter paper surface was found to exhibit the similar topographical image to that of the original filter paper, and the

roughness average values ( $R_a$  : 69 nm) of the modified filter paper was also the same as that ( $R_a$ : 67 nm) of the original one.

The clear void moieties were observed on the modified filter paper surface (see Figure 2-8), and such void moieties should interact smoothly with oil droplets to afford the superoleophilic characteristic on the modified surface due to the lower surface tension of oils than that of water. On the other hand, the architecture of the similar roughness surface for the modified filter paper to that of the original filter paper suggests that the surface modification of the filter paper would be due to the two-dimensional modification, providing the thin coating fluorinated nanocomposite surface; because the  $R_F-(VM)_n-R_F$  oligomer should undergo the smooth sol-gel reaction in the presence of the **AM-Cellu** under non-catalytic conditions to supply the two-dimensional cross-linked silica network structures on the surface. Thus, such smooth roughness surface would provide the superhydrophobic characteristic on the modified surface related to the presence of the longer fluoroalkyl groups in the nanocomposites.

Heretofore, there have been numerous reports on the creation of the superhydrophobic/superoleophilic filter paper through the architecture of the roughness surface by using a variety of methods, such as a porous film formation composed of poly(tetrafluoroethylene) nanoparticles<sup>8)</sup>, spray coating with hydrophobic silica

nanoparticles suspension<sup>7)</sup>, the treatment with a mixture of hydrophobic silica nanoparticles and polystyrene solution in toluene<sup>27)</sup>, and two step dip coating, which consists of the first dip coating of calcium carbonate and subsequently, the coating with alkyl ketene dimer<sup>5)</sup>. These superhydrophobic surfaces are in general realized by enhancing the surface roughness. However, FE-SEM and DFM measurements illustrated in Figures 2-8 and 2-10 show that the surface morphology of the present superoleophilic/superhydrophobic surface is quite similar to that of the parent filter paper, and the enhancement of the surface roughness was not observed during the surface modification process. This surface modification method without the enhancement of the surface roughness for affording the superhydrophobic characteristic will become the first example.

#### **2.3.4. Separation of W/O Emulsion by Using the Modified Filter Paper Treated with the $R_F-(VM-SiO_2)_n-R_F/AM-Cellu$ Nanocomposites as the Separation Membrane**

The superoleophilic surface has in general a strong affinity toward oils. Thus, the surfaces possessing the superoleophilic/superhydrophobic characteristic can simultaneously repels water and strongly absorbs oils. Such behavior should be applicable to the oil/water separating materials.<sup>5, 7, 28, 29)</sup> Thus, the water-in-oil (W/O) emulsion was tried to separate by

using the modified filter paper treated with the  $R_F-(VM-SiO_2)_n-R_F/AM-Cellu$  nanocomposites as the separation membrane. The surfactant (span 80: 20.0 mg)-stabilized water (0.05 ml)-in-oil (1, 2-dichloroethane: 5.00 ml) (W/O) emulsion was prepared under ultrasonic conditions for 5 min at room temperature. The original non-treated filter paper was also used as the separation membrane under similar conditions, for comparison. These results are shown in Figure 2-11.

The original filter paper was not effective for the membrane to separate the W/O emulsion under reduced pressure conditions. However, interestingly, it was demonstrated that the present modified filter paper is effective for the separation of the W/O emulsion, and only transparent colorless oil has been isolated under reduced pressure. In fact, as shown in Figure 2-11-[B], optical micrograph showed that the water droplet cannot be detected at all in the isolated colorless oil, although the water droplet can be easily detected in the case of the use of the original filter paper (see Figure 2-11-[A]).

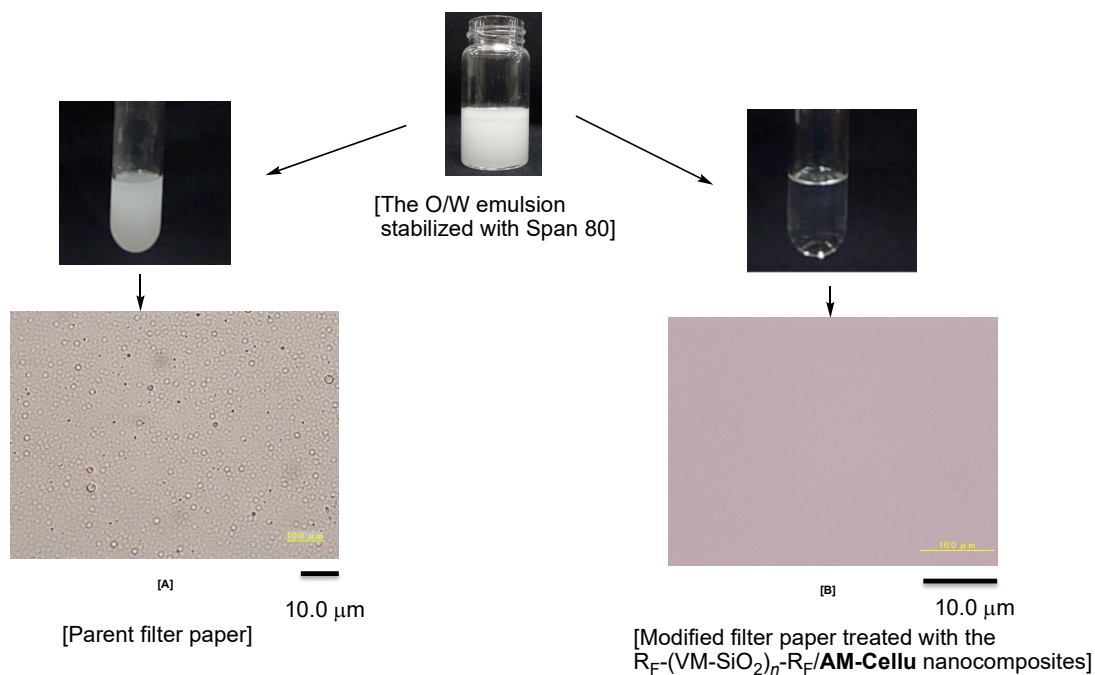


Figure 2-11 Photograph of optical microscopy of the isolated oil after the separation of the W/O emulsion by using the parent filter paper and the modified filter paper treated with the  $R_F-(VM-SiO_2)_n-R_F/AM-Cellu$  nanocomposites

The reusability was studied for the modified filter paper as the separation membrane, and the colorless oil was quantitatively isolated under similar conditions even after the use of the W/O emulsion three times as the following recovered ratios: first time 95 %; second time 94 %; third time 95 %.

In this way, the present  $R_F-(VM-SiO_2)_n-R_F/AM-Cellu$  nanocomposites may be developed in the new separation membrane for the mixture of oil and water in a wide variety of fields.

## 2.4. Conclusion

In summary, a simple strategy for creation of novel thermoresponsive surface has been developed by using the fluoroalkyl end-capped vinyltrimthoxysilane oligomeric silica/**AM-Cellu** nanocomposites  $[R_F-(VM-SiO_2)_n-R_F/AM-Cellu]$ . The resulting surfaces are sensitive to the temperature changes. Especially, it was demonstrated that the modified surface treated with the  $R_F-(VM-SiO_2)_n-R_F/AM-Cellu$  nanocomposites can afford from highly oleophobic/superhydrophilic to superoleophilic/superhydrophobic characteristics on the modified glass surface corresponding to the temperature changes from 20 to 70 °C. Interestingly, such fluorinated nanocomposites were applied to the surface modification of filter paper to provide a superoleophilic/superhydrophobic characteristic on the modified surface. More interestingly, the modified filter paper possessing a superoleophilic/superhydrophobic characteristic was also applied to the membrane for the separation of the W/O emulsion to isolate the colorless oil. Therefore, the present fluorinated nanocomposites have high potential for the novel separation membrane of the mixtures of oil and water in a wide variety of fields including the organic synthetic area.

## References

- 1) D. Klemm, B. Heublein, H.-P. Fink, and A. Bohn, *Angew. Chem. Int. Ed.*, **44**, 3358 (2005).
- 2) Y. Habibi, L. Lucia, and O. J. Rojas, *Chem. Rev.*, **110**, 3479 (2010).
- 3) H. Teisala, M. Tuominen, and J. Kuusipalo, *Adv. Mater. Interfaces*, **1**, 1300026 (1 - 20) (2014).
- 4) S. Li, Y. Wei, and J. Huang, *Chem. Lett.*, **39**, 20 (2010).
- 5) T. Arbatan, L. Zhang, X.-Ya Fang, and W. Shen, *Chem. Eng. J.*, **210**, 74 (2012).
- 6) H. Yang and Y. Deng, *J. Colloid Interface Sci.*, **325**, 588 (2008).
- 7) J. Li, H. Wan, Y. Ye, H. Zhou, and J. Chen, *Appl. Surface Sci.*, **261**, 470 (2012).
- 8) C. Du, J. Wang, Z. Chen, and D. Chen, *Appl. Surface Sci.*, **313**, 304 (2014).
- 9) S. Li, H. Xie, S. Zhang, and X. Wang, *Chem. Commun.*, **46**, 4857 (2007).
- 10) S. Li, S. Zhang, and X. Wang, *Langmuir*, **24**, 5585 (2008).
- 11) D. Nystrom, J. Lindqvist, E. Ostmark, A. Hult, and E. Malmstrom, *Chem. Commun.*, **34**, 3594 (2006).
- 12) A. Calmark and E. Malmstrom, *J. Am. Chem. Soc.*, **124**, 900 (2002).
- 13) T. Wang, X. Hu, and S. Dong, *Chem. Commun.*, **18**, 1849 (2007).

- 14) H. Sawada, *Polym. Chem.*, **3**, 46 (2012).
- 15) Y. Goto, H. Takashima, K. Takishita, and H. Sawada, *J. Colloid Interface Sci.*, **362**, 375 (2011).
- 16) Y. Oikawa, T. Saito, M. Yamada, M. Sugita, and H. Sawada, *ACS Appl. Mater. Interfaces*, **7**, 13782 (2015).
- 17) T. Saito, Y. Tsushima, and H. Sawada, *Colloid Polym. Sci.*, **293**, 65 (2015).
- 18) A. Ratcha, T. Saito, R. Takahashi, S. Kongparakul, and H. Sawada, *Colloid Polym. Sci.*, **294**, 1529 (2016).
- 19) J. Suzuki, Y. Takegahara, Y. Oikawa, M. Chiba, S. Yamada, M. Sugiya, and H. Sawada, *J. Sol-Gel Sci. Technol.*, **81**, 611 (2017).
- 20) H. Sawada and M. Nakayama, *J. Chem. Soc., Chem. Commun.*, **10**, 677 (1991).
- 21) H. Sawada, T. Suzuki, H. Takashima, and K. Takishita, *Colloid Polym. Sci.*, **286**, 1569 (2008).
- 22) H. Sawada, Y. Ikematsu, T. Kawase, and Y. Hayakawa, *Langmuir*, **12**, 3529 (1996).
- 23) Y. Hirokawa and T. Tanaka, *J. Chem. Phys.*, **81**, 6379 (1984).
- 24) Y. Si and Z. Guo, *Chem. Lett.*, **44**, 874 (2015).
- 25) K. Liu, Y. Tian, and L. Jiang, *Prog. Mater. Sci.*, **58**, 503 (2013).
- 26) E. Celia, T. Darmanin, E. T. de Givenchy, S. Amigoni, and F. Guittard,



*J. Colloid Interface Sci.*, **402**, 1 (2013).

27) S. Wang, M. Li, and Q. Lu, *ACS Appl. Mater. Interfaces*, **2**, 677 (2010).

28) M. Zhang, C. Wang, S. Wang, Y. Shi, and J. Li, *Appl. Surface Sci.*, **261**, 764 (2012).

29) M. Zhang, C. Wang, S. Wang, Y. Shi, and J. Li, *Carbohydrate Polym.*, **97**, 59 (2013).

## CHAPTER 3

**Preparation of Fluoroalkyl End-capped Oligomer/Cyclodextrin Polymer**

**Composites: Development of Fluorinated Composite Material Having a  
Higher Adsorption Ability toward Organic Molecules**

### 3.1. Introduction

There has been a great interest in cyclodextrins which consist of a hydrophilic exterior and a hydrophobic interior capable of binding small hydrophobic structures, due to their ability to form inclusion complexes with a wide variety of water-insoluble compounds.<sup>1 ~ 4)</sup> Cyclodextrins have been predominantly used for the stabilization, solubilization and formulation of drugs, and for the separation of the isomers and analogs in analytical chemistry.<sup>5, 6)</sup> However, cyclodextrins possess a solubility toward water, limiting its reusability as the adsorbent for these compounds. Therefore, it is deeply desirable to develop the water-insoluble cyclodextrin polymers. In fact, there have been numerous reports on the synthesis of the water-insoluble cyclodextrin polymers by the use of epichlorohydrin and diisocyanates as the crosslinking agents, so far.<sup>7 ~ 11)</sup> These water-insoluble cyclodextrin polymers thus obtained have been applied to the adsorbents for the organic pollutants such as phenol, *p*-nitrophenol, benzoic acid, *p*-nitrobenzoic acid, 4-*t*-butylbenzoic acid, and bisphenol A.<sup>12 ~ 14)</sup> Hitherto, there have been comprehensively studied on the synthesis and applications of two fluoroalkyl end-capped oligomers [ $R_F-(M)_n-R_F$ ;  $R_F$  = fluoroalkyl group,  $M$  = radical polymerizable monomer] by the use of fluoroalkanoyl peroxide [ $R_F-C(=O)-OO-(O=)C-R_F$ ] as a key intermediate.<sup>15 ~ 19)</sup> In these

two fluoroalkyl end-capped oligomers, especially, two fluoroalkyl end-capped vinyltrimethoxysilane oligomer  $[\text{R}_\text{F}-(\text{CH}_2\text{CHSi}(\text{OMe}_3)_n-\text{R}_\text{F})$ ;  $\text{R}_\text{F} = \text{CF}(\text{CF}_3)\text{OC}_3\text{F}_7$ ) has been already applied to the composite reactions with not only talc fine particles in the presence of low-molecular weight organic molecules but also organic polymers such as poly(terafluoroethylene) fine particles to afford the corresponding fluorinated oligomeric silica nanocomposites – encapsulated these guest molecules.<sup>20 ~ 22]</sup> It was also demonstrated that these fluorinated nanocomposites can exhibit a superoleophilic/superhydrophobic characteristic toward the modified surface, although the corresponding original fluorinated oligomeric silica nanoparticles  $[\text{R}_\text{F}-(\text{CH}_2\text{CHSiO}_2)_n-\text{R}_\text{F}]$  can give a usual oleophobic/superhydrophobic property on their modified surface.<sup>20]</sup> In addition, these fluorinated nanocomposites are applicable to the packing materials for the column chromatography to separate the mixture of oil and water.<sup>21, 22]</sup> From the developmental viewpoint of the cyclodextrin polymer derivatives possessing a higher adsorption ability toward a variety of organic molecules in aqueous media than that of the pristine cyclodextrin polymers, it is of particular interest to explore the cyclodextrin polymer derivatives possessing a superoleophilic/superhydrophobic characteristic; however, such studies have been heretofore very limited. This chapter shows that two fluoroalkyl end-capped vinyltrimethoxysilane oligomer can be applicable to the sol-gel reaction in the

presence of  $\alpha$ -,  $\beta$ -,  $\gamma$ -cyclodextrin polymers ( $\alpha$ -,  $\beta$ -,  $\gamma$ -CDPs) under alkaline conditions to afford the corresponding fluorinated oligomeric silica/ $\alpha$ -,  $\beta$ -,  $\gamma$ -CDPs composites. Interestingly, these fluorinated composites thus obtained were found to provide a higher adsorption ability toward low-molecular weight aromatic compounds such as bisphenol A and bisphenol AF in the aqueous solutions than that of the pristine  $\alpha$ -,  $\beta$ -,  $\gamma$ -CDPs. More interestingly, a higher adsorption behavior toward the volatile organic compounds such as toluene, xylenes, trichloroethylene and tetrachloroethylene was also observed by using these fluorinated composites. These results will be described in this chapter.

## 3.2. Experimental

### 3.2.1 Measurements

Dynamic light scattering (DLS) measurements were measured by using Otsuka Electronics DLS-7000 HL (Tokyo, Japan). Micrometer size-controlled composite particles were measured by using laser diffraction particle size analyzer: Shimadzu SALD-200 V (Kyoto, Japan). Field emission scanning electron micrographs (FE-SEM) were obtained using JEOL JSM-7000F (Tokyo, Japan). Thermal analyses were recorded on NETZSCH JAPAN TG-DTA2010SE $\alpha$  differential thermobalance (Kanagawa, Japan). Contact angles were measured using a Kyowa Interface Science Drop Master 300 (Saitama, Japan). Dynamic force microscopy (DFM) was recorded by using SII Nano Technology Inc. E-sweep (Chiba, Japan). HPLC (high performance liquid chromatography) analyses were conducted on a Shimadzu LC10A (Kyoto, Japan). GC-Mass spectra were recorded on a JEOL JMS-Q1000GC K9 (Tokyo, Japan).

### 3.2.2. Materials

$\alpha$ -,  $\beta$ - and  $\gamma$ -cyclodextrin polymers ( $\alpha$ -,  $\beta$ -,  $\gamma$ -CDPs) were received from Kankyo Kogaku (Hirosaki, Japan). Fluoroalkyl end-capped vinyltrimethoxysilane oligomer [ $R_F-(CH_2CHSi(OMe)_3)_n-R_F$ ;  $n = 2, 3$ ;  $R_F = CF(CF_3)OC_3F_7$ ;  $R_F-(VM)_n-R_F$ ] was synthesized according to the previously reported method.<sup>23)</sup> Glass plate (borosilicate glass) [micro cover glass: 18 mm x 18 mm] was purchased from Matsunami glass Ind. Ltd. (Osaka, Japan) and was used after washing well with 1, 2-dichloromethane. Bisphenol A and bisphenol AF were purchased from Tokyo Chemical Industrial Co. (Tokyo, Japan).

### 3.2.3. Preparation of fluoroalkyl end-capped vinyltrimethoxysilane oligomeric silica/ $\alpha$ -CDP composites [ $R_F-(VM-SiO_2)_n-R_F/\alpha$ -CDP]

A typical procedure for the preparation of  $R_F-(VM-SiO_2)_n-R_F/\alpha$ -CDP composites is as follows: To methanol solution (5 ml) containing fluoroalkyl end-capped vinyltrimethoxysilane oligomer [ $R_F-(VM)_n-R_F$ ] (300 mg) was added  $\alpha$ -CDP (10 mg). The mixture was stirred with a magnetic stirring bar at room temperature for 10 min. 25 % aqueous ammonia solution (1.0 ml) was added to the methanol solution, and was

successively stirred at room temperature for 5 hrs. After the solvent was evaporated off, methanol was added to the obtained crude products. The methanol suspension thus obtained was stirred with magnetic stirring bar at room temperature for 1 day, and then was centrifuged for 30 min. The expected fluorinated oligomeric silica/ $\alpha$ -CDP composites were easily separated from the methanol solution, and was successively washed several times with methanol. After centrifugal separation of this solution, the obtained product was dried under vacuum at 50 °C for 1 day to produce the purified fluorinated composite white colored powders (190 mg). Other fluorinated composites were prepared under similar conditions.

#### **3.2.4. Surface modification of glass treated with the $R_F-(VM-SiO_2)_n-R_F/\alpha$ -CDP composites**

To methanol solution (5 ml) containing  $R_F-(VM)_n-R_F$  oligomer (300 mg) was added  $\alpha$ -CDP (10 mg). The mixture was stirred with a magnetic stirring bar at room temperature for 10 min. 25 % aqueous ammonia solution (1.0 ml) was added to the methanol solution, and was successively stirred at room temperature for 5 hrs. The glass plate was dipped into this methanol solution at room temperature and left for 1 min. These glass plates were lifted



from the solutions at a constant rate of 0.5 mm/min and subjected to the treatment for 1 day at room temperature; finally, these were dried under vacuum for 1 day at room temperature. After drying, the contact angles of dodecane and water were measured by the deposit of each droplet (2  $\mu$ l) on the modified glasses.

### **3.2.5. Preparation of the surfactant-stabilized water in oil (toluene) emulsion**

The surfactant (span 80: 30 mg) was added into the mixture of water (0.05 ml) and toluene (5.0 ml). The expected white-colored W/O emulsion was easily prepared through the ultrasonic irradiation of the obtained mixture for 5 min at room temperature. Other W/O (oil: 1, 2-dichloroethane) emulsion was also prepared under similar conditions.

### **3.2.6. Adsorption of bisphenol A in the aqueous solution by using the $R_F-(CH_2CHSiO_2)_n-R_F/\beta$ -CDPs composites**

Solid-phase extraction cartridge connected with the polyethylene frit containing the  $R_F-(CH_2CHSiO_2)_n-R_F/\beta$ -CDPs composite powders (20 mg: Run 20 in Table 3-1) was used for the adsorption of bisphenol A. 5 ml of aqueous methanol solution (concentration of

methanol: 6 %) containing bisphenol A ( $0.1 \text{ mmol/dm}^3$ ) was applied to the cartridge, and the obtained eluent was analyzed by HPLC [Shimadzu LC10A; column: RP-18PA<sup>TR</sup> (4.6 mm I.D. = 150 mm); injection volume: 10 ml; mobile phase: methanol/water/phosphoric acid (70.0/29.9/0.1 (vol/vol/vol); detection wavelength: 278 nm) to detect the residual bisphenol A. Schematic process for analyzing the residual bisphenol A was illustrated in Scheme 3-2, and the residual bisphenol AF was also analyzed under similar conditions. In addition, Schematic illustration for the adsorption and desorption of BPA through the recycling process by using the  $R_F-(CH_2CHSiO_2)_n-R_F/\beta$ -CDPs composite powders as the packing material is shown in Scheme 3-3.

### **3.2.7. Adsorption of volatile organic compounds (VOCs) in the aqueous solutions by using the $R_F-(CH_2CHSiO_2)_n-R_F/CDPs$ composites**

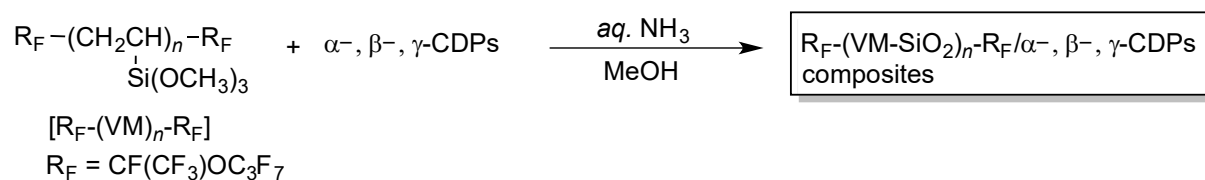
5 ml of 0.1 % methanol solution containing VOCs (concentration of each VOC:  $100 \text{ } \mu\text{g/dm}^3$ ) was poured into the solid-phase extraction cartridge connected with the polyethylene frit containing the  $R_F-(CH_2CHSiO_2)_n-R_F/CDPs$  composite powders (20 mg), and the eluent thus obtained was added into the head space vial. Head space operating conditions were 30 min for sample equilibration at a temperature of 60 °C, and successively

subjected to analysis by head space gas chromatography/mass spectrometer (conditions: capillary column: Aquatic<sup>TR</sup>: 0.25 mm I.D. = 60 m df = 1.4  $\mu$ m; inlet temperature: 200 °C; injection volume: 2 ml; carrier gas: Helium; column oven temperature: from 40 °C to 200 °C (programming rate: 10 °C/min); ion source temperature: 200 °C; ionization energy: 70 eV). The adsorption ratios (%) of VOCs were determined based on the calibration curve created by using the corresponding pristine VOCs having known concentrations. Schematic outline for the analytical measurements of the adsorption ratios of the VOCs is illustrated in Scheme 3-4.

### 3.3. Results and discussion

#### 3.3.1. Preparation of $R_F-(VM-SiO_2)_n-R_F/\alpha-, \beta-, \gamma\text{-CDPs}$ composites

Fluoroalkyl end-capped vinyltrimethoxysilane oligomer  $[R_F-(CH_2CHSi(OMe)_3)_n-R_F]$ :  $n = 2, 3$ ;  $R_F = CF(CF_3)OC_3F_7$ :  $R_F-(VM)_n-R_F$ ] was found to undergo the sol-gel reaction under alkaline conditions in the presence of  $\alpha-, \beta-, \gamma\text{-CDPs}$  at room temperature to provide the corresponding fluorinated oligomeric silica/ $\alpha-, \beta-, \gamma\text{-CDPs}$  composites. The results are shown in Scheme 3-1 and Table 3-1.



Scheme 3-1 Preparation of  $R_F-(VM-SiO_2)_n-R_F/\alpha-, \beta-, \gamma\text{-CDPs}$  composites

Table 3-1 Preparation of  $R_F-(VM-SiO_2)_n-R_F/ \alpha-, \beta-, \gamma-$ CDPs composites

Run	CDPs (mg)	$R_F-(VM)_n-R_F$ (mg)	MeOH (ml)	aq. $NH_3$ (ml)	Yield <sup>a)</sup> (%)	Size of the composites <sup>b)</sup> ( $\mu m$ )
1	$\alpha$ -CDP (10)	300	5	1	38	$5.2 \pm 0.4$
2	$\beta$ -CDP (10)	300	5	1	56	$2.8 \pm 0.2$
3	$\gamma$ -CDP (10)	300	5	1	40	$4.9 \pm 0.3$
4	$\alpha$ -CDP (25)	300	5	1	61	$6.7 \pm 0.4$
5	$\beta$ -CDP (25)	300	5	1	53	$4.1 \pm 0.2$
6	$\gamma$ -CDP (25)	300	5	1	58	$6.9 \pm 0.3$
7	$\alpha$ -CDP (50)	300	5	1	62	$10.9 \pm 0.4$
8	$\beta$ -CDP (50)	300	5	1	55	$4.3 \pm 0.3$
9	$\gamma$ -CDP (50)	300	5	1	58	$6.6 \pm 0.4$
10	$\alpha$ -CDP (100)	300	5	1	63	$16.7 \pm 0.4$
11	$\beta$ -CDP (100)	300	5	1	64	$10.1 \pm 0.3$
12	$\gamma$ -CDP (100)	300	5	1	61	$9.6 \pm 0.4$
13	$\alpha$ -CDP (200)	300	5	1	70	$10.1 \pm 0.3$
14	$\beta$ -CDP (200)	300	5	1	66	$11.2 \pm 0.3$
15	$\gamma$ -CDP (200)	300	5	1	62	$12.5 \pm 0.3$
16	$\alpha$ -CDP (300)	300	5	1	67	$12.6 \pm 0.3$
17	$\beta$ -CDP (300)	300	5	1	71	$8.4 \pm 0.3$
18	$\gamma$ -CDP (300)	300	5	1	72	$11.9 \pm 0.3$
19	$\alpha$ -CDP (200)	200	5	1	78	$20.5 \pm 0.4$
20	$\beta$ -CDP (200)	200	5	1	69	$7.3 \pm 0.3$
21	$\gamma$ -CDP (200)	200	5	1	67	$11.7 \pm 0.5$
22	$\beta$ -CDP (200)	100	5	1	77	$20.4 \pm 0.4$
Original $R_F-(VM-SiO_2)_n-R_F$ nanoparticle						$27.7 \pm 6.7 \text{ nm}^c$
Original $\alpha$ -CDP						$15.8 \pm 0.2 \mu m^b$
$\beta$ -CDP						$16.6 \pm 0.3 \mu m^b$
$\gamma$ -CDP						$17.1 \pm 0.4 \mu m^b$

a) Yields are based on  $R_F-(VM-SiO_2)_n-R_F$  oligomer and CDPs

b) Determined by laser diffraction particle size analyzer in methanol

c) Determined by dynamic light scattering (DLS) measurements in methanol

As shown in Scheme 3-1 and Table 3-1, the expected composites

[ $R_F-(VM-SiO_2)_n-R_F/\alpha-, \beta-, \gamma$ -CDPs] were obtained as 38 ~ 78 % isolated yields through the sol-gel reaction of the  $R_F-(VM)_n-R_F$  oligomer in the presence of CDPs under alkaline conditions. Table 3-1 shows that the yields of the composites are sensitive to the feed ratios of CDPs and  $R_F-(VM)_n-R_F$  oligomer employed, increasing with greater feed ratios of CDPs in the oligomer – CDPs. In addition, the size of the composites was found to increase with the increase of the feed ratios of CDPs. These findings would be due to the presence of micrometer-size controlled CDPs particles.

The pristine CDPs have no solubility toward both water and fluorinated aliphatic solvents [1 : 1 mixed solvents (AK-225<sup>TR</sup>) of 1, 1-dichloro-2, 2, 3, 3, 3-pentafluoropropane and 1, 3-dichloro-1, 2, 2, 3, 3-pentafluoropropane]; however, the CDPs have a dispersibility toward not only water but also some organic solvents such as dimethyl sulfoxide (DMSO), 1, 2-dichloroethane and *N, N*-dimethylformamide (DMF). On the other hand, the fluorinated composites in Table 3-1 were found to give an extremely poor dispersibility in water; however, these composites afforded good dispersibility and stability in traditional organic media such as tetrahydrofuran, DMSO, 1, 2-dichloroethane, DMF, methanol, and 2-propanol including aliphatic solvents: AK-225<sup>TR</sup>. Such dispersibility toward the fluorinated composites; that is, no dispersibility toward water and a good dispersibility toward fluorinated aliphatic solvents, quite different from the pristine CDPs, would be due

to the presence of the fluoroalkyl segments in the composites illustrated in Scheme 3-1.

The sizes of the composites in methanol were measured by laser diffraction particle analyzer at 25 °C (Table 3-1). Each size of these fluorinated composites is micrometer size-controlled fine particles: 3 ~ 17  $\mu\text{m}$  as shown in Table 3-1, on the contrary, the size of the pristine CDPs is 16 ~ 17  $\mu\text{m}$  levels. The decrease of the size of the obtained composites, compared to that of the pristine CDPs would be due to the agglomeration and aggregation of the pristine CDPs.

FE-SEM photograph of the  $\text{R}_\text{F}-(\text{VM-SiO}_2)_n-\text{R}_\text{F}$ /CDPs composite powders (Runs 16, 17 and 18 in Table 3-1) was recorded in order to clarify the morphology of the obtained composites. The FE-SEM measurements of pristine CDPs particle powders and  $\text{R}_\text{F}-(\text{VM-SiO}_2)_n-\text{R}_\text{F}$  oligomeric nanoparticle powders, which were prepared under alkaline conditions, were also measured under similar conditions, for comparison. The results are shown in Figures 3-1 ~ 3-3.

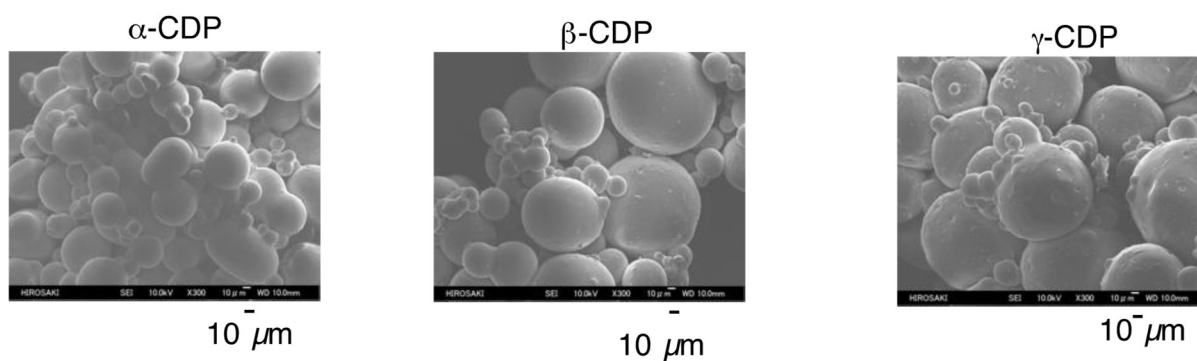


Figure 3-1 Field emission scanning electron microscopy (FE-SEM) image of pristine  $\alpha$ -CDP,  $\beta$ -CDP and  $\gamma$ -CDP powders

Figure 3-1 shows that the pristine  $\alpha$ -,  $\beta$ -,  $\gamma$ -CDPs particles are irregular in size, and FE-SEM picture of the  $R_F-(VM-SiO_2)_n-R_F$  oligomeric particle powders shows the formation of nanometer size-controlled fine particles (see Figure 3-2).

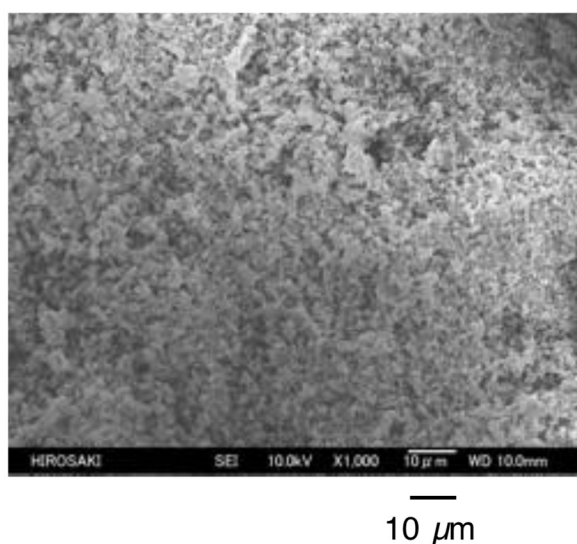


Figure 3-2 FE-SEM image of the pristine  $R_F-(VM-SiO_2)_n-R_F$  nanoparticle powders



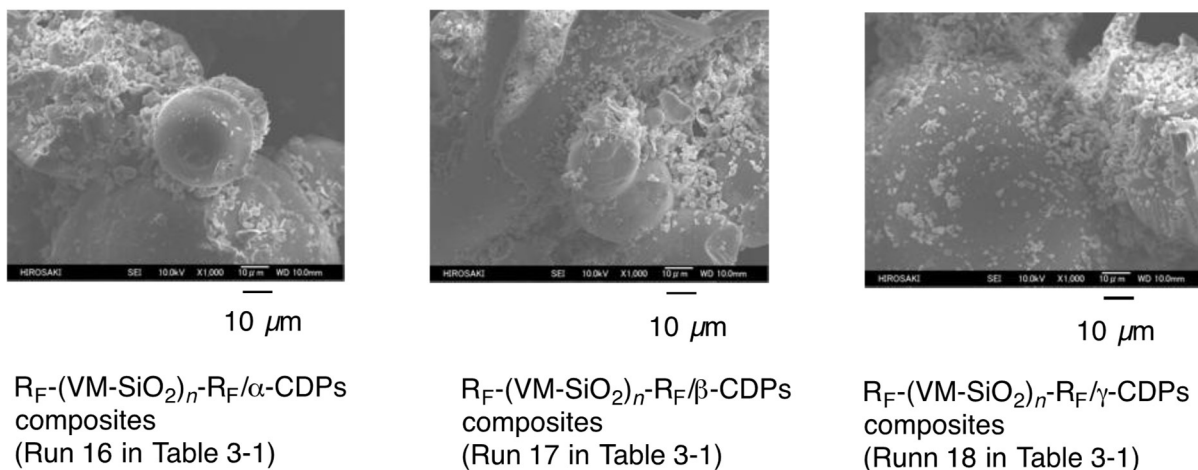


Figure 3-3 FE-SEM images of  $R_F-(VM-SiO_2)_n-R_F/\alpha-, \beta-, \gamma$ -CDPs composite powders

In contrast, electron micrographs of the present  $R_F-(VM-SiO_2)_n-R_F/\alpha$ -CDP,  $\beta$ -CDP, and  $\gamma$ -CDP composites show that the  $R_F-(VM-SiO_2)_n-R_F$  oligomeric nanoparticles are uniformly coated on each CDP particle surface to provide the corresponding fluorinated oligomeric silica/CDPs composites.

In order to verify the presence of the  $R_F-(VM-SiO_2)_n-R_F$  oligomeric nanoparticles in the composites, thermal stability of the fluorinated composites in Table 3-1 was studied by thermogravimetric analyses, in which the weight loss of these composites was measured by raising the temperature around 800 °C (the heating rate: 10 °C min<sup>-1</sup>) in air atmosphere, and the results were shown in Figures 3-4 ~ 3-6.

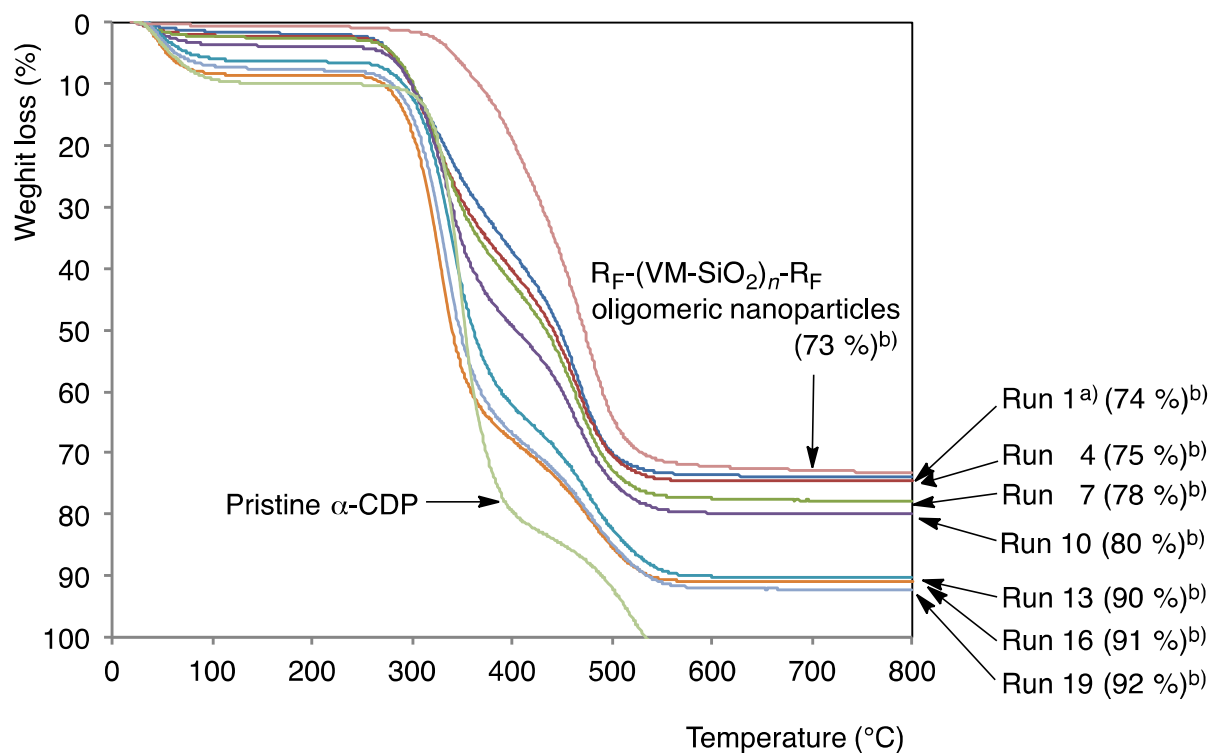


Figure 3-4 Thermogravimetric analyses of  $R_F-(VM-SiO_2)_n-R_F/\alpha$ -CDP composites

a) Run No. corresponds to that of Table 3-1

b) Weight loss (%) at 800 °C

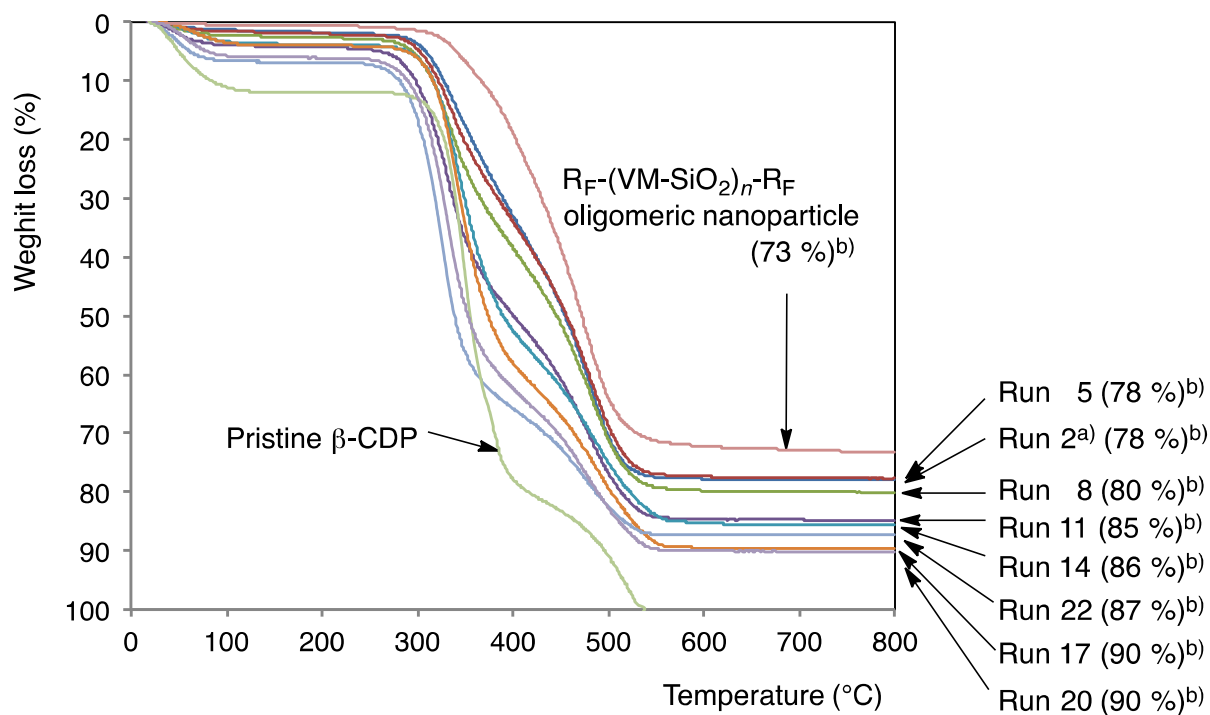


Figure 3-5 Thermogravimetric analyses of  $R_F-(VM-SiO_2)_n-R_F/\beta\text{-CDP}$  composites  
a) Run No. corresponds to that of Table 3-1  
b) Weight loss (%) at 800 °C

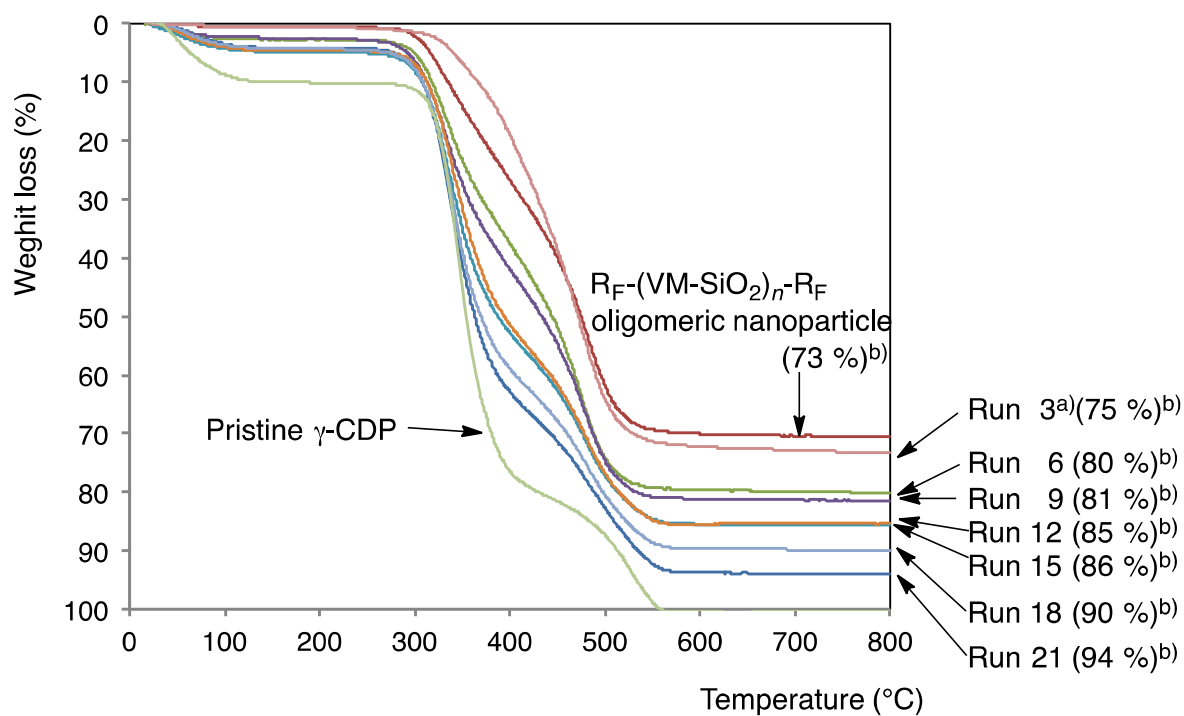


Figure 3-6 Thermogravimetric analyses of  $R_F-(VM-SiO_2)_n-R_F/\gamma\text{-CDP}$  composites  
a) Run No. corresponds to that of Table 3-1  
b) Weight loss (%) at 800 °C

As shown in Figure 3-4, the pristine  $R_F-(VM-SiO_2)_n-R_F$  oligomeric nanoparticles, which were prepared by the sol-gel reaction of  $R_F-(VM)_n-R_F$  oligomer under alkaline conditions in Scheme 3-1, afforded the 73 % weight loss around at 530 °C, owing to the partial formation of silica gel during the calcination process. Pristine  $\alpha$ -CDP afforded a perfect weight loss at around 540 °C. In contrast, the  $R_F-(VM-SiO_2)_n-R_F/\alpha$ -CDP composites (Runs 1, 4, 7, 10, 13 and 16 in Table 3-1) were found to provide the weight loss behavior in proportion to the contents of the  $R_F-(VM-SiO_2)_n-R_F$  oligomeric nanoparticles in the composites after calcination at 800 °C, and the contents of  $\alpha$ -CDP in the composites were estimated to be from 1 to 19 %. Similar TGA curves for the  $R_F-(VM-SiO_2)_n-R_F/\beta$ -CDP and  $\gamma$ -CDP composites were observed, and the contents of  $\beta$ -CDP and  $\gamma$ -CDP in the  $R_F-(VM-SiO_2)_n-R_F$  composites were also estimated under similar conditions. The results are as follows:

Contents (%) of CDPs in the composites:

$\alpha$ -CDP	Run 1 1	Run 4 2	Run 7 5	Run 10 7	Run 13 17	Run 16 18	Run 19 19	
<hr/>								
$\beta$ -CDP	Run 2 5	Run 5 5	Run 8 7	Run 11 12	Run 14 13	Run 17 17	Run 20 17	Run 22 14
<hr/>								
$\gamma$ -CDP	Run 3 2	Run 6 7	Run 9 8	Run 12 12	Run 15 13	Run 18 17	Run 21 21	

The contents of CDPs in the obtained composites were found to increase from 1 ~ 5 % to 17 ~ 18 % with increasing the feed ratios of CDPs in the CDPs – oligomer (300 mg) from 10 to 300 mg in the composites reactions (illustrated in Scheme 3-1).

### 3.3.2. Surface property of $R_F-(VM-SiO_2)_n-R_F/CDPs$ composites

In order to clarify the surface active characteristics of the present composites in Table 3-1, these fluorinated composites were applied to the surface modification of glass to measure the dodecane and water contact angle values on the modified glass surfaces. The results are shown in Table 3-2.

Table 3-2 Contact angles of dodecane and water on the modified glasses treated with the  $R_F-(VM-SiO_2)_n-R_F/CDPs$  composites

	Dodecane (degree)	Water(degree)
$R_F-(VM-SiO_2)_n-R_F/\alpha$ -CDP composites (Runs 1, 4, 7, 10, 13, 16 and 19)*	0	180
$R_F-(VM-SiO_2)_n-R_F/\beta$ -CDP composites (Runs 2, 5, 8, 11, 14, 17, 20 and 22)	0	180
$R_F-(VM-SiO_2)_n-R_F/\gamma$ -CDP composites (Runs 3, 6, 9, 12, 15, 18 and 21)	0	180
-----		
$R_F-(VM-SiO_2)_n-R_F$ oligomeric nanoparticles	48	180

\*) Each Run No. corresponds to that of Table 3-1

It is well known that  $R_F-(CH_2CHSi(OMe)_3)_n-R_F$  oligomer can undergo the sol-gel reaction to afford the corresponding fluoroalkyl end-capped oligomeric silica nanoparticles  $[R_F-(CH_2CHSiO_2)_n-R_F]$ .<sup>20)</sup>  $R_F-(CH_2CHSiO_2)_n-R_F$  oligomeric nanoparticles thus obtained were also applied to the surface modification to provide an oleophobic/superhydrophobic characteristic on the modified glass surface.<sup>20)</sup> In fact, as shown in Table 3-2, the dodecane and water contact angle values on the modified glass surface treated with the  $R_F-(CH_2CHSiO_2)_n-R_F$  oligomeric nanoparticles are 48 and 180 degrees to exhibit the oleophobic and superhydrophobic characteristic. However, interestingly, it was demonstrated that the  $R_F-(CH_2CHSiO_2)_n-R_F$ /CDPs composites illustrated in Table 3-2 can afford a superoleophilic/superhydrophobic characteristic; because the dodecane and water contact angle values are 0 and 180 degrees in each case, although each composite contains the longer fluoroalkyl groups possessing a good oleophobic property.

There have been heretofore a variety of reports on the creation of the superoleophilic/superhydrophobic surface through the architecture of the roughness surface by using a variety of methods, such as a porous film formation composed of poly(tetrafluoroethylene) nanoparticles<sup>24)</sup>, spray coating with hydrophobic silica nanoparticles suspension<sup>25)</sup>, the treatment with a mixture of hydrophobic silica nanoparticles and polystyrene solution in toluene<sup>26)</sup>. Especially, the introduction of a proper

rough surface microstructure should make a flat hydrophobic surface superhydrophobic, owing to the introduction of an air cushion beneath the water droplet; in contrast, a flat oleophilic surface should become superoleophilic through the capillary effect.<sup>27 ~ 35)</sup> Thus, in order to verify such unique surface wettability, FE-SEM measurements and dynamic force microscopy (DFM) measurements were tried to study on the surface roughness of the modified glass surface by the treatments of the  $R_F-(CH_2CHSiO_2)_n-R_F/\alpha$ -CDP composites (Run 16 in Table 3-1). The modified glass surface treated with the  $R_F-(CH_2CHSiO_2)_n-R_F$  oligomeric nanoparticles were also studied under similar conditions, for comparison. The results are shown in Figure 3-7.

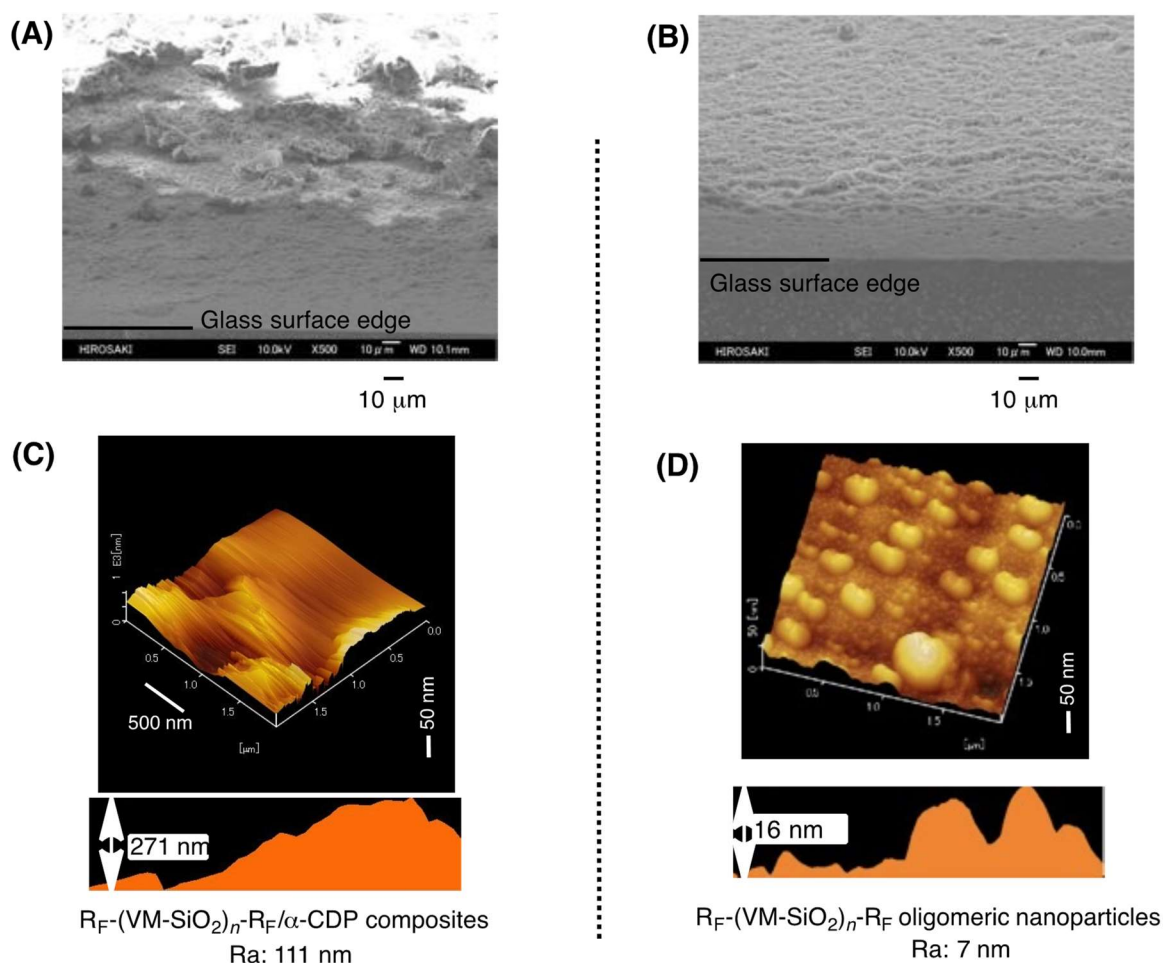


Figure 3-7 FE-SEM (Field Emission Scanning Electron Microscopy) images of the modified glass surface treated with the  $R_F-(VM-SiO_2)_n-R_F/\alpha-CDP$  composites (A), the  $R_F-(VM-SiO_2)_n-R_F$  nanoparticles (B), and DFM (Dynamic Force Microscopy) topographic images of the modified glass surface treated with the  $R_F-(VM-SiO_2)_n-R_F/\alpha-CDP$  composites (C), the  $R_F-(VM-SiO_2)_n-R_F$  nanoparticles (D)

As shown in Figure 3-7-(A), the architecture of the effective roughness surface was observed on the modified glass surface, compared with that [Figure 3-7-(B)] of the modified glass surface treated with the  $R_F-(CH_2CHSiO_2)_n-R_F$  oligomeric nanoparticles. Especially, the topographical image of the modified surface treated with the  $R_F-(CH_2CHSiO_2)_n-R_F/\alpha-CDP$  composites afforded an effective roughness characteristic, and a higher roughness average values: Ra: 111 nm than that (Ra: 7 nm) of the pristine



$R_F-(CH_2CHSiO_2)_n-R_F$  oligomeric nanoparticles can be observed. Such higher roughness value is due to the presence of micrometer size-controlled  $\alpha$ -CDP particles in the composites, providing a superoleophilic/superhydrophobic characteristic on the modified surface. Similar higher roughness values ( $R_a$ ): 135 nm and 82 nm were obtained on the modified glass surfaces treated with the  $R_F-(CH_2CHSiO_2)_n-R_F/\beta$ -CDP composites (Run 17 in Table 3-1) and the  $R_F-(CH_2CHSiO_2)_n-R_F/\gamma$ -CDP composites (Run 18 in Table 3-1), respectively (data not shown). Such higher roughness surfaces would interact with oil (dodecane) possessing the lower surface tension than that of water to give the superoleophilic characteristic, because an oil droplet could easily penetrate the very small orifice between the microsize-controlled composites particles. In contrast, the fluoroalkyl segments in the composites can be arranged on the modified roughness surface to afford the superhydrophobic characteristic.

### **3.3.3. Application of $R_F-(VM-SiO_2)_n-R_F$ /CDPs composites to the separation of the mixture of oil and water**

In this way, it was demonstrated that the present fluorinated composites can provide a superoleophilic/superhydrophobic property. The superoleophilic surface possesses in

general a strong affinity toward oils. Therefore, the surfaces having the superoleophilic/superhydrophobic characteristic can simultaneously repels water and strongly absorbs oils, of whose behavior should be applicable to the separation of oil and water.<sup>36 ~ 39)</sup> Thus, three kinds of mixtures of oil and water such as the O/W emulsions (oils: 1, 2-dichloroethane and toluene) and the mixture of water [5 ml: water was colored with  $\text{CuSO}_4 \cdot 5\text{H}_2\text{O}$  (200 mg)] and 1, 2-dichloroethane (5 ml) were tried to separate by using the present composites. The traditional silica-gel (Wakogel<sup>TR</sup> C-500HG: average particle size: 21  $\mu\text{m}$ ) was not effective for the packing material for column chromatography to separate these mixtures under reduced pressure. However, interestingly, the only transparent colorless oils can be isolated under similar conditions by using the  $\text{R}_\text{F}-(\text{CH}_2\text{CHSiO}_2)_n-\text{R}_\text{F}$ /CDPs composite powders as the packing materials for column chromatography. The recovery ratios ( $w/w_0$ ) ( $w$ : weight of the isolated transparent colorless oil;  $w_0$ : weight of the used oil) of the isolated transparent colorless oils from the mixtures of oil and water are shown in Table 3-3.

Table 3-3 Recovery ratios of oils from the mixtures of oils and water by using the  $R_F-(CH_2CHSiO_2)_n-R_F$ /CDPs composites as the packing materials for column chromatography

Composites		Recovery ratio (%)	
Mixture of 1,2-dichloroethane and water		oil: 1,2-dichloroethane	W/O emulsion oil: toluene
$R_F-(CH_2CHSiO_2)_n-R_F/\alpha$ -CDP composites			
Run 1*	80	82	82
Run 16	73	75	79
-----			
$R_F-(CH_2CHSiO_2)_n-R_F/\beta$ -CDP composites			
Run 2	67	78	76
Run 17	70	81	81
-----			
$R_F-(CH_2CHSiO_2)_n-R_F/\gamma$ -CDP composites			
Run 3	77	78	77
Run 18	77	82	83

\*Each Run No. corresponds to that of Table 3-1

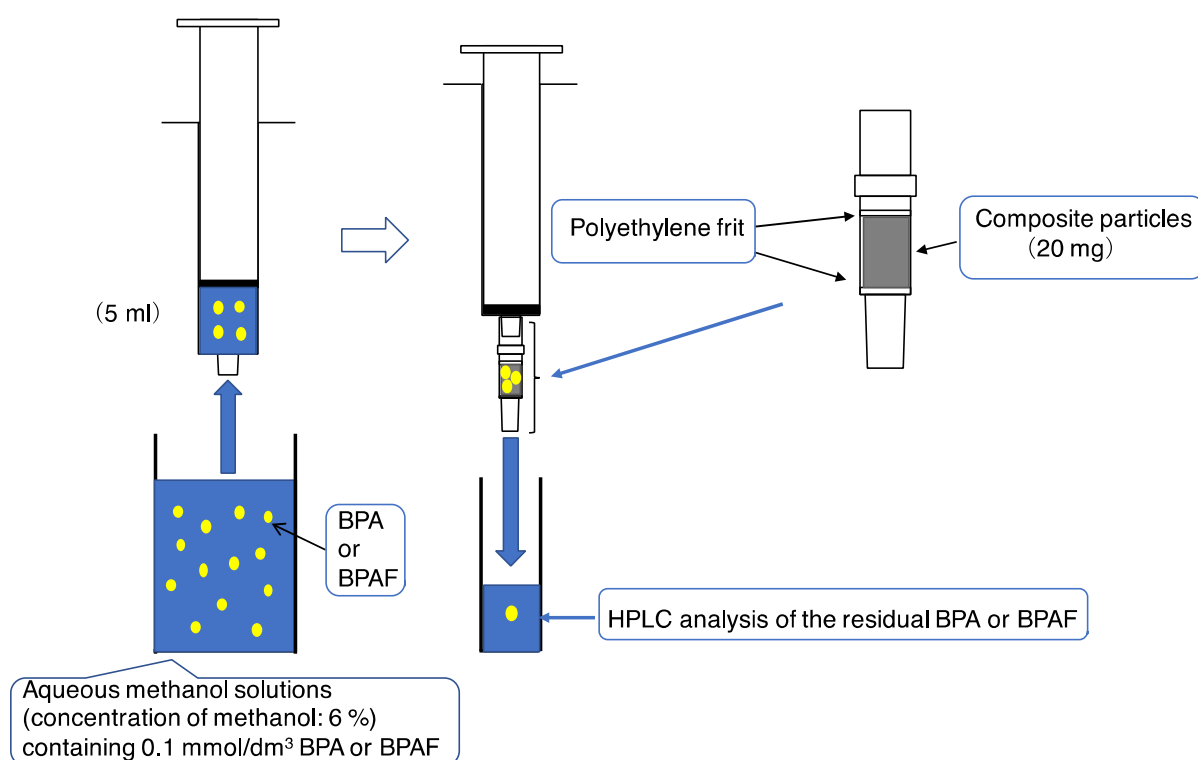
As shown in Table 3-3, the  $R_F-(CH_2CHSiO_2)_n-R_F/\alpha$ -,  $\beta$ -  $\gamma$ - CDPs composites (Runs 1, 2 and 3), which were prepared under the feed ratios of CDPs/oligomer: 10/300, were found to provide a similarly good recovery ratios to those of the other fluorinated composites, which were prepared under the feed ratios of CDPs/oligomer: 300/300. This finding would be due to the superoleophilic/superhydrophobic characteristic in each composite illustrated

in Table 3-2, and the composites possessing such wettability can strongly interact with oils in the aqueous solutions to isolate only oils from the mixtures.

#### **3.3.4. Adsorption of organic molecules by using the $R_F-(CH_2CHSiO_2)_n-R_F$ /CDPs composites**

The traditional organic dyes in many industries such as plastics, textile and cosmetics are in general common water pollutants and we can detect trace quantities in industrial wastewater. Thus, it is very important to develop new technologies to eliminate them.<sup>40)</sup> Hitherto, water-insoluble cyclodextrin polymers (CDPs) have been applied for the removal of various organic dyes from aqueous solutions.<sup>40~47)</sup> From this point of view, it is deeply desirable to develop new CDP derivatives possessing a higher adsorption ability, compared to that of the pristine CDPs. Here the present  $R_F-(CH_2CHSiO_2)_n-R_F$ /CDPs composites were investigated for adsorption of aromatic compounds such as bisphenol A and bisphenol AF in their aqueous methanol solutions. Schematic illustration for the adsorption process of bisphenol A (BPA) or bisphenol AF (BPAF) by using the solid-phase extraction cartridge connected with the polyethylene frit packed with the  $R_F-(CH_2CHSiO_2)_n-R_F$ /CDPs composite powders is illustrated in Scheme 3-2. The adsorption ability of BPA and BPAF

has been also investigated by using the pristine CDPs (20 mg), and the  $R_F-(CH_2CHSiO_2)_n-R_F$ /PTFE (polyterafluoroethylene) composites (20 mg) possessing a superoleophilic/superhydrophobic property<sup>22)</sup> under similar conditions, for comparison. These results are shown in Table 3-4.



Scheme 3-2 Schematic outline for the analysis of the adsorption ratios of bisphenol A (BPA) or bisphenol AF (BPAF) by using the solid-phase extraction cartridge connected with the polyethylene frit packed with the  $R_F-(CH_2CHSiO_2)_n-R_F$ /CDPs composite powders

Table 3-4 Adsorption ratio (%) of BPA and BPAF using the  $R_F-(CH_2CHSiO_2)_n-R_F/CDPs$  composites

CDPs in the composites Run*	Adsorption ratio (%)	
	BPA	BPAF
$\alpha$ -CDP		
19	47	52
10	--	34
-----		
$\beta$ -CDP		
20	100	93
11	--	94
-----		
$\gamma$ -CDP		
21	58	69
12	--	54
-----		
Pristine $\alpha$ -CDP	48	61
$\beta$ -CDP	75	73
$\gamma$ -CDP	59	64
-----		
$R_F-(CH_2CHSiO_2)_n-R_F/PTFE^{**}$	--	5

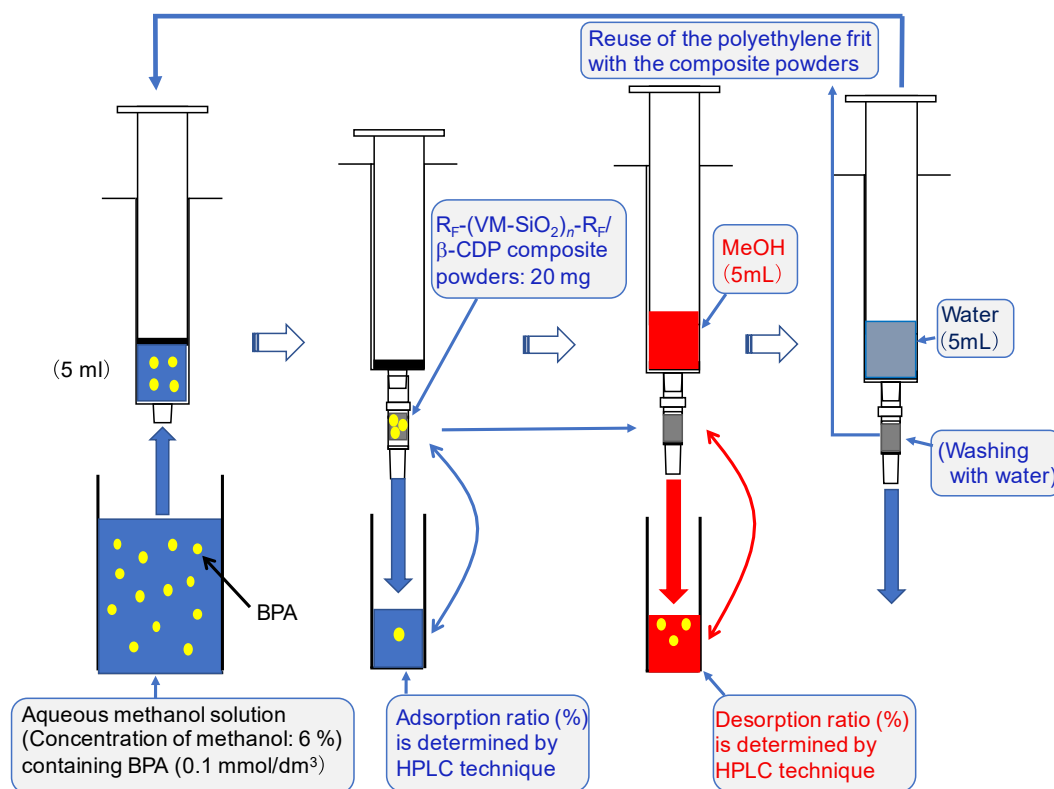
\*Each Run No. corresponds to that of Table 3-1

\*\*Preparative feed ratio of PTFE/oligomer (mg/mg): 100/300

As shown in Table 3-4, the adsorption ability of BPA and BPAF is sensitive to the structures of CDPs in the  $R_F-(CH_2CHSiO_2)_n-R_F/CDPs$  composites, and the highest adsorption ability of BPA or BPAF was observed by the use of the  $\beta$ -CDP in the composites, respectively. It was also demonstrated that the  $R_F-(CH_2CHSiO_2)_n-R_F/\beta$ -CDP composites can enhance the adsorption ability of BPA and BPAF, effectively than that of the pristine  $\beta$ -CDP under similar conditions, indicating that since the present  $R_F-(CH_2CHSiO_2)_n-R_F/\beta$ -CDP composites can exhibit a superoleophilic characteristic with a superhydrophobic property, such superoleophilic characteristic should interact strongly with

oleophilic organic molecules in the aqueous solutions to give a higher adsorption ability; although the pristine  $\beta$ -CDP cannot possess such higher oleophilic property. Especially, the size-fitness of the interior cavity of  $\beta$ -CDP (not  $\alpha$ - and  $\gamma$ -CDPs) in the composites toward BPA or BPAF can provide a higher adsorption ability to form the inclusion derivatives with such aromatic compounds. From this finding, it is suggested that the higher adsorption ratios of BPA or BPAF should be much related to the presence of CDPs in the composites. In fact, the  $R_F-(CH_2CHSiO_2)_n-R_F/PTFE$  composites<sup>22)</sup>, which can exhibit a similar superoleophilic/superhydrophobic characteristic, were unable to provide the adsorption ability as shown in Table 3-4.

The reusability was studied for the  $R_F-(CH_2CHSiO_2)_n-R_F/\beta$ -CDP composite powders (20 mg: Run 22 in Table 3-1) as the packing material for the solid-phase extraction cartridge for the adsorption and desorption of BPA. Scheme 3-3 shows the schematic outline for the recycling process for the adsorption and desorption of BPA by using the  $R_F-(CH_2CHSiO_2)_n-R_F/\beta$ -CDP composite powders as the packing material.



Scheme 3-3 Schematic outline for the recycling process for the adsorption and desorption of BPA by using the  $R_F-(CH_2CHSiO_2)_n-R_F/\beta\text{-CDP}$  composite powders as the packing material

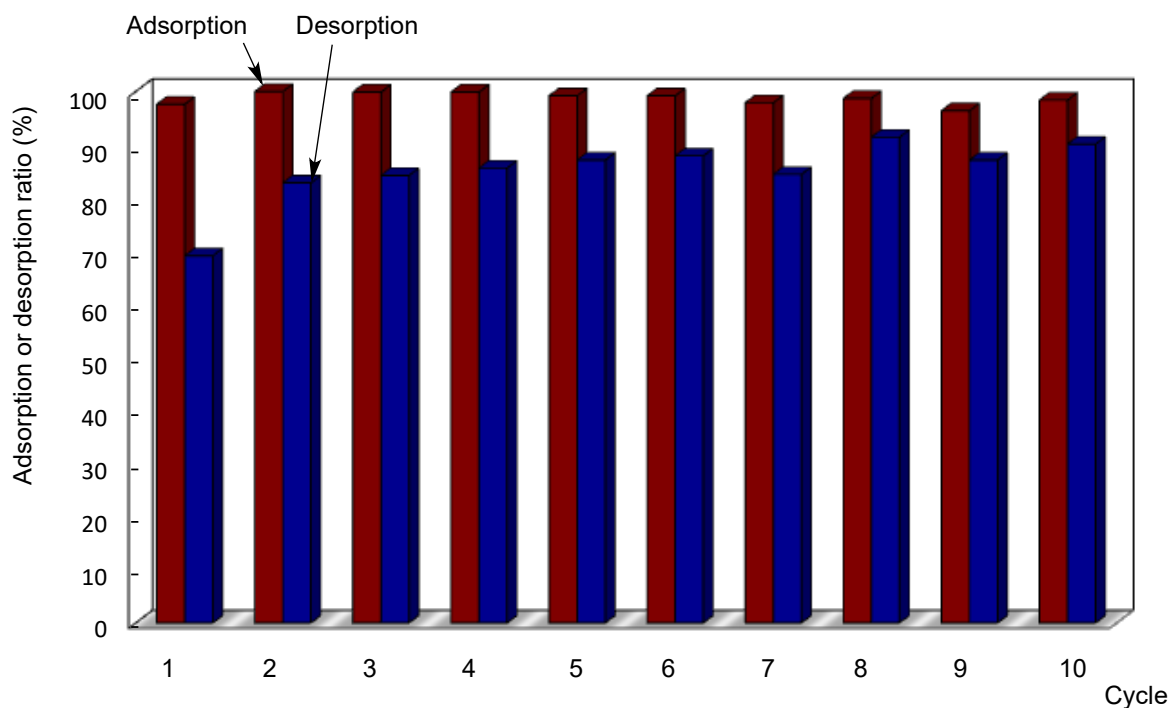


Figure 3-8 Relationship between the recyclability of the  $R_F-(CH_2CHSiO_2)_n-R_F/\beta\text{-CDP}$  composites (Run 22 in Table 3-1) as the packing material, and the adsorption and desorption ratios of BPA in each cycle

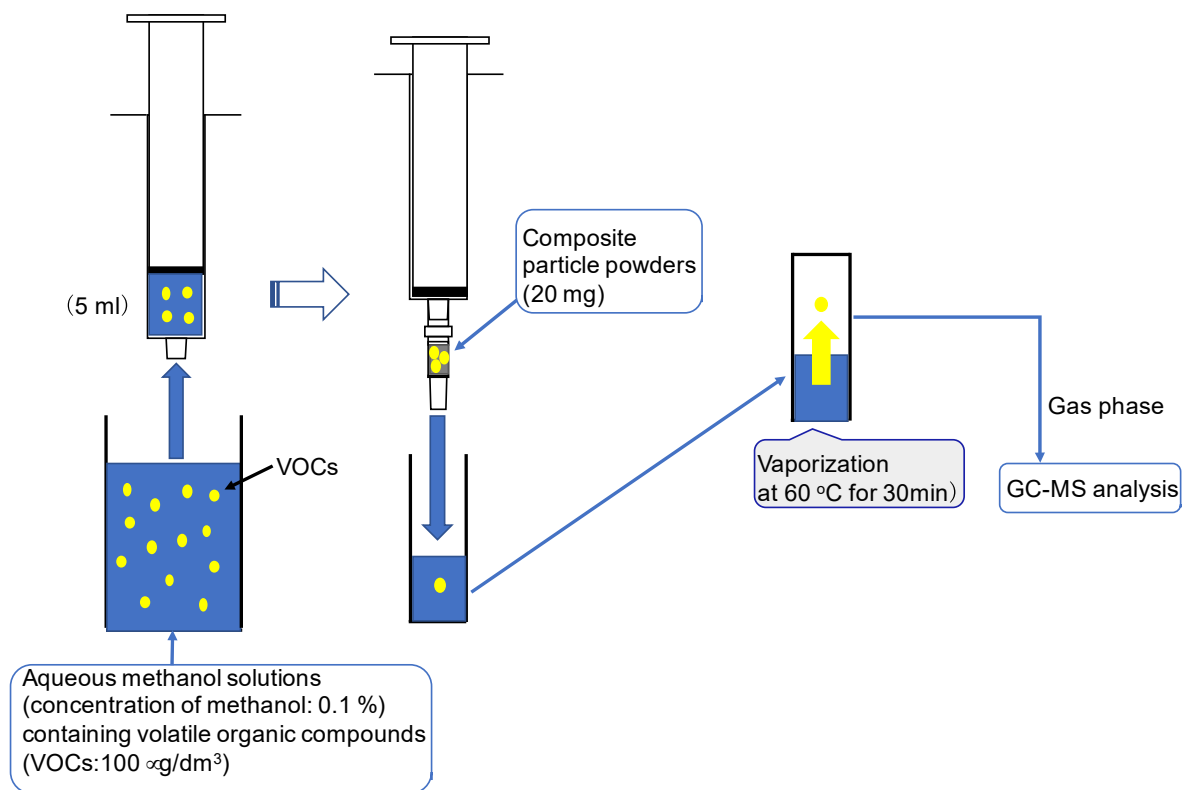


As shown in Scheme 3-3 and Figure 3-8, a good recyclability was observed for the use of the  $R_F-(CH_2CHSiO_2)_n-R_F/\beta$ -CDP composite powders as the packing material for the adsorption and desorption of the BPA even after 10 cycle, and the adsorption and desorption ratios in each cycle are 98 ~ 100 % and 69 ~ 91 %, respectively. In this way, the present  $R_F-(CH_2CHSiO_2)_n-R_F/\beta$ -CDP composites may be developed as the new adsorbent toward the aromatic molecules in their aqueous solutions, especially, the trace amounts of toxic aromatic compounds in industrial wastewater.

Recently, there is a serious problem in increasing environmental pollution, such as the discharge of the industrial wastewater including volatile organic compounds (VOC).<sup>48,</sup>

<sup>49)</sup> From this point of view, it is suggested that the present  $R_F-(CH_2CHSiO_2)_n-R_F/CDPs$  composites would have high potential for the application of novel adsorbent toward not only aromatic compounds such as BPA but also a variety of VOCs. Thus, the  $R_F-(CH_2CHSiO_2)_n-R_F/CDPs$  composites (Runs 19, 20 and 21 in Table 3-1) have been applied to the packing materials for the adsorption of VOCs such as benzene, toluene, xylenes, trichloroethylene, tetrachloroethylene, chloroform, and tetrachlorometane by using the head space – gas chromatograph/mass spectrometer (GC/MS) measurements (the analytical measurement outline: see Scheme 3-4). The adsorption ability of the VOCs was also studied by using the pristine CDPs under similar conditions, for comparison. The

results are shown in Table 3-5.



Scheme 3-4 Schematic outline for the analysis of the adsorption ratios of the VOCs by the head space – GC/MS measurements

Table 3-5 Adsorption ratios of VOCs by the use of  $R_F-(CH_2CHSiO_2)_n-R_F$ /CDPs composites (Run 19, 20, and 21 in Table 3-1)

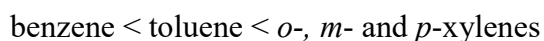
VOC	Adsorption ratio (%)					
	CDPs in the composites			Pristine CDPs		
	$\alpha$ -CDP	$\beta$ -CDP	$\gamma$ -CDP	$\alpha$ -CDP	$\beta$ -CDP	$\gamma$ -CDP
PhH	27	47	25	14	17	4
PhMe	67	73	69	18	15	6
<i>o</i> -Xylene	89	92	93	13	20	19
<i>m</i> - and <i>p</i> -Xylenes	94	95	95	24	21	18
$CH_2=CHCl$	3	0	6	12	4	3
$Cl_2C=CH_2$	25	2	16	21	6	6
$CHCl=CHCl$ ( <i>cis</i> )	28	11	12	21	8	0
$Cl_2C=CHCl$	48	47	40	22	17	11
$Cl_2C=CCl_2$	86	92	91	7	24	20
$ClCH_2CH=CHCl$ ( <i>cis</i> )	52	32	19	29	6	0
$ClCH_2CH=CHCl$ ( <i>trans</i> )	55	32	19	31	0	0
$Cl_2CH_2$	15	1	6	14	1	0
$CHCl_3$	23	35	15	15	12	0
$CCl_4$	59	86	67	13	32	15

As shown in Table 3-5, the  $R_F-(CH_2CHSiO_2)_n-R_F$ /CDPs composites were found to exhibit a higher adsorption ability for VOCs, compared to that of the pristine CDPs.  $R_F-(CH_2CHSiO_2)_n-R_F/\beta$ -CDP composites can possess a higher adsorption ability, quite similar to that of BPA and BPAF illustrated in Table 3-4.

VOCs such as  $CH_2=CHCl$ ,  $Cl_2C=CH_2$ ,  $CHCl=CHCl$ , and  $Cl_2CH_2$ , the  $R_F-(CH_2CHSiO_2)_n-R_F$ /CDPs composites afforded a similar adsorption behavior to that of the pristine CDPs. However, in the cases of the tri- and tetra-chlorinated VOCs such as  $Cl_2C=CHCl$ ,  $Cl_2C=CCl_2$ ,  $CHCl_3$  and  $CCl_4$ , interestingly, these VOCs can be easily

adsorbed by the  $R_F-(CH_2CHSiO_2)_n-R_F/CDPs$  composites, especially by the  $R_F-(CH_2CHSiO_2)_n-R_F/\beta$ -CDP composites. These findings would be due to the increase of the oleophilicity of VOCs by introducing the additional chlorine atoms into VOCs; because the  $R_F-(CH_2CHSiO_2)_n-R_F/CDPs$  composites can possess a superoleophilic property to interact with more oleophilic organic molecules. On the other hand, dichlorinated VOCs such as  $ClCH_2CH=CHCl$  (*cis* and *trans*) can give a higher adsorption ability than the pristine CDPs, quite different from the similar dichlorinated VOCs such as  $CH_2=CHCl$  and  $Cl_2C=CH_2$ . This finding would be due to the longer carbon chains (three carbon chains) to give more oleophilic property.

In the cases of aromatic VOCs such as benzene, toluene, *o*-, *m*-, and *p*-xylenes, these aromatic VOCs are likely to interact with the  $R_F-(CH_2CHSiO_2)_n-R_F/CDPs$  composites to afford higher adsorption ratios than the pristine CDPs. Interestingly, higher adsorption ratios from 25 to 95 % were obtained with the increase of the oleophobicity of the VOCs as following:



More interestingly, the highest adsorption ability toward these VOCs was observed by using the  $R_F-(CH_2CHSiO_2)_n-R_F/\beta$ -CDP composites. This finding is due to the size-fitness of the interior cavity of  $\beta$ -CDP toward these aromatic VOCs.

### 3.4. Conclusion

Fluoroalkyl end-capped vinyltrimethoxysilane oligomeric silica/ $\alpha$ -,  $\beta$ -,  $\gamma$ -cyclodextrin polymers (CDPs) composites  $[R_F-(CH_2CHSiO_2)_n-R_F/CDPs]$  were prepared by the sol-gel reactions of the corresponding oligomer in the presence of CDPs under alkaline conditions. These obtained fluorinated composites were found to exhibit a superoleophilic/superhydrophobic characteristic on the modified surface, although the corresponding fluoroalkyl end-capped oligomeric silica nanoparticles can give a oleophobic/superhydrophobic property on the modified surface. The  $R_F-(CH_2CHSiO_2)_n-R_F/CDPs$  composites possessing a superoleophilic/superhydrophobic characteristic have been applied to the packing material for the column chromatography to separate the mixture of oil/water and the W/O emulsions to isolate the transparent colorless oils. In addition, the  $R_F-(CH_2CHSiO_2)_n-R_F/CDPs$  composites have been also applied to the packing material for the solid-phase extraction cartridge to adsorb the aromatic compounds such as BPA and BPAF in their aqueous solutions, and the highest adsorption behavior for these compounds was observed in the  $R_F-(CH_2CHSiO_2)_n-R_F/\beta$ -CDP composites. In addition to the adsorption of the aromatic compounds, the  $R_F-(CH_2CHSiO_2)_n-R_F/CDPs$  composites have been also applied to the adsorption of the VOCs by the head-space – GC/MS

technique. In a wide variety of VOCs, more oleophilic aromatic VOCs can afford a higher adsorption ability toward the present  $R_F-(CH_2CHSiO_2)_n-R_F/CDPs$  composites, especially, the  $R_F-(CH_2CHSiO_2)_n-R_F/\beta$ -CDPs composites, compared to that of the pristine CDPs. In the cases of chlorinated aliphatic VOCs, tri- and tetra-chlorinated VOCs can provide a higher adsorption ability toward the fluorinated CDPs composites, especially fluorinated  $\beta$ -CDP composites. These findings would be due to the effective oleophilic – oleophilic interaction between the oleophilic VOCs and the fluorinated CDPs composites possessing a superoleophilic property. In this way, the present fluorinated CDPs composites would have high potential for the development of not only the practical oil/water separation materials but also the new sorbents to remove the organic pollutants in the industrial wastewater.

## References

- 1) G. Crini and P.-M. Badot Eds., “*Sorption Process and Pollution – Conventional and Non-Conventional Sorbents for Pollutant Removal from Wastewaters*”, Presses Universitaires de Franche-Comte (2010).
- 2) G. Crini, *Prog. Polym. Sci.*, **30**, 38 (2005).
- 3) M. L. Bender and M. Komiyama, *Cyclodextrin Chemistry*, Spronger-Verlag, New York (1978).
- 4) I. Tabushi, *Acc. Chem. Res.*, **15**, 66 (1982).
- 5) S. Tang, L. Kong, J. Ou, Y. Liu, and H. Zou, *J. Mol. Recognit.*, **19**, 39 (2006).
- 6) H. Asanuma, M. Kakazu, M. Shibata, T. Hishiya, and M. Komiyama, *Supramol. Sci.*, **5**, 417 (1998).
- 7) G. Crini, C. Cosentino, S. Bertini, A. Naggi, G. Torri, C. Vechhi, L. Janus, and M. Morcellet, *Carbohydr. Res.*, 308, 37 (1998).
- 8) L. Moine, C. Amiel, W. Brown, and P. Guerin, *Polym. Int.*, **50**, 663 (2001).
- 9) M. Raoov, S. Mohamad, and M. R. Abas, *Int. J. Mol. Sci.*, **15**, 100 (2014).
- 10) H. Yamasaki, Y. Nagasawa, N. Uchida, and K. Fukunaga, *Kobunshi Ronbunshu*, **70**, 572 (2013).

- 11) T. Hishiya, M. Shibata, M. Kakazu, H. Asanuma, and M. Komiyama, *Macromolecules*, **32**, 2265 (1999).
- 12) G. Crini, S. Bertini, G. Torri, A. Naggi, D. Sforzini, C. Vecchi, L. Janus, Y. Lekchiri, and M. Morcellet, *J. Appl. Polym. Sci.*, **68**, 1973 (1998).
- 13) M. Kitaoka and K. Hayashi, *J. Incl. Phenom. Macrocyclic Chem.*, **44**, 429 (2002).
- 14) J. C. Yu, Z. T. Jiang, H. Y. Liu, L. Yu, and L. Zhang, *Anal. Chim. Acta*, **477**, 93 (2003).
- 15) B. Ameduri and H. Sawada (Eds.), *Fluorinated Polymers: Volume 1, "Synthesis, Properties, Processing and Simulation"*, Cambridge, RSC (2016);
- 16) B. Ameduri and H. Sawada (Eds.), *Fluorinated Polymers: Volume 2, "Applications"*, Cambridge, RSC (2016).
- 17) H. Sawada, *Chem. Rev.*, **96**, 1779 (1996).
- 18) H. Sawada, *Prog. Polym. Sci.*, **32**, 509 (2007).
- 19) H. Sawada, *Polym. Chem.*, **3**, 46 (2012).
- 20) H. Sawada, T. Suzuki, H. Takashima, and K. Takishita, *Colloid Polym. Sci.*, **286**, 1569 (2008).
- 21) Y. Oikawa, T. Saito, S. Yamada, M. Sugiya and H. Sawada, *ACS Appl. Mater. Interfaces*, **7**, 13782 (2015).
- 22) J. Suzuki, Y. Takegahara, Y. Oikawa, M. Chiba, S. Yamada, M. Sugiya, and H. Sawada,



- J. Sol-Gel Sci. Technol.*, **81**, 611 (2017).
- 23) H. Sawada and M. Nakayama, *J. Chem. Soc., Chem. Commun.*, 677 (1991).
- 24) C. Su, J. Wang, Z. Chen, and D. Chen, *Appl. Surface Sci.*, **313**, 304 (2014).
- 25) J. Li, H. Wan, Y. Ye, H. Zhou, and J. Chen, *Appl. Surface Sci.*, **261**, 470 (2012).
- 26) E. Celia, T. Darmanin, E. T. de Givenchy, S. Amigoni, and F. Guiiard, *J. Colloid Interface Sci.*, **402**, 1 (2013).
- 27) M. Liu and L. Jiang, *Adv. Funct. Mater.*, **20**, 3753 (2010).
- 28) Q. M. Pan, M. Wang, and H. B. Wang, *Appl. Surf. Sci.*, **254**, 6002 (2008).
- 29) C. X. Wang, T. J. Yao, J. Wu, C. Ma, Z. X. Fan, Z. Y. Wang, Y. R. Cheng, Q. Lin, and B. Yang, *ACS Appl. Mater. Interfaces*, **1**, 2613 (2009).
- 30) B. Wang, J. Li, G. Y. Wang, W. X. Liang, Y. B. Zhang, L. Shi, Z. Guo, and W. M. Liu, *ACS Appl. Mater. Interfaces*, **5**, 1827 (2013).
- 31) W. X. Liang and Z. G. Guo, *RSC Adv.*, **3**, 16469 (2013).
- 32) J. Zhang and S. Seeger, *Adv. Funct. Mater.*, **21**, 4699 (2019).
- 33) X. Y. Zhou, Z. Z. Zhang, X. H. Xu, F. Guo, X. T. Zhu, X. H. Men, and B. Ge, *ACS Appl. Mater. Interfaces*, **5**, 7208 (2013).
- 34) S. H. Wang, M. Li, and Q. H. Lu, *ACS Appl. Mater. Interfaces*, **2**, 677 (2010).
- 35) X. Liu, L. Ge, W. Li, X. Wang, and F. Li, *ACS Appl. Mater. Interfaces*, **7**, 791 (2015).

- 36) M. Zhang, C. Wang, S. Wang, Y. Shi, and J. Li, *Carbohydr. Polym.*, **97**, 59 (2013).
- 37) T. Arbatan, L. Zhang, X.-Y. Fang, and W. Shen, *Chem. Eng. J.*, **210**, 74 (2012).
- 38) H. Sawada, Y. Suto, T. Saito, Y. Oikawa, K. Yamashita, S. Yamada, M. Sugiya, and J. Suzuki, *Polymers*, **9**, 92 (1 ~ 14) (2017); doi:10.3390/polym9030092.
- 39) S. Katayama, S. Fujii, T. Saito, S. Yamazaki, and H. Sawada, *Polymers*, **9**, 292 (1 ~ 17) (2017); doi:10.3390/polym9070292.
- 40) G. Crini, *Bioresource Technol.*, **90**, 193 (2003).
- 41) M. Weickenmeier, G. Wenz, and J. Huff, *Macromol. Rapid Commun.*, **18**, 1117 (1997).
- 42) K. Sreenivasan, *J. Appl. Polym. Sci.*, **68**, 1857 (1998).
- 43) A. Binello, B. Robaldo, A. Barge, R. Cavalli, and G. Cravotto, *J. Appl. Polym. Sci.*, **107**, 2549 (2008).
- 44) J. Kiji, H. Kunishi, T. Okano, T. Terashima, and K. Motomura, *Angew. Makromol. Chem.*, **199**, 207 (1992).
- 45) H. Yamasaki, Y. Makihara, and K. Fukunaga, *J. Chem. Technol. Biotechnol.*, **81**, 1271 (2006).
- 46) G. Crini, C. Cosentino, S. Bertini, A. Naggi, G. Torri, C. Vecchi, L. Janus, and M. Morcellet, *Carbohydr. Res.*, **308**, 37 (1998).
- 47) K.-P. Lee, S.-H. Choi, E.-N. Ryu, J. J. Ryoo, J. H. Park, Y. Kim, and M. H. Hyun,

*Anal. Sci.*, **18**, 31 (2002).

48) A. K. Kota, G. Kwon, W. Choi, J. M. Mabry, and A. Tuteja, *Nat. Commun.*, **3**, 1025 (2012).

49) S. Parak, E. S. Lee, and W. R. W. Sulaiman, *J. Ind. Eng. Chem.*, **21**, 1239 (2015).

## Conclusions

The results obtained from this study are summarized as follows.

1. Fluoroalkyl end-capped vinyltrimethoxysilane oligomer [ $R_F-(CH_2CHSi(OMe)_3)_n-R_F$ ;  $R_F = CF(CF_3)OC_3F_7$ ,  $n = 2, 3$ ;  $R_F-(VM)_n-R_F$  oligomer] can undergo the sol-gel reaction in the presence of poly(tetrafluoroethylene) (PTFE) fine particles under alkaline conditions to afford the corresponding fluorinated oligomeric silica/PTFE nanocomposites [ $R_F-(VM-SiO_2)_n-R_F/PTFE$  nanocomposites]. Interestingly, the modified glass, PTFE sheet and filter paper surfaces treated with the obtained nanocomposites were found to exhibit a superoleophilic/superhydrophobic characteristic; although the original PTFE sheet and the modified glass surface treated with the  $R_F-(VM)_n-R_F$  oligomeric silica nanoparticles [ $R_F-(VM-SiO_2)_n-R_F$ ] can provide the usual oleophobic/hydrophobic and oleophobic/superhydrophobic properties, respectively. The modified filter paper was applied to the separation membrane for the mixture of oil/water. In addition, the fluorinated PTFE nanocomposite white-colored powders thus obtained were applied to the packing material for the column chromatography to separate the mixture of oil/water and water-in-oil (W/O) emulsions. The reusability was also studied for the present nanocomposite particle powders as the

packing material for the separation of not only the mixture of oil/water but also the W/O emulsions, and the colorless oil was quantitatively isolated under similar conditions even after the use of the packing materials five times.

2. Fluoroalkyl end-capped vinyltrimethoxysilane oligomeric silica/alkyl-modified cellulose (**AM-Cellu**) nanocomposites [ $R_F-(CH_2-CHSiO_2)_n-R_F/AM-Cellu$ ;  $n = 2, 3$ ;  $R_F = CF(CF_3)OC_3F_7$ ] were prepared by the sol-gel reactions of the corresponding oligomer [ $R_F-(CH_2-CHSi(OMe)_3)_n-R_F$ ] in the presence of **AM-Cellu**. The nanocomposites thus obtained were applied to the surface modification of glass to exhibit a highly oleophobic/superhydrophilic characteristic on the modified surface at 20 °C. Interestingly, a temperature dependence of contact angle values of dodecane and water was observed on the modified surface at 20 ~ 70 °C, and the dodecane contact angle values were found to decrease with increasing the temperatures from 20 to 70 °C to provide from highly oleophobic to superoleophilic characteristics on the surface. On the other hand, the increase of water contact angle values was observed with increasing the temperatures under similar conditions to supply from superhydrophilic to superhydrophobic characteristics on the modified surface. The corresponding

nanocomposites were also applied to the surface modification of filter paper under similar conditions to afford a superoleophilic/superhydrophobic characteristic on the surface. It was demonstrated that the modified filter paper is effective for the separation membrane for W/O emulsion to isolate the transparent colorless oil.

3. Fluoroalkyl end-capped vinyltrimethoxysilane oligomer  $[R_F-(CH_2CHSi(OMe)_3)_n-R_F]$ ;  $R_F = CF(CF_3)OCF_7$ ,  $n = 2, 3$ ;  $R_F-(VM)_n-R_F$ ] was applied to the preparation of fluoroalkyl end-capped vinyltrimethoxysilane oligomer/ $\alpha$ ,  $\beta$ ,  $\gamma$ -cyclodextrin polymers ( $\alpha$ ,  $\beta$ ,  $\gamma$ -CDPs) composites  $[R_F-(VM-SiO_2)_n-R_F/\alpha$ ,  $\beta$ ,  $\gamma$ -CDPs] by the sol-gel reaction of the corresponding oligomer in the presence of the  $\alpha$ ,  $\beta$ ,  $\gamma$ -CDPs under alkaline conditions. The  $R_F-(VM-SiO_2)_n-R_F/\alpha$ ,  $\beta$ ,  $\gamma$ -CDPs composites thus obtained were found to give a good dispersibility toward the traditional organic media except for water, and were applied to the surface modification of glass to provide a superoleophilic/superhydrophobic characteristic on the modified surface, although the corresponding  $R_F-(VM-SiO_2)_n-R_F$  nanocomposites can give a usual oleophobic/superhydrophobic property on the surface. These composites powders were also found to be applicable to the packing material for

the column chromatography to separate the mixture of oil/water and the water in oil (W/O) emulsions. More interestingly, these composite powders were found to have a higher adsorption ability toward not only low-molecular weight aromatic compounds such as bisphenol A and bisphenol AF but also volatile organic compounds, compared to that of the pristine  $\alpha$ ,  $\beta$ ,  $\gamma$ -CDPs.

## Publications

- 1) J. Suzuki, Y. Takegahara, Y. Oikawa, M. Chiba, S. Yamada, M. Sugiya, and H. Sawada, "Preparation of Fluoroalkyl End-Capped Vinyltrimethoxysilane Oligomeric Silica/Poly(tetrafluoroethylene) Nanocomposites Possessing a Superoleophilic/Superhydrophobic Characteristic: Application to the Separation of Oil and Water", *J. Sol-Gel Sci. Technol.*, **81**, 611 ~ 622 (2017).
- 2) H. Sawada, Y. Suto, T. Saito, Y. Oikawa, K. Yamashita, S. Yamada, M. Sugiya, and J. Suzuki, "Preparation of  $R_F-(VM-SiO_2)_n-R_F/AM$ -Cellu Nanocomposites, and Use Thereof for the Modification of Glass and Filter Paper Surfaces: Creation of a Glass Thermoresponsive Switching Behavior and an Efficient Separation Paper Membrane", *Polymers*, **9**, 92 (1 ~14) (2017).
- 3) J. Suzuki, Y. Takegahara, Y. Oikawa, Y. Aomi, and H. Sawada, "Preparation of Fluoroalkyl End-Capped Oligomer/Cyclodextrin Polymer Composites: Development of Fluorinated Composite Material Having a Higher Adsorption



Ability toward Organic Molecules”, *J. Encap. Adsorp. Sci.*, **8**, 117 ~ 138 (2018).

## Acknowledgements

The author would like to express his deepest gratitude to Prof. Hideo Sawada for his guidance and valuable discussions on this study.

He deeply thanks to Prof. Isoshi Nukatsuka, Associate Prof. Jun Kawakami, Associate Prof. Masanobu Sagisaka, and Associate Prof. Fumihiko Kitagawa, for their kind advices and discussions. He would also deeply thank to Dr. Masashi Sugiya and Mr. Satoshi Yamada of Nippon Chemical Industrial Co., Ltd, Dr. Yuri Oikawa, Mr. Yutaro Takegahara, Mr. Masaya Chiba, Mr. Yuki Suto, Mr. Tomoya Saito, Mr. Katsumi Yamashita, Mr. Yuta Aomi of Department of Frontier Materials Chemistry, Graduate School of Science and Technology, Hirosaki University, for their kind advices and discussions, respectively. He wishes to extend his thank to all of students of a laboratory for their advices and discussions.

He would also like to thank to his manager and co-workers for their cooperation and support.

Finally, he would like to especially thank to his wife and daughters for their understanding, encouragement and sacrifice throughout his study.